THE COMPRESSION IGNITION OF FUEL-OXIDANT MIXTURES

by

H.C. WATSON

Thesis submitted for the degree of

Doctor of Philosophy

in the Faculty of Engineering

University of London

City and Guilds College,

Imperial College of Science and Technology,

London, S.W.7.

January 1969

ABSTRACT

This thesis presents an analytical method for predicting the autoignition of fuel-oxidant mixtures in a system where the fluid properties are spatially uniform and the density-time variation is prescribed. Application of the method has permitted comparison of predicted results with experimental observations of the autoignition of hydrogen-oxygen-argon mixtures in a single-shot compression machine. Hydrogen was selected as fuel because it was one of the few fuels used in reciprocating engines for which the kinetic data, required for the predictions, are available in the literature.

Comparisons have been made between predicted and observed results of the induction-times to autoignition over the H_2-O_2 composition range from .05 to 2.5 of the stoichiometric value. When the predictions were calculated from existing kinetic-data only qualitative agreement was obtained between predicted and observed results. To obtain quantitative agreement it proved necessary to adjust the forward rates of six reactions, in a kinetic model of nine reactions for the species H_2, O_2, H, O, OH and H_2O. These 'effective' reaction-rates contribute to the knowledge of the hydrogen-oxygen reaction in the previously unexplored pressure range of 10 to 25 atmospheres and temperatures in the region 850 to 1200°K.

The combination of compression machine and prediction technique has application to future kinetic studies, not only in establishing the importance of the additional species HO_2 and H_2O_2 in the hydrogen reaction, but also in deriving the ignition

kinetics of other fuel-oxidant mixtures. These studies, and the present investigation, will assist in predicting the ignition of simple fuels in reciprocating engines.

——— ooo ———

ACKNOWLEDGEMENTS

The diverse nature of the present work is such that I have acquired knowledge of numerous fields of science. This would not have been possible without assistance and counsel from many persons:

I wish to thank Professor D.B. Spalding for initiating the project, for the interest he maintained in it and the guidance he gave as the work progressed. He and Mr. A.D. Gosman have had a most valuable influence on the presentation of this thesis. Their belief, and rightly, in the guiding principles: ease of reading and continuity of thought; will, I hope, be reflected throughout the thesis.

To Dr. G.A. Karim, I owe my gratitude for his enthusiastic supervision. His encouragement in times of difficulty and his eagerness for success were a valuable driving force.

Mr. N.P.W. Moore deserves my sincere thanks for the assistance he has given me in finalising this work.

To others, too numerous to mention individually, I acknowledge their collective contribution to both scientific and non-scientific matters.

I also acknowledge the financial support given to me by the Science Research Council.

CONTENTS

page

page

page

CHAPTER 1

INTRODUCTION

1.1 Historical Background

The goal of the combustion engineer in power-plant design must always be to predict quantitatively, by way of mathematical analysis, the performance of the machine he designs. Only when accurate prediction is possible can he rest assured that changes in operating conditions or design detail can be accounted for with certainty and without recourse to experiment.

The reward will surely be economy of effort. For example; much experimental effort is being directed to reduce atmospheric pollution caused by automobile exhaust-gases. If it were possible, by prediction, to relate the level of polluants in the exhaust gas to any combination of engine variables, then a combination could be selected so as to minimise the polluant level. At present, we must try to find this optimum solution by laborious experimental procedure.

The presently reported work falls short of predicting such a general case as given in the example. However, it has been possible to predict results, agreeing closely with experiment, for the compression to self-ignition of a 'simple' fuel in a piston-cylinder machine. The study has been confined to this problem, where the whole charge simultaneously ignites, to simplify the mathematical analysis of the igniting system. The analysis is simplified in that there is no need to consider the partial-differential equations which describe the spatial variation of the properties of the cylinder charge in spark-ignited, or diesel-engine, combustion problems. Instead, the equations reduce to ordinary-differential form because

the fluid properties remain uniform throughout the charge at all times.

The study has considered the 'simple' fuel hydrogen, rather than a hydro-carbon fuel, because the chemical kinetics of its ignition reaction are available in the literature. Not only have models been proposed to describe the steps in the hydrogen chain-reaction, but also values for the reaction rates of many of these steps have been given. These kinetic data are required for the mathematical description of chemical reaction occurring in the piston-in-cylinder system.

It is the consideration of the detailed chemical-kinetics in which the present study is more exact than previous work (Karim [29.]*), when engine autoignition was predicted by making simplifications; especially to the kinetic model which was reduced to a single-step reaction, the rate of which was assumed to represent the rate of dominant reaction in the chain mechanism. Thus, it was not possible, as now, to predict the production and survival of intermediate chemical species formed during reaction.

The present investigation was initiated by Spalding [50.], who proposed a method for predicting the onset of 'knock' in gasoline engines. Overall reaction-kinetic data was to be obtained from a study of the autoignition of fuels under experimental conditions, more controlled, but closely reproducing those of the autoigniting 'end-gas', remote from the sparking-plug of a firing engine. That is, under 'knocking' conditions. For this study, a compression machine was to be built, capable of reproducing the density-time history of the 'end-gas'. The kinetic data obtained from the re-

---

* Square brackets indicate reference numerals.

sults of the experiments with the machine, would then be used to calculate, by way of a single equation, the operating conditions at which the onset of 'knock' would occur in any engine.

It was the reluctance to accept the restrictions imposed by the consideration of overall kinetics (see Watson [59.] and Annand [2.]) that Spalding's proposal was modified to the present objectives, given below, in which account is taken of the detailed kinetics.

1.2 The Present Study

There were four main objectives to the investigation. They were:

1. to establish an analytical method for predicting autoignition in a system having spatially-uniform fluid properties and subjected to a prescribed density-time variation.
2. to observe experimentally the autoignition of hydrogen-oxygen-inert mixtures in such a system. More specifically, to obtain pressure- and density-time records, over a wide range of mixture composition, for charges compressed to autoignition in a compression apparatus.
3. to investigate the extent to which the existing chemical-kinetic data, reported in the literature, could be used for predicting hydrogen autoignition as observed in the experimental tests.
4. to derive, if possible, kinetic data of the hydrogen reaction which could be used for predicting autoignition, in agreement with experiment, in systems of the type considered.

The methods used in achieving these objectives may be summarised as follows:

1. The chemical-kinetic and gas-dynamic equations, describing the reaction of the compressed gaseous mixture, were reduced to (n+1)* non-linear, first order, differential equations. A computer programme was written to execute the numerical method of solution.

2. A pneumatically-driven compression-machine was designed and constructed. The cylinder of the machine, in which the reactant-gas was compressed to autoignition, was instrumented with pressure and displacement transducers so that continuous records could be obtained of the cylinder pressure and volume with respect to time.

3. Pressure-time histories of autoignition, predicted from a range of plausible reaction-kinetic data, were compared with the experimental pressure-time records. The kinetic data was said to represent truly the reactions leading to ignition only when there was quantitative agreement between predicted and experimental results for a wide range of compression paths and of pre-compression states: mixture composition, temperature and pressure.

4. The strategy used to derive reaction-kinetic data has been more modest than the exact procedure, and has thus avoided an examination of hundreds of experimental results and searches in multi-dimensional space for the kinetic data. The method used to obtain values for the kinetic data was to consider a plausible set of elementary reactions of known or proveable importance. Then, the rate constant of each reaction was systematically adjusted until a set of values was obtained which gave predicted autoignition data, in agreement with experiment, over a wide range of mixture composition.

---

* n is the number of species participating in the reaction.

1.3 Outline of Thesis

There are eight chapters in the thesis, the first of which is this introduction.

The next two chapters are concerned with the mathemtical analysis of the reacting system subjected to a prescribed density change. Chapter 2 considers the derivation of the equations and the procedure of numerical solution. In Chapter 3, the input data (thermodynamic and transport properties, chemical-kinetic and heat-transfer data) are provided for the calculation, by a computer programme, of the variation with time of parameters such as pressure, temperature, species concentration and combustion-energy release-rates.

Chapters 4 and 5 describe the experimental contribution. The former outlines the design, construction and operational procedure of the apparatus, while a more detailed description of the apparatus may be found in Appendix D. Chapter 5 contains the results of the experimental investigations: the assessment of the modes of piston-motion attainable with the apparatus; the tests to obtain the constants of a formula for predicting the heat-transfer rate at the gas-to-wall interface; and the study of hydrogen-oxygen autoignition over the mixture range 0.05 to 2.5 of the stoichiometric value; revealed for the first time, is the two-stage ignition behaviour of hydrogen at a narrow band of experimental conditions.

Comparisons are made between predicted and observed autoignition data in Chapter 6. Predictions are calculated from combinations of kinetic models and reaction-rate data for the species H_2, O_2, H, O, OH, H_2O, HO_2 and H_2O_2. The comparions show that while qualitative agreement exists between prediction and experiment, quantitative agreement does not.

Thus, in Chapter 7, reaction-rate constants are derived which, in a 9-step kinetic-model, give agreement between predicted and observed autoignition data. The kinetic model is then extended to include reactions of the species HO_2 and H_2O_2 and the resultant implications are discussed.

The last chapter, Chapter 8, contains a summary of the results of this thesis and recommendations for future studies.

CHAPTER 2

MATHEMATICAL ANALYSIS AND METHOD OF SOLUTION

2.1 Introduction

2.11 The object of the chapter

The present task is the analysis of a reacting system subjected to a prescribed variation of density with time. The gaesous system, contained by a moving piston in a closed cylinder, is assumed to have no spatial property variation, so that the conservation laws of energy and mass need only be expressed through ordinary-differential equations, and the conservation of momentum can be ignored. Additional algebraic and differential equations will be required to express the boundary conditions, and to describe the thermodynamic and chemical-kinetic properties of the fluid.

The first objective of this chapter is to present these equations in forms which lead to ease of manipulation for solution in the prediction procedure. It is for ease of solution and because of the importance of reaction chemistry to the problem, that the equations are subdivided into two sections: thermodynamic and chemical-kinetic equations.

The second object of the chapter is to present the procedure by which the equations are solved and predictions made.

2.12 The relevance of previous work to the present problem

Before proceeding to the analysis, we will digress slightly and indicate how the analysis differs from, and extends, previous related studies involving detailed chemical-kinetics.

The essential difference between the present task and previous tasks is that the problem considered is a transient combustion-phenomenon rather than continuous reaction in a steady flow. Two examples of these steady-flow problems are: 1. an examination of the flow of reacting H_2-O_2 mixtures within a well-stirred reactor by Jenkins, Spalding and Yumlu [25.]. They simplified the analysis by assuming that mixing between reactant-gas and products was both instantaneous and complete, and that pressure variation within the reactor could be neglected. 2. Further flow studies have been made of the hydrogen reaction in adiabatic-parallel ducts. Momtchiloff et al. [38.] and Pergament [41.] predicted the variation of parameters such as reactant concentrations and temperature along the duct, while Bascombe [4.] and Brokaw [8.] predicted ignition delays only. Again, in all their mathematical models complete and instantaneous mixing of reactants and products was assumed.

Here too, in 2.21 we shall make the same important assumption that mixing is complete. This is certainly true at time $t = 0$, when the gaseous charge is premixed. But as the system density is altered, by the movement of the piston down the cylinder, gas close to the walls may not have the same properties as the bulk of the charge. However, it will be shown that during compression extensive mixing does occur, indicating that the assumption of equal pressure, temperature and species concentration etc. at every point of the charge is close to reality.

However, although the fluid properties are assumed to be spatially uniform the conditions at the system boundary are different from those of the steady-flow examples discussed. Heat transfer cannot be neglected for the piston-in-cylinder system, and while

there is no fluid flow through the boundary, we shall have to allow for work done at the boundary. Although these differences considerably alter the mathematical formulation of the problem, we shall see later, in this and subsequent chapters, that much can be learnt from the solution procedures adopted in the prediction of combustion in steady flow.

2.2 The Derivation of Equations

2.21 The system considered

a) The boundaries of the system.

The system considered is that bounded by the cylinder walls, the cylinder-head face and the moving boundary of the piston crown.

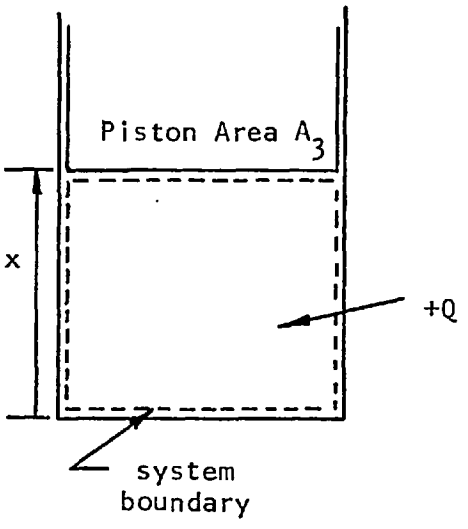

Fig. 2.21-1
The system considered

b) Assumptions about the system.

1. The system is at all times homogeneous.

2. The gases obey the ideal gas laws.

3. There is no loss of mass from the system.

4. Gravitational and gas motion forces may be neglected.

5. There is immediate equalisation of pressure throughout the system.

2.22 The derivation of equations

a) Thermodynamic equations.

Energy conservation; the 1st law of thermodynamics:

$$dQ - dW = dE \qquad 2.22\text{-}1$$

for the system $dE = dU$ 2.22-2

where Q is the heat flux across the system boundary and W is the work at the boundary, while E and U are the total energy and internal energy respectively.

Mass conservation; the system mass M is given by:

$$M = \rho x A_3 \qquad 2.22\text{-}3$$

in terms of the density, ρ; the piston area, A_3; and displacement x.

The total internal-energy is the summation of the component internal-energies, U_i:

$$U = M\Sigma\sigma_i U_i \qquad 2.22\text{-}4$$

where σ_i is the concentration of the i^{th} species.

The constituent energy above the reference temperature T_R is given by:

$$U_i = \int_{T_R}^{T} C_{v_i}\, dT + U_{R_i} \qquad 2.22\text{-}5$$

The reference internal-energy U_{R_i} includes the heat of formation and C_{v_i} is the specific heat at constant volume.

The density and temperature are related to the pressure, p, by the equation of state:

$$p = \rho R\Sigma(\sigma_i)T \qquad 2.22\text{-}6$$

Further, we need to know a relation between piston displacement and time of the form

$$x = f(t) \qquad 2.22\text{-}7$$

whence, by differentiation:

$$\frac{dx}{dt} = f'(t) \qquad 2.22\text{-}8$$

We may now proceed to rearrange the above equations, to obtain the energy-conservation equation in terms of concentration and temperature only.

Firstly, the differential of the internal energy is found by substitution of equation 2.22-5 in 2.22-4 and differentiating to give:

$$dU = M\Sigma\left(\int_{T_R}^{T} C_{v_i}\, dT + U_{R_i}\right) d\sigma_i + M\Sigma\sigma_i\, C_{v_i}\, dT \qquad 2.22\text{-}9$$

Next, the work term for the system is given by:

$$dW = pdV \qquad 2.22\text{-}10$$

Since the volume V is xA_3, we may write dV as:

$$dV = A_3 f'(t)$$

and as the pressure may be expressed via equations 2.22-6, 2.22-3 and 2.22-7, we can rewrite equation 2.22-10 as:

$$dW = \frac{MRf'(t)T\Sigma(\sigma_i)}{f(t)} \qquad 2.22\text{-}11$$

We will show later in section 3.25 that it is possible to express dQ in terms involving temperature and concentration only.

By substituting equations 2.22-9 and 2.22-11 in equation 2.22-1 we have the energy-conservation equation in the following form:

$$\frac{MRf'(t)T\Sigma(\sigma_i)}{f(t)} + M\Sigma\left(\int_{T_R}^{T} C_{v_i}\, dT + U_{R_i}\right)\frac{d\sigma_i}{dt} + M\Sigma(C_{v_i}\sigma_i)\frac{dT}{dt} - \frac{dQ}{dt} = 0. \qquad 2.22\text{-}12$$

b) Chemical-kinetic equations.

i) The reaction-rate expressions.

Let g be the total number of reactants of species S_i, and h be the total number of products of the j^{th} chemical reaction.

This general reaction may be written as:

$$\sum_{i=1}^{g} \alpha_{ijr} S_i \rightleftarrows \sum_{i=1}^{h} \alpha_{ijp} S_i \qquad 2.22\text{-}13$$

where α_{ijr} and α_{ijp} are the stoichiometric coefficients of the reactants and products respectively.

The forward-reaction rate for the j^{th} reaction is given by:

$$\dot{m}'''_{jf} = k_{jf} \rho^{g} \prod_{i=1}^{g} (\sigma_i) \qquad 2.22\text{-}14$$

where the rate constant k_{jf} is of the form:

$$k_{jf} = A_j T^{B_j} e^{-E_j/RT} \qquad 2.22\text{-}15$$

A_j, B_j and E_j are constants for each reaction.

The backward rate-constant is related to the forward by the equilibrium constant K_{cj}:

$$k_{jb} = k_{jf}/K_{cj} \qquad 2.22\text{-}16$$

The concentration-based constant is related to the pressure-based equilibrium-constant K_{pj} by:

$$K_{cj} = K_{pj} (RT)^{\left[\sum_{i=1}^{h} (\alpha_{ijp}) - \sum_{i=1}^{g} (\alpha_{ijr})\right]} \qquad 2.22\text{-}17$$

The net-reaction rate, the summation of the forward and backward rates, is:

$$\dot{m}'''_{j} = k_{jf} \rho^{g} \cdot \prod_{i=1}^{g} (\sigma_i) - k_{jb} \rho^{h} \cdot \prod_{i=1}^{h} (\sigma_i) \qquad 2.22\text{-}18$$

For the reactions of termolecular order, the mass of the third body, M, is taken as 1, and its molecular weight is taken as the mean molecular-weight. Thus its concentration may be found from:

$$\sigma_M = \frac{1}{W_M} = \Sigma\sigma_i \quad . \qquad 2.22\text{-}19$$

ii) The equations for species continuity.

Suppose that the total number of species considered is n, of which the first n_a are atomic. The net formation of i^{th} molecular species is given by the equation of molecular continuity:

$$\rho \frac{d\sigma_i}{dt} = - \left[\sum_{j=1}^{N} (\alpha_{ijr} \dot{m}_j''' - \alpha_{ijp} \dot{m}_j''') \right] \qquad 2.22\text{-}20$$

for $i = n_a+1, n$.

Now, if in the q^{th} molecular species there are B_{iq} atoms of species i, atomic continuity is given by:

$$\frac{m_i}{W_{A_i}} = \sigma_i + \sum_{q=n_a+1}^{n} (B_{iq}\sigma_q) \quad . \qquad 2.22\text{-}21$$

This, when differentiated, with respect to time, is:

$$\frac{d\sigma_i}{dt} = - \sum_{q=n_a+1}^{n} (B_{iq} \frac{d\sigma_q}{dt}) \quad . \qquad 2.22\text{-}22$$

This completes the mathematical description of the problem.

2.23 Summary of the problem

a) The equations to be solved

The equations to be solved have been reviewed, they consist of n+1, simultaneous, non-linear, ordinary-differential equations.

From thermodynamics we have one equation for the conservation of energy (2.22-12). The remaining n equations express the kinetics of the chemical reaction; n_a describe atomic continuity (2.22-22) and $n-n_a$ describe the molecular continuity (2.22-20).

Now we can proceed to the task of reducing the differential equations to algebraic ones; then, with the aid of the digital computer we may descend to arithmetic and provide numerical solutions. In the next section 2.3, the process of reducing the equations will be described.

b) The input information

Before we may proceed from algebraic to arithmetic solutions we shall require input data with which we may obtain our goal, the numerical predictions. From an examination of the differential equations it is plain to see what this data is.

In the energy equation (2.22-12), the following information is required:

1. for the work term, the first term; a relation for the piston displacement with time. That is, a prescribed density-time variation.

2. for the combustion-energy term, the second term; the specific heats and heats of formation of each constituent species.

3. for the fourth term; an expression for the rate of heat transfer.

The kinetic data required in the species continuity equations (2.22-20 and 2.22-22) are:

1. a set of elementary reaction-steps to describe the transformation of reactants to combustion products.

2. the rate constants of each reaction.

3. the equilibrium constant of each reaction.

Last, we shall require the boundary conditions for all the variables at the initiation of the integration procedure.

How this information is obtained is the province of Chapter 3. The immediate task is the reduction of the differential equations to algebraic ones.

2.3 The Method of Solution

2.31 The task

In section 2.2 it was shown that, in a system subjected to a prescribed density-time variation, chemical reaction is governed by the differential equations, 2.22-12, 2.22-20 and 2.22-22, together with the boundary conditions for all the variables and auxiliary thermodynamic, heat-transfer and chemical-kinetic relations. Solution of the equations will yield the time variation of the dependent variables, σ_i, p, T etc.

The task of the present section is to derive a solution procedure for the mathematical problem. Because of the number and non-linearity of the equations an exact solution is not possible. The solution procedure must be a numerical one; the main elements of its derivation are: 1. the reduction of the differential equations to a set of simultaneous, algebraic finite-difference equations; 2. the recasting of the equations into a suitable form for solution by an iterative, successive-substitution technique and 3. the outline of the iterative-solution procedure.

The solution procedure arrived at should have the following desirable properties:

1. Accuracy. The algebraic equations represent approximations to the differential equations. There will, in general, be a difference between the convergent solutions of the former and the exact solutions of the latter. The difference is termed the trunca-

tion error, and an attempt will be made to keep this as small as possible.

2. Convergence. Convergence is the property of an iterative method of solving a set of simultaneous-algebraic equations to proceed in a regular fashion towards their solution. A satisfactory method must be convergent under all circumstances, and must converge rapidly so that the method is not time consuming.

2.32 Possible solution procedures

There are two ways of deriving finite-difference equations from differential ones: by way of Taylor-series expansions; and by integration over finite periods of time, together with assumptions about the behaviour of the variables over this period of time. The second method has been adopted because of practical difficulties with the first: the determination of the derivatives of the functions to be integrated.

Once the algebraic equations have been derived, a procedure has to be developed for solving them. When the equations are few in number and linear, or may be linearised, standard matrix-inversion techniques may be used. Momtchlioff et al. [38.], for example, used a Runge-Kutta integration procedure and matrix inversion to solve the steady-flow reaction problem outlined in section 2.12. However, because the equations of the present analysis are numerous (up to 10) and the energy equation (2.22-12) is highly non-linear, successive-substitution techniques are employed.* In these, initial guesses for the values of the variables are substituted into successive-

---

* The wisdom of this decision is now questionable. Wolfshtein [60.] showed that the equations may be recast. He outlined a Runge-Kutta procedure for their solution. As yet (1968) the relative merits of the two procedures have not been compared.

substitution formulae which have been derived from the algebraic equations, and new values are computed; then these values are used as new guesses and so on.

Not all iterative schemes converge infallibly to the solution. The conditions for the convergence of linear equations have been established.* The conditions for convergence of non-linear equations are complex and difficult to establish. Thus, as we proceed, we must realise that convergence may not always be obtained, and be prepared to modify the procedure to obtain convergence.

Having indicated the outline of the successive-substitution procedure we will now proceed to the details, and show that two methods are used. Which of the two methods is used is dependent upon the rapidity of convergence of the simpler procedure.

2.33 The solution of the finite-difference equations

a) The reduction of the equations

We have chosen to integrate the differential equations over a finite period of time, Δt. If Δt is small enough then we may assume the values, at the beginning of the step at time t, exist throughout the step (as in Euler's method). However, if larger increments are taken and increased truncation error is to be avoided, we must make a better assumption for the values of the variables during the step. We shall assume that the variables take the mean of their values at the beginning and end of the step. That is:

$$\left.\begin{aligned} T &= T + \Delta T/2 \\ \text{and} \quad \sigma_i &= \sigma_i + \Delta\sigma_i/2 \end{aligned}\right\} \qquad 2.33\text{-}1$$

where ΔT and $\Delta\sigma_i$ are the incremental values of temperature and

---

* See, for example Verga [57.].

concentration respectively.

Thus, for example, the energy equation (2.22-12) when rearranged becomes:

$$\Delta T = [\Delta Q - \frac{f'(t)(T + \frac{\Delta T}{2})\Sigma(\sigma_i + \frac{\Delta\sigma_i}{2})\,\Delta t}{f(t)}$$

$$- \Sigma(\int_{T_R}^{T} C_{v_i}\, dT + U_{R_i})\Delta\sigma_i] \;\; \Sigma(C_{v_i}(\sigma_i + \frac{\Delta\sigma_i}{2}) \qquad 2.33\text{-}2$$

Although the assumption of equation 3.33-1 permits an increase in the size of the time step, Δt, and thus a reduction in the number of steps to cover the entire period of integration, there is a penalty to pay: the incremental values now appear on the right-hand side of equation 2.33-2 and in the finite-difference forms[+] of the continuity equations obtained from 2.22-20 and 2.22-22. The penalty is not a light one, as the degree of the continuity equations for those species involved in termolecular reactions will be raised from first to third. Thus we will now be faced with the solution of quadratic and frequently cubic simultaneous-equations to find the concentration increments over any time step.

b) The two iterative methods

Two procedures are used to solve, by iteration, the algebraic equations. The first method, denoted TYPE I, employs simple successive substitution; while for TYPE II the procedure is modified. The new value of the variable to be substituted in the equations is predicted from the previous substitution history. How the type of procedure is selected in described in (c).

[+] The simplicity of defining these equations does not warrant the space. They are obtained by substituting equation 2.33-1 into equation 2.22-15 through to 2.22-22.

The TYPE I method. Initial guesses are made for all the values of the incremental variables and then substituted into the finite difference equations from 2.22-20 and 2.22-22, and in 2.33-2. Evaluation of the equations leads to new values for the variables. If these values differ from those used in their computation then the new values are re-substituted, and so on, until agreement is obtained.

The TYPE II method. This method employs two modifications to the TYPE I procedure:

i) Solutions to the continuity equations and energy equation are obtained successively instead of simultaneously. For a given ΔT, the values of $\Delta\sigma_i$ may be found from the continuity equations alone. Knowing the $\Delta\sigma_i$ values we may solve the energy equation, 2.33-2, to obtain a better value of ΔT with which to solve the continuity equations, and so on.

ii) To obtain rapid convergence in this two-stage procedure, a Newton-Raphson prediction is employed to modify the values to be substituted into the equations. The algebraic equations must be slightly recast to effect the prediction.

Suppose any one of the arguments of temperature or concentration increments are represented by Δy. At time t, the appropriate energy or species continuity equation defines Δy_n, the value of Δy in the n^{th} iteration, and is of the form

$$\Delta y_n = f(\Delta y, \sigma_i, T, \ldots)_{n-1} \quad . \qquad 2.33\text{-}3$$

We define f(y) as:

$$f(y)_n = \Delta y_n - f(\Delta y, \sigma_i, T, \ldots)_n \quad . \qquad 2.33\text{-}4$$

The equation which $f(\Delta y, \ldots)$ represents will be satisfied when

$$f(y)_n = 0 \quad . \qquad 2.33\text{-}5$$

The Newton-Raphson predictor [38.] for predicting the n^{th} interative value of Δy is:

$$\Delta y_n = \Delta y_{n-1} - f(y)_{n-1} \cdot \frac{\Delta y_{n-1} - \Delta y_{n-2}}{f(y)_{n-1} - f(y)_{n-2}} \qquad 2.33\text{-}6$$

The values for $f(y)_{n-1}$ and $f(y)_{n-2}$ will already have been calculated in the two previous iterations.

c) The combined solution procedure

How the two iterative solution procedures are combined and initiated is illustrated by the flow chart, figure 2.33-1. When the time interval for integration has been set, a decision is made as to the likelihood of the TYPE I procedure converging rapidly. This decision is based on the convergence history over the previous time steps.* If TYPE I procedure is adopted, then the first guesses are given by:

$$\Delta y_1 = \Delta y^1 \qquad 2.33\text{-}7$$

where Δy^1 was the value at convergence over the previous time increment.+

The TYPE II procedure requires two values, Δy_1 and Δy_2, before the Newton-Raphson prediction can be used. As may be seen in the flow chart the values ascribed to these are:

$$\left.\begin{aligned} \Delta y_1 &= \Delta y^1 \\ \Delta y_2 &= .95\ \Delta y^1 \end{aligned}\right\} \text{ for all } y \qquad 2.33\text{-}8$$

at the commencement of iteration over a new time step. Similarly,

---

* The details of the decision-making flow-process may be found in the description of the computer programme, in Appendix A.

+ It will be shown in Appendix A that the time increment is itself adjustable and Δy^1 will have to be modified accordingly.

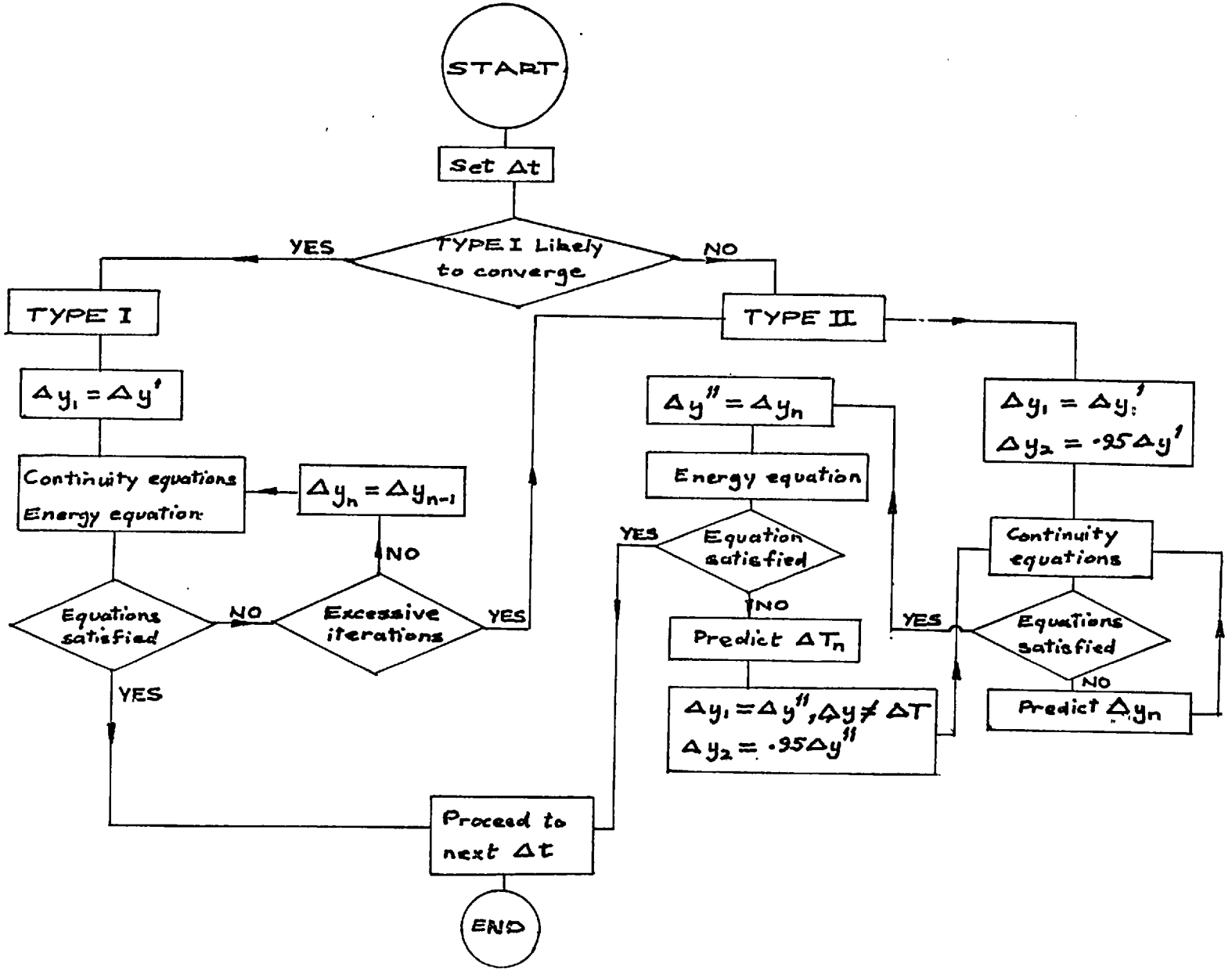

Fig 2.33-1 Flow Chart for Iteration Procedures

prior to each subsequent iteration of the continuity equations Δy_1 and Δy_2 are defined as:

$$\left.\begin{aligned} \Delta y_1 &= \Delta y'' \\ \Delta y_2 &= .95\ \Delta y'' \end{aligned}\right\} \quad y \neq \Delta T \qquad 2.33\text{-}9$$

where $\Delta y''$ was the value at convergence for the previous value of ΔT.

The two iteration procedures have now been outlined. It is apparent that the TYPE II procedure could be used at all times, but because in practice its execution time is about twice that of TYPE I, it is worthwhile to run the two procedures in parallel. To generalise, the TYPE I procedure is successful during the early compression and late expansion processes, away from the ignition zone where the large rates of reaction give rise to divergence.

2.4 Closure

In the present chapter, differential equations were deduced to describe the process occurring in a reacting system and then the equations were reduced to algebraic form. The chapter ended with a means of solving them. Now, we may descend from the algebra to arithmetic and, with the aid of the digital computer, predict the solutions to particular problems in terms of numbers. The computer programme written to execute the predictions may be found in Appendix A. It was clear from the differential equations that to obtain the numerical solutions input data would be required: boundary conditions, heat-transfer, thermodynamic and chemical-kinetic data. It has been necessary to establish much of this data from experiment or by statistical methods because available values are either inconsistent or imprecise. How this was done is the topic of the next chapter.

CHAPTER 3

AUXILIARY INPUT DATA

3.1 Introduction

3.11 The input data examined

This chapter describes the input data which permits, when combined with the numerical procedure evolved in Chapter 2, the prediction of the progress of reaction in the compression-machine system. It became clear in the derivation of the differential equations (section 2.2) what input data was required.

The data flow chart, fig 2.11-1, summarises this data and shows where it is used in the equations. Here we shall describe how the data is obtained.

The need to devote a chapter to describing input data arises mainly from difficulties in obtaining adequate chemical-kinetic and heat-transfer data: Although in the literature there is an abundance of kinetic data for the H_2-O_2 reaction, there exists no single reaction model with a consistent set of reaction rates which is applicable to the range of temperature and pressure encountered in the experimental-autoignition tests. Many equations have been formulated for predicting gas-wall heat-transfer in piston engines, but we shall discover that none of the existing procedures accurately predicted the heat-transfer observed in the compression machine.

We shall examine alternative kinetic models and select a representative model on the basis of the available evidence. The reaction-rate literature will be studied and mean reaction-rates obtained by statistical methods. Accurate prediction of heat transfer will be achieved by correlating the observed values by dimensional analysis.

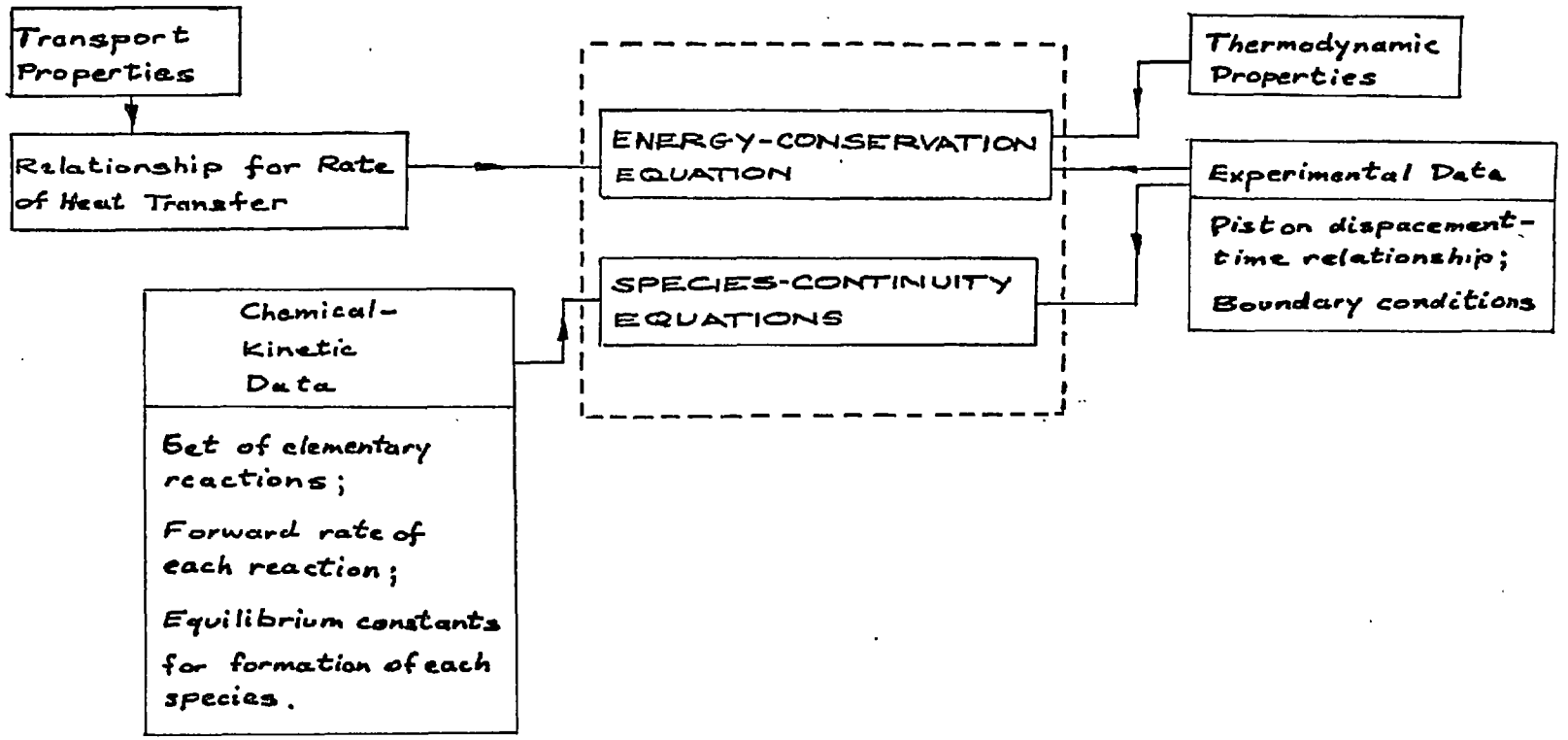

Fig 2.11-1 Data Flow Chart

Frequently throughout this chapter we shall call upon tabulated data: equilibrium constants, thermodynamic properties etc. To avoid interpolation between tabulated values we will fit the data to suitable expressions.

At the end of the chapter, we will review the data required from the present experimental tests.

3.2 The Equation for the Rate of Heat Transfer

3.21 The task

It was in the equation for the energy conservation (2.22-1) that we introduced the term to describe heat transfer from the gas to the wall boundary of the system. The object of this section is to obtain an equation to describe this term as a function of known or measured quantities. In doing so we shall need to pre-suppose knowledge of the experimental results, in the form of pressure- and volume-time histories of the compression in the apparatus of non-reacting air charges.

The first conclusion, drawn from the experimental measurements, is that the gas-wall heat-transfer is not negligible. In a typical test the observed peak-pressure was 10% less than the adiabatic pressure calculated at the same cylinder volume. We cannot therefore assume $\frac{dQ}{dt} = 0$ and we must proceed to find a relation which predicts the observed pressure-time histories.

3.22 The importance of conductive heat-transfer

It is likely that all three heat-transfer mechanisms: conduction, convection and radiation; have a role in the heat-transfer process. A preliminary assessment was made to establish that in

the compression machine, as in conventional piston-engines, the role of conduction in the heat-transfer process was not important. For this reason a simplified conduction model was examined. The decay of temperature with time was calculated* for an air charge in the cylinder. It was assumed that the initial temperature, pressure and cylinder-configuration corresponded to the conditions which would exist at the end of a representative compression-stroke. Thus the decay of temperature was calculated under conditions when the rate of heat transfer would be a maximum. With this maximum rate of heat transfer for the entire duration of the compression stroke the spatial-average loss of temperature corresponded to less than half the difference between the adiabatic and observed temperatures. In a more realistic conduction model with the temperature varying with time, rising from the wall temperature to the final value, there would be less heat-transfer than in this worst-case calculation. It was therefore possible to proceed, confident that the role of conduction was not important in the present heat-transfer prediction.

3.23 Available expressions for predicting engine heat-transfer

Many equations have been proposed for predicting engine heat-transfer, but no one equation exists for predicting heat transfer for a wide range of engine configurations. Because engine heat-transfer is a transient phenomenon it is difficult to make accurate experimental measurements of heat-flux rates. Thus the constants in equations for predicting heat-transfer are frequently uncertain and lack the desired universal application.

The most notable equations for predicting heat-transfer are those due to Eichelberg [15.], Annand [1.] and Overbye et al. [40.].

---

* Using established methods for predicting temperature decay in solids. For example Carslaw and Jaegar [11.].

All three were used to predict pressure-time histories of air charges under the same conditions as experimental tests in the compression machine. Comparison between observed- and predicted-pressure histories demonstrated that none of the three expressions accurately predicted the observed results. Milkins [37.], a co-worker on the heat-transfer analysis, presents the details.

3.24 The path

Because the available equations had proved inadequate, an analysis of heat transfer in the compression machine was performed. Air charges were compressed in the compression machine* varying the volume ratio at the end of compression, but holding constant other parameters such as compression-stroke-time; starting pressures and temperatures; and wall surface-temperatures. Pressure- and volume-time records from these tests were analysed by the method which is presented in Appendix B. In general terms, this method compares, over a small time increment, the actual and adiabatic pressure developments. The difference between the two is attributed to heat transfer. Thus heat-flux rates and overall surface-heat-transfer coefficient may be calculated.

The results of the analysis will now be presented and then we shall show how they have been correlated to provide a single equation for predicting the observed heat-transfer.

3.25 Analysis of results

Fig 3.25-1 shows the typical variation with time of the surface-heat-transfer coefficient at three compression ratios. Two features of the curves are worthy of note: 1. the peak values of the coefficient increases with increasing compression ratio; 2. all the

---

* See section 5.12.

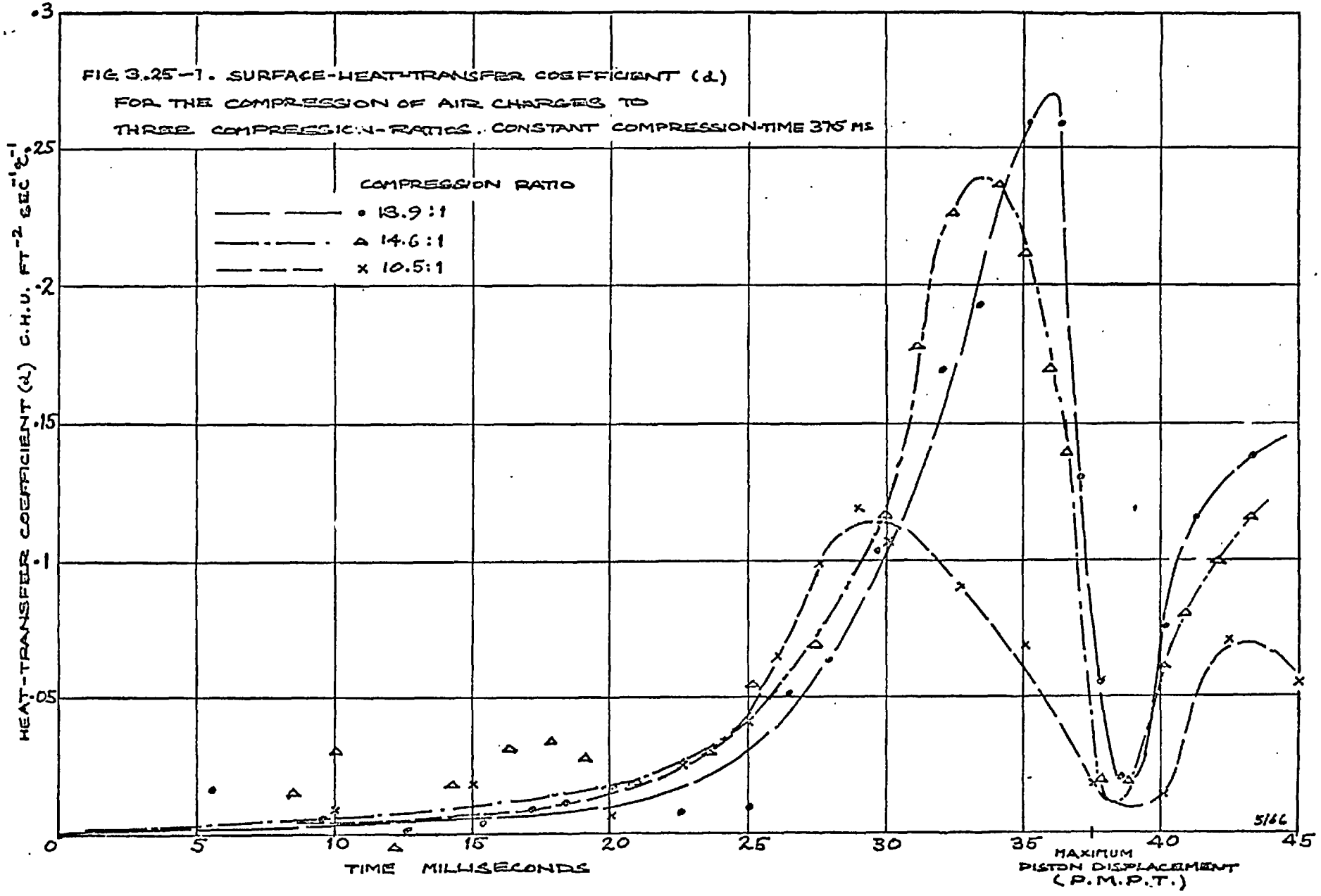
FIG. 3.25-1. SURFACE-HEAT-TRANSFER COEFFICIENT (d)
FOR THE COMPRESSION OF AIR CHARGES TO
THREE COMPRESSION-RATIOS. CONSTANT COMPRESSION-TIME 375 MS
COMPRESSION RATIO
• 13.9 : 1
△ 14.6 : 1
× 10.5 : 1
HEAT-TRANSFER COEFFICIENT (d) C.H.U. FT⁻² SEC⁻¹ ℃⁻¹
·3
·25
·2
·15
·1
·05
0
5
10
15
20
25
30
35
40
45
TIME MILLISECONDS
MAXIMUM PISTON DISPLACEMENT (P.M.P.T.)
5/16

curves exhibit minimum values shortly after the point of maximum piston-travel, here after referred to as P.M.P.T. We shall, in the light of the method used to correlate these curves and further evidence, be able to offer reasons for these two features in section 3.27.

There is reasonable agreement between current measurements of the heat-transfer coefficients and that of other workers. For example, Annand [1.] deduced from Elser's data [17.] that during compression and prior to ignition the maximum value of apparent-heat-transfer coefficient was .075 Chu $ft^{-2}s^{-1}$ at a compression ratio of 12.8.1. This is about 60% of the present measurement. The difference is probably accounted for by the influence on convection of the different stroke-bore ratios in the engine and the compression machine.

In order to correlate the results over a range of compression ratios, dimensional analysis of the convection within the system has been performed. The relative triviality of conduction has been established in 3.22 and radiation has, for the present, been ignored because of the low temperatures of the compressed gas. The dimensional analysis showed that the parameters affecting convective heat-transfer may be grouped in the following way:-

$$Nu = f(Re, Pr, r \ldots) \qquad 3.25\text{-}1$$

where Nu is the Nusselt number

Re is the Reynolds number

Pr is the Prandtl number

and r is the compression ratio.

Over the considered temperature range, the Prandtl number for air is constant within 5%. The variable length x in the compression-ratio may be incorporated into Re and Nu as the length dimension.

Thus we may express equation 3.25-1 as:-

$$Nu = f(Re)$$

$$\text{or} \quad \frac{\alpha x}{k} = f\left(\frac{\rho v x}{\mu}\right) \qquad 3.25\text{-}2$$

where α is the heat-transfer coefficient

k is the spatial-mean thermal-conductivity of the gas

ρ is the density

v is velocity = dx/dt

and μ is the spatial-mean viscosity of the gas.

Clearly, the choice of piston velocity for the velocity term in the Reynolds number is arbitrary. As has been pointed out by Knight [33.] this term should represent the velocity of that part of the gas by which heat is convected from the bulk to the walls. Since we have at present no measurement of the gas velocity, we shall assume that there exists some relation between it and the piston velocity, which will be accounted for in the coefficients of equation 3.25-2.

For the three results of fig 3.25-1 the Nusselt and Reynolds numbers have been plotted on a log basis in fig 3.25-2. This shows that during the compression stroke, as soon as the heat-transfer coefficient becomes significant (i.e. beyond 20 ms) a straight line correlation exists, given by

$$Nu = .97\ Re^{.66} \qquad 3.25\text{-}3$$

3.26 The final equation

The range of applicability of equation 3.25-3 was tested by predicting pressure records, using the main computer programme (Appendix A), and comparing the results with those observed experi-

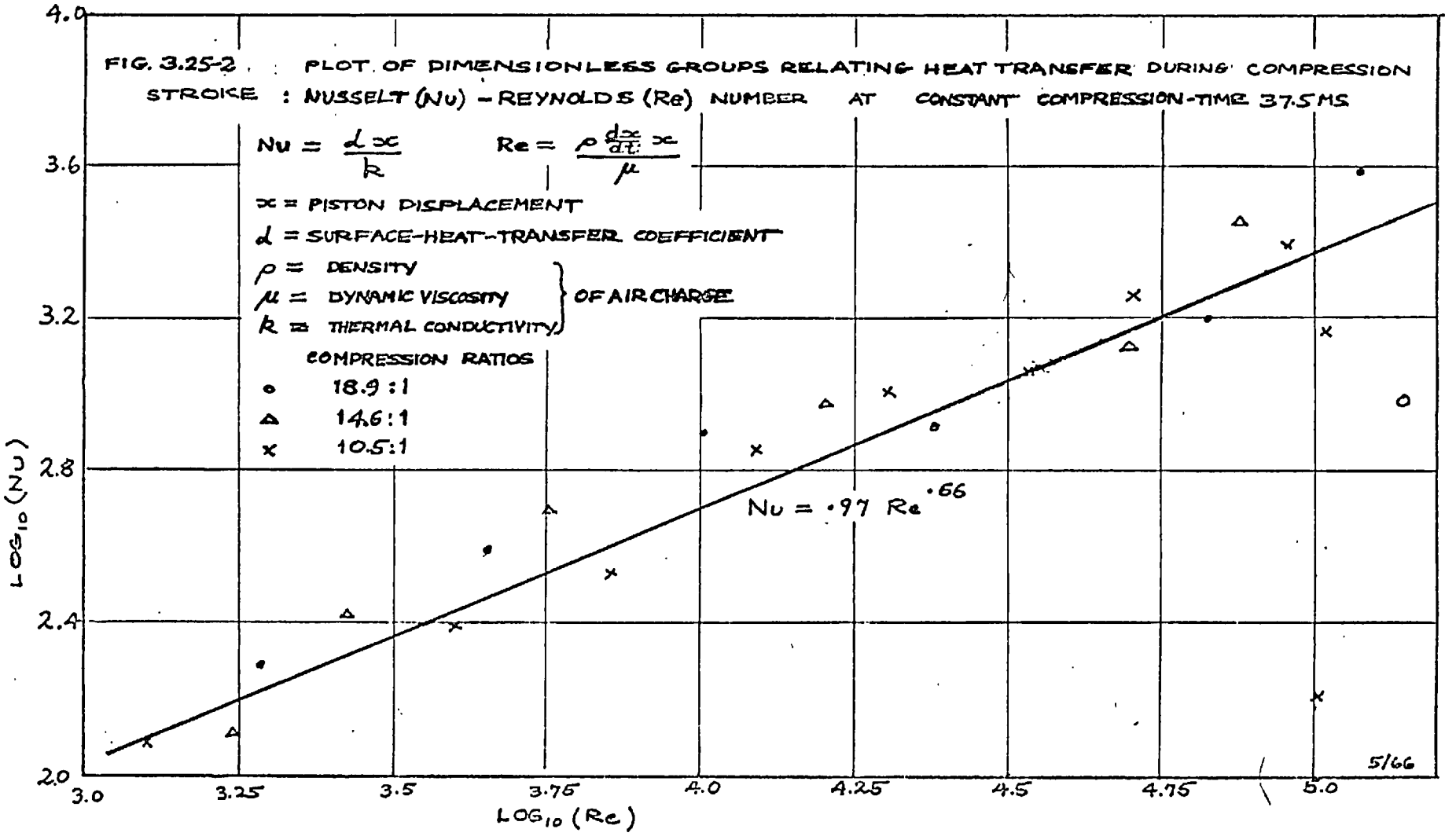
FIG. 3.25-2 : PLOT OF DIMENSIONLESS GROUPS RELATING HEAT TRANSFER DURING COMPRESSION STROKE : NUSSELT (Nu) – REYNOLDS (Re) NUMBER AT CONSTANT COMPRESSION-TIME 37.5 MS
Nu = $\frac{\alpha x}{k}$ Re = $\frac{\rho \frac{dx}{dt} x}{\mu}$
x = PISTON DISPLACEMENT
α = SURFACE-HEAT-TRANSFER COEFFICIENT
ρ = DENSITY
μ = DYNAMIC VISCOSITY } OF AIR CHARGE
k = THERMAL CONDUCTIVITY
COMPRESSION RATIOS
18.9 : 1
14.6 : 1
10.5 : 1
Nu = .97 Re^.66
5/66
LOG10 (Nu)
LOG10 (Re)
4.0
3.6
3.2
2.8
2.4
2.0
3.0
3.25
3.5
3.75
4.0
4.25
4.5
4.75
5.0

mentally. The comparisons showed that predictions were within $\pm$ 5. lbf in^{-2} of the experimental values. Adjusting the proportionality constant of equation 3.25-3 to .93 gave better agreement, $\pm$ 2.5 lbf in^{-2} over the entire duration of the tests. See for example fig 3.26-1. Thus the final equation for predicting heat-transfer is:

$$Nu = .93\ Re^{.66} \quad . \qquad 3.26\text{-}1.$$

3.27 Concluding discussion

Plainly, equation 3.26-1 predicts zero heat-transfer when the Reynolds number is zero at the point of maximum piston-travel. There are two reasons why this does not lead to erroneous predictions: 1.) at maximum stroke the heat-transfer coefficient is small (see fig 3.25-1); 2.) the duration of small Reynolds number is short, for example, for the test shown in fig 3.26-1 the Reynolds number is less than 10^3 for only 0.2 ms.

We have shown that it is possible to relate Nusselt and Reynolds numbers, thus implying that forced convection takes place within the cylinder. A transparent model of the piston and cylinder was made and the air motion within the cylinder was recorded, during compression and expansion, by photographing a tracer suspended in the gas. These experiments are reported in Appendix E. The results showed that during compression a toroidal vortex pattern of recirculating flow was set up. When the direction of piston motion was reversed, expanding the charge, the direction of the recirculating flow was reversed.

These results enable us to explain the shape of the heat-transfer coefficient curves of fig 3.25-1. The small coefficients around P.M.P.T. correspond to the relatively quiescent period when the flow

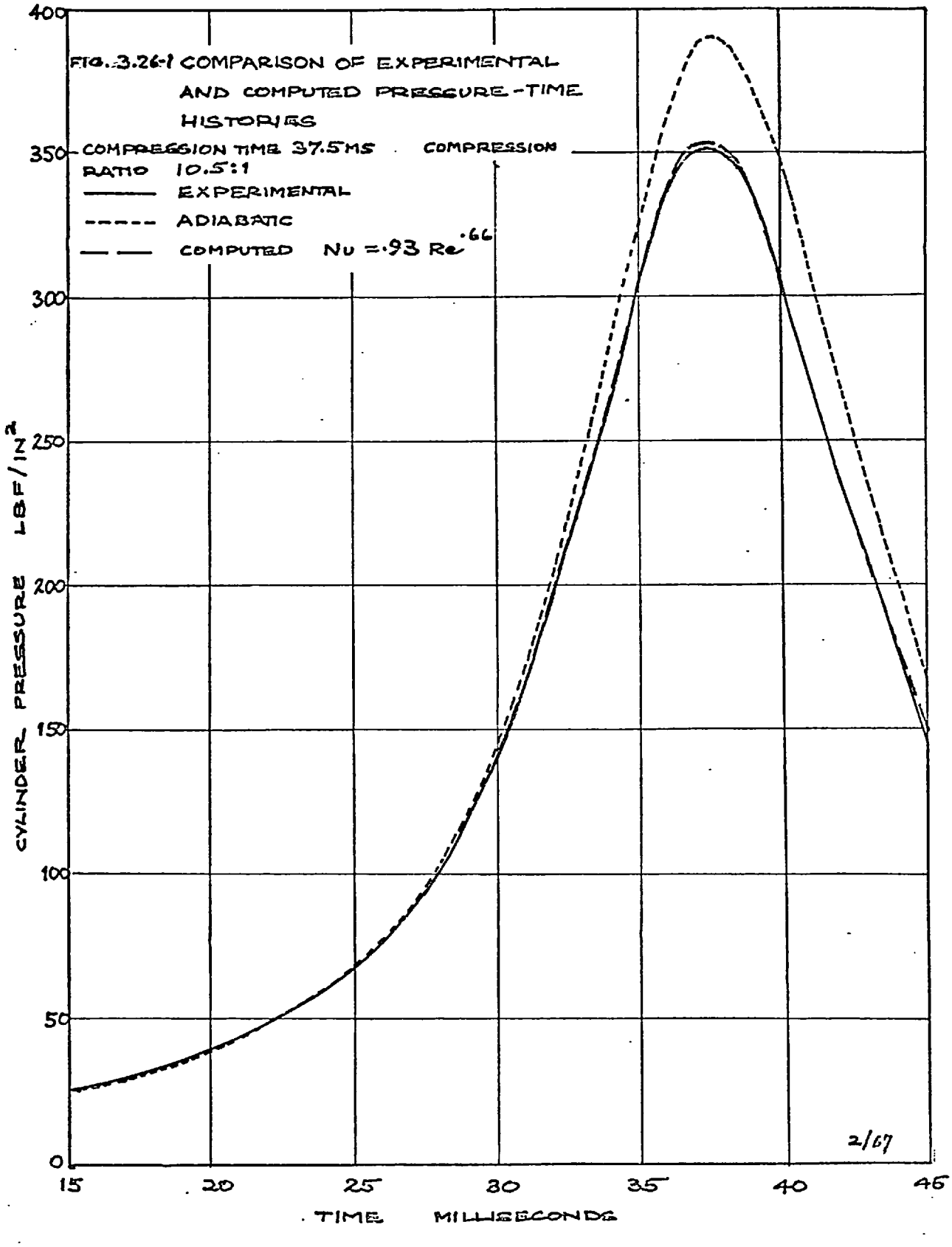
FIG. 3.26-1 COMPARISON OF EXPERIMENTAL AND COMPUTED PRESSURE-TIME HISTORIES
COMPRESSION TIME 37.5MS COMPRESSION RATIO 10.5:1
EXPERIMENTAL
ADIABATIC
COMPUTED Nu = .93 Re^.66
CYLINDER PRESSURE LBF/IN²
TIME MILLISECONDS
2/67
0
50
100
150
200
250
300
350
400
15
20
25
30
35
40
46

pattern in the cylinder is reversing. The increase in peak coefficient, with increasing compression-rates, indicates increased convection within the cylinder as the piston speed increases.

But the most important deduction that we can make from the flow study is that considerable mixing takes place in the period before P.M.P.T. Later, we will show in section 6.12 that this period is critical in that there are reasons for predicting autoignition records in which ignition occurs just before or at P.M.P.T. For these predictions, we may now justify the mixing assumption made in deriving the predicting equations (see section 2.21) that there was no spatial variation in the thermodynamic properties of the reactant-gas charge.

3.3 Thermodynamic and Transport Properties

3.31 The data required

It has been shown in section 2.23 that we needed the molar specific heat of each species to calculate the total energy of the system, representing the third term of the energy equation, 2.22-12. From the preceeding section we saw that the last term of that equation - the heat-transfer contribution; could be predicted from knowledge of the system properties, including the spatial-mean viscosity and thermal-conductivity of the fluid. These then are the thermodynamic and transport properties which we should specify.

3.32 The molar-specific-heat

The JANAF tables [25.] record the molar-specific-heats as functions of temperature for all the common gases. A computer programme has been written to fit these data to polynomial expressions of temperature and the results have been reported* for the coefficients

---

* Karim and Watson [30.].

of polynomials of orders 3 to 9. Extracted from these results, in table 3.31-1, are the coefficients of the optimum orders (i.e. with minimum fitting-error), for the temperature range 300-3000°K.

The polynomial expressions not only enable rapid calculation, in the computer, of specific heats, thus avoiding interpolating routines, but also permit the rapid evaluation of the coefficient of a polynomial representing the internal energy of the mean composition of a mixture of gases. The procedure is to multiply the polynomial coefficients of each species by the concentration of that species. The proportionated ccefficients of the same order are summated, yielding polynomial coefficients which, at the particular temperature, may then be evaluated for the mean-mixture specific-heat or integrated, before evaluation, for the mean-mixture internal-energy.

3.33 Thermal conductivity and viscosity of the fluid

Temperature explicit expressions for both air and argon*, for both these properties, have been reported by Hilsenrath et al. [23.]. Although similar data is available for H_2, O_2 and H_2O, that of the other reacting species is not readily available. Moreover, to find the values for the mean-mixture composition is a complex procedure.+ Because of this and two more reasons: 1. the heat-transfer equation uses constants derived from tests in the machine and therefore errors will tend to cancel. 2. heat transfer rarely represents more than 18% of the system energy; the policy adopted has been to use only the viscosity and thermal conductivity of the largest component in the gaseous mixture. In practice, the satisfactory prediction of the pressure development, prior

---

* The diluent used in the hydrogen autoignition tests.

\+ See, for example Reid and Sherwood [44.].

TABLE 3.33-1 COEFFICIENTS OF OPTIMISED-ORDER POLYNOMIAL EXPRESSIONS FOR MOLAR SPECIFIC-HEAT CALS $(GM.MOL)^{-1}\ {}^{\circ}K^{-1}$

Fitted Temperature Range 300-3000°K

$$C_p = \sum_{j=1}^{n+1} C_j T^{j-1}$$

where C_p molar specific-heat at constant pressure
C coefficient
j coefficient no.
n order of polynomial
T temperature °K

Species Number	Species	α_1	α_2	α_3	α_4	α_5	α_6	α_7	Max % Error & Location	Maximum Numerical Error & Location
1	H_2	0.67717E01	0.75962E-03	-0.13791E-05	0.164-15E-08	-0.65103E-12	0.84921E-16		0.442 (400°K)	0.03081 (400°K)
2	O_2	0.63698E01	0.17998E-02	0.15815E-05	-0.21810E-08	0.85804E-12	-0.11137E-15		0.416 (900°K)	0.0314 (900°K)
3	N_2	0.70807E01	-0.18787E-02	0.54419E-05	-0.38815E-08	0.11679E-11	-0.12910E-15		-.270 (600°K)	-.01948 (600°K)
4	H	0.49680E01								
5	O	0.56794E01	-0.21957E-02	0.27335E-05	-0.16397E-08	0.46886E-12	-0.15100E-16		-0.194 (400°K)	-0.01007 (400°K)
6	N	0.49692E01	-0.57129E-05	0.78368E-08	-0.25396E-11	-0.13827E-14	0.69541E-18		0.002 (600°K)	0.00010 (600°K)
7	OH	0.77485E01	-0.32194E-02	0.46180E-05	-0.22728E-08	0.50157E-12	-0.41704E-16		0.147 ((400°K)	0.10420 (400°K)
8	NO	0.71946E01	-0.17124E-02	0.59265E-05	-0.46178E-08	0.14826E-11	-0.17222E-15		-0.579 (400°K)	-0.41479 (400°K)
9	H_2O	0.79526E01	-0.12299E-02	0.58635E-05	-0.35407E-08	0.89235E-12	-0.84303E-16		-0.099 (400°K)	-0.00815 (400°K)
10	HO_2	0.60279E01	0.90143E-02	-0.48245E-05	0.12889E-08	-0.13645E-12			-0.378 (400°K)	-.03373 (400°K)
11	H_2O_2	0.32546E01	0.351283E-01	-0.48991E-04	0.4021E-07	-0.18851E-10	0.47744E-14	-0.52856E-18	0.034 (700°K)	0.00470 (700°K)

to ignition, in all the tests is the justification of the policy.

3.4 Chemical-kinetic data

3.41 The task

Firstly the task is to specify a set of elementary reactions which describe the oxidation of hydrogen to its products of combustion. Then secondly, to obtain the rates of each reaction and their temperature dependence. As we have shown in the analysis (equation 2.22-15) it is usual to express these rate constants by the Arrhenius equation. We may describe our second task more specifically as: to define the three constants A_j, B_j and E_j of the Arrhenius equation for each reaction.

The task is not an easy one. Although many workers have researched into the kinetic data of the hydrogen reaction, there is a diversity of opinion on the importance of individual reactions and there exist wide variations in reported values of the reaction rates. The reason for this is plain; it is not possible to examine experimentally each reaction in turn and measure the rate and temperature dependence with which it proceeds from reactants to products; in practice one must always examine the simultaneous progress of many reactions, and the values calculated for any one will be dependent upon those given to the others.

Nonetheless, we must endeavour to find as simple a scheme of reactions as possible, out of the 50 or more plausible reactions up to termolecular order; including only those which actively participate in the progress of the overall reaction, and thus influence the numerical predictions. Simplicity of the scheme will speed the computation of the predictions we make, and also give us hope that some day we may be

able to predict the reaction of more complex fuels in which the hydrogen reaction is but a part.

3.42 The possible reaction scheme

Some of the important species participating in the hydrogen reaction are H_2, O_2, H, O, OH and H_2O. Further species which may also be formed are HO_2, H_2O_2 and O_3. For the first six species the only important bimolecular reactions are I, II, III, IV, IX and XXIV listed in table 3.42-1. These six reactions give rise to large numbers of radicals which can only be removed by recombination at the wall or by way of termolecular reactions. The former method is unlikely due to the time available for reaction being small compared to the diffusion time of the component species to the walls. Possible termolecular reactions are V, VI, VII, VIII and XXV.

For the additional species HO_2, H_2O_2 and O_3, the importance of reactions involving O_3 is most uncertain; while for HO_2 and H_2O_2 there are many known reactions. The HO_2 formation reaction is kinetically well established as an explanation of the second explosion limit* and the presence of H_2O_2 was established experimentally by absorption spectroscopy by Holt and Oldenberg [24.]. Thus we can suppose that although some HO_2 formed may be removed by reactions XI to XV, H_2O_2 will be formed by XVI or XX. Decomposition of H_2O_2 by reaction within the gas phase may take place by reaction XVII, XXVIII or IX.

3.43 The selected reaction scheme

For simplicity, we shall initially neglect the species HO_2, H_2O_2 and O_3. Of the eleven remaining reactions XXIV and XXV may

---

* See, for example Lewis and von Elbe [34.].

Table 3.42-1 Reaction System

$H_2 + OH \rightleftharpoons H_2O + H$	I
$H + O_2 \rightleftharpoons OH + O$	II
$H_2 + O \rightleftharpoons OH + H$	III
$H_2O + O \rightleftharpoons OH + OH$	IV
$H + OH + M \rightleftharpoons H_2O + M$	V
$O + O + M \rightleftharpoons O_2 + M$	VI
$H + H + M \rightleftharpoons H_2 + M$	VII
$O + H + M \rightleftharpoons OH + M$	VIII
$H_2 + O_2 \rightleftharpoons OH + OH$	IX
$H + O_2 + M \rightleftharpoons HO_2 + M$	X
$HO_2 + H \rightleftharpoons OH + OH$	XI
$HO_2 + O \rightleftharpoons OH + O_2$	XII
$HO_2 + OH \rightleftharpoons H_2O + O_2$	XIII
$HO_2 + H \rightleftharpoons H_2O + O$	XIV
$HO_2 + H \rightleftharpoons H_2 + O_2$	XV
$HO_2 + HO_2 \rightleftharpoons H_2O_2 + O_2$	XVI
$H_2O_2 + M \rightleftharpoons OH + OH + M$	XVII
$H + H_2O_2 \rightleftharpoons H_2O + OH$	XVIII
$OH + H_2O_2 \rightleftharpoons H_2O + HO_2$	XIX
$H_2 + HO_2 \rightleftharpoons H_2O_2 + H$	XX
$H_2 + O_2 \rightleftharpoons H_2O + O$	XXIV
$H_2 + O + M \rightleftharpoons H_2O + M$	XXV

dismissed because of their small (+ .9 K cal) and large (- 120.6 K cal) respective heats of formation and because they are 'spin-forbidden' reactions. We now have the same scheme of reactions as used by Jenkins et al. [26.]. Their results indicated that the reactor temperature was less responsive to changes in the rates of reactions VI to IX than to I to V. The latter five reactions were the scheme which we used at the outset of our prediction calculations. Later, many more reactions had to be added as we will show in Chapter 6.

3.44 The reaction-rate constants

A preliminary survey of the literature revealed a divergence of opinion amongst workers as to the representative values of the reaction-rate constants. The values obtained were dependent upon many factors such as: the type of experiment, the complexity of the reaction scheme used in the computation of the values, etc.

A detailed survey was made, making use of existing surveys* and personal research into the recent publications. The results are summarised and presented graphically in Appendix C. From the scattered values, plotted on the curves, specific values for the constants of the Arrhenius reaction-rate equation have been obtained by fitting the constants by the method of least squares.

It is possible that such a statistical method could, if the number of points to be fitted were few, lead to values for the constants which are inconsistent with theoretical considerations+, although representative of the available data. Mindful of this, we shall show in Chapter 6, that autoignition predictions were also

---

* References [5.], [35.] and [42.].

+ Again see Appendix C.

made from data derived in stirred reactor experiments [26.] but the predicted results did not differ substantially from those using the presently surveyed reaction-rate values.

3.45 The equilibrium constants

We saw in section 3.22b that, having established the forward reaction-rate constant, the backward rate constant could be obtained from the equilibrium constant by the relation 2.22-16. Tabulated values of the pressure-based equilibrium-constant are readily available in the JANAF tables [25.] at increments of 100°C. As we require the equilibrium constants as continuous functions of temperature we may avoid interpolation by fitting to an appropriate equation. It is easy to argue that both forward and backward rate constants may be expressed by the Arrhenius equation. Therefore, the equilibrium constant will also be represented by the same equation.

The fitting procedure and results have been reported elsewhere:* the conclusion drawn was that the general Arrhenius expression, with all three constants A, B and E optimised to fit the tabulated data, gave the best fitted curves - deviation between fitted and tabulated values was never worse than 1.75% over the temperature range 300-3000°K. The constants are tabulated later with the forward reaction rates of each reaction, in table 7.23-1.

3.5 The experimental data

We have now gathered together all the data necessary to begin our predictions except for the boundary conditions and the specification of the density-time relationship.

The boundary conditions: starting values of temperature, pressure and species concentrations; are specified from the experimental

---

* See Karim and Watson [30.].

conditions.

The density-time variation is less easy to specify. By analysis it is possible to obtain an equation for the motion of the compression piston in its cylinder. However, in Appendix F, a brief examination of the machine piston-motion, reveals that the frictional force is a complex function, probably of piston acceleration as well as static friction, so that the piston motion cannot be expressed reliably as an explicit function of time.

Instead, we shall in our computation use the experimentally-measured piston-displacements of the test whose pressure, temperature etc.we wish to predict.

Closure. This concludes the presentation of the data. We shall now describe the experimental apparatus and then experimental results which we may compare with those predicted by the procedure of Chapter 2 from the data of this chapter.

CHAPTER 4

THE EXPERIMENTAL APPARATUS

4.1 Introduction

4.11 Outline of the chapter

In the present chapter we shall describe, in outline, the novel compression-machine which has been constructed to comply with the demands of the theory in Chapter 2, and other specifications which give the apparatus a wide range of application to piston-engine research. The detailed description of the apparatus is given in Appendix D.

We shall describe how experimental measurements are made and what the precision of measurement is. Upon this precision depends the reliability of the chemical-kinetic data we shall establish in Chapter 7.

At the end of the present chapter, some of the merits of the apparatus are described in its application to the derivation of reaction kinetics from autoignition experiments and to the study of other problems related to piston-engine combustion research.

4.12 The task

The experimental task was to design, construct and develop an apparatus which could be used to study the compression to autoignition of reactant-gas mixtures. The measurements to be made in the apparatus were the variation of the gas volume and pressure with time.

The apparatus, to be consistent with the theory developed in the earlier chapters, should have the following desirable features:

1. it should be possible to determine accurately the pressure, temperature and composition of the gaseous charge prior to the compression process.

2. the charge should be free from contaminants, which may influence the kinetics of the reaction being studied, such as: lubricants or residual gases and solid deposits from earlier tests.

3. the volume path should be: continuously variable with time; adjustable; yet reproducible.

4. there should be no loss of charge from the system during the prescribed change in volume.

In addition, since the construction of the apparatus will be costly, both in labour and material, the apparatus should be versatile: its range application should not be restricted to our present needs only,but should be capable of extension to future studies of engine-related combustion-phenomena.

4.13 The path

A critical examination of existing apparatus revealed that no suitable machine existed which complied with the specification set out in the preceding section. Research piston-engines* were rejected because they did not comply with points 1., 2. and 3. In the alternative type of apparatus, rapid-compression machines, charges are rapidly compressed by a piston whose motion is such that the cylinder volume is reduced to a final fixed value. Thus they do not permit the production of a continuously varying density-time history (point 3.), which must be achieved if the process we are to study is to be representative of piston-engine combustion.

---

* Of the C.F.R. or Ricardo E6 type.

The solution lay in the design of a novel machine which complied with all the design requirements by combining the advantages of the research engine with those of rapid-compression machines: combining the continually-varying piston-motion of the former with the single-operating cycle of the latter. Such an apparatus has been called a 'slow-compression' machine.*

We shall now proceed to the description of this machine and its associated apparatus.

4.2 The Compression Machine

4.21 Its principles of operation

Fig.4.21-1 shows a schematic layout of the compression machine and its control systems.

The machine consists of a large double-ended cylinder containing a driving piston, from which two shafts extend through both ends of the cylinder. The lower shaft acts as the piston of the compression cylinder, while the upper shaft engages with a quick-release mechanism. With the mechanism engaged, high pressure air (100 to 700 lbf in^{-2}) is admitted to the driving chamber behind the driving piston. On release the pistons accelerate and pressure in the chamber in front of the driving piston increases from its starting value (4 to 40 lbf in^{-2}) retarding the motion and then returning the piston along its cylinder. Oscillatory motion continues until damped out by friction.

The piston motion, piston speed and compression ratio achieved on the first cycle may be varied by adjusting the pressures at piston release, and the volumes of the chambers on each side of the

---

* This term was coined by Spalding [50]. We have throughout the text abbreviated it to 'compression' machine.

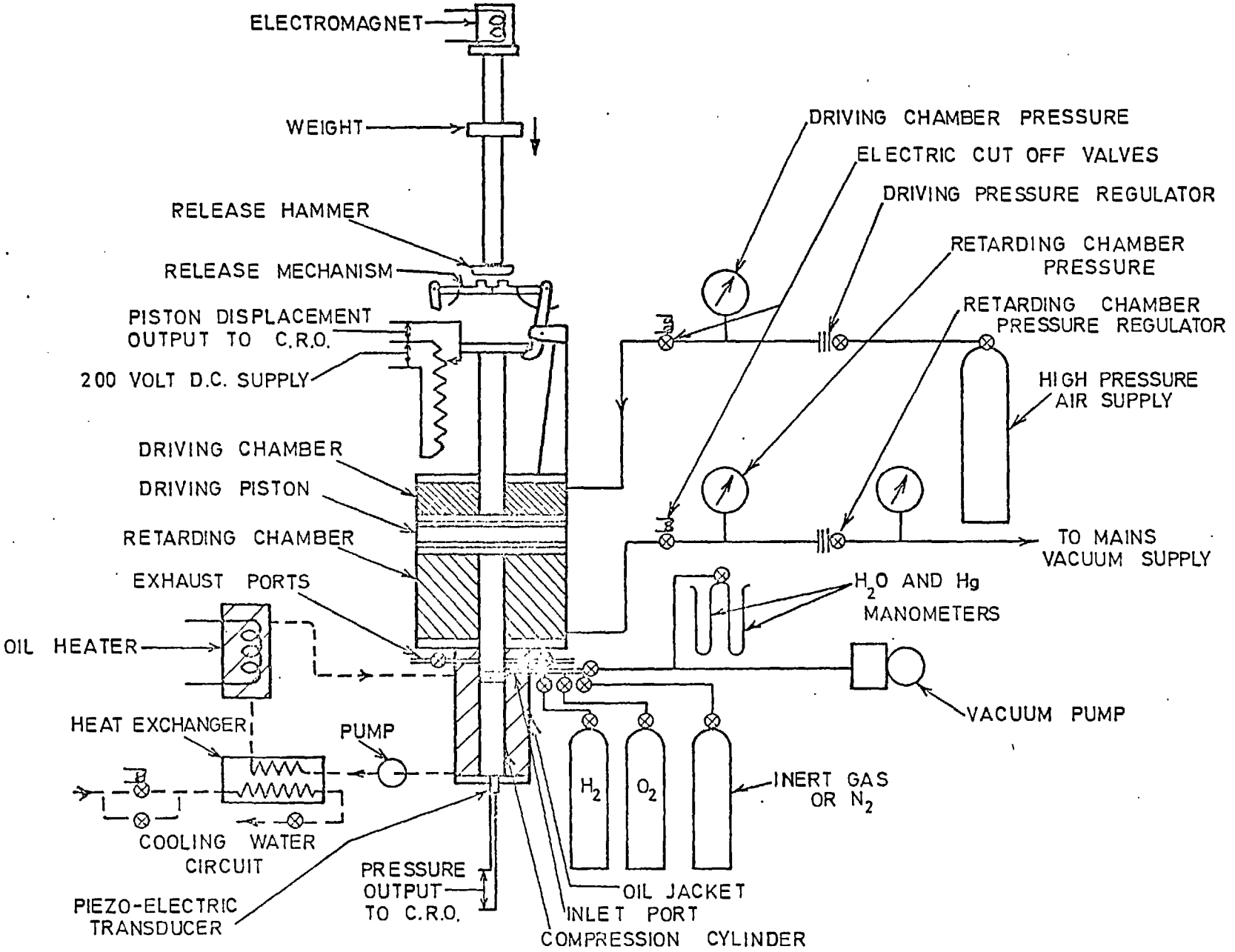

FIG 4.21-1 SCHEMATIC DIAGRAM — COMPRESSION IGNITION MACHINE TEST RIG

driving piston. The relationship between the control variables and the piston motion is discussed in Appendix F.

The compression cylinder is charged with reactant-gas when the pistons are held in the locked position: the cylinder is evacuated and the gases are individually admitted, the mixture composition being determined from the partial pressure of each component. The walls of the cylinder are uniformly heated by an oil jacket, and the reactant-gas temperature is allowed to rise to the wall temperature before the pistons are released to compress the charge.

During compression transducers are used to monitor the cylinder pressure and volume, and their outputs are displayed on a cathode-ray-oscilloscope.

The details of the compression machine are presented in Appendix D. Many of its novel features, such as the piston rings which provide unlubricated sealing of the compression cylinder, are described.

4.3 Experimental Measurements

4.31 The requirements

The object in constructing the apparatus was to measure the relation with time of the compression-cylinder pressure and volume. The precision with which these parameters are measured will determine the accuracy of any data which we derive from the experimental tests.

We recall that, in the prediction of autoignition, we needed the time differential of the cylinder volume.* Thus we need all possible precision in the measurement of the volume, as errors in

---

* Strictly, required in equation 2.22-8 is the piston displacement, to which the cylinder volume is directly proportional.

measurement will be amplified on differentiation.

The pressure is the parameter which will be compared with predicted values, and we cannot claim greater accuracy for our prediction technique than that achieved in the experimental measurements. Further, the point of ignition* may be defined more exactly, especially when ignition is early of P.M.P.T. (the point of maximum piston travel), from a rate-of-pressure-rise, dp/dt, record than from the pressure itself. Thus the simultaneous and accurate display of both dp/dt and pressure records is essential.

We have indicated the need for the precise measurement of both cylinder pressure and volume. Now we shall show how the measurements have been made and estimate the errors in the measurements.

4.32 The measurement of cylinder pressure

a) The pressure transducer

Cylinder pressure is, almost universally, measured in reciprocating engines by piezo-electric transducers, because of their rapid response and trouble-free operation. The transducer, of this type, which finally proved adequate for the present measurements was a Kistler 701/X unit, which incorporated a compensator for mechanical vibration. Without this compensation facility, tests in the compression machine had shown that vibration, set up by the sudden acceleration of the pistons, excited the transducers at their natural transverse frequency causing oscillations in the recorded pressure and particularly in the rate-of-pressure-rise.

Shock tube testing+ of the 701/X and other transducers demonstrated that the pressure front of a shock wave could be measured

---

* Defined in section 5.21.

+ Using standard test procedure, see for example, Schweppe et al. [48.].

up to 8% less than its actual value, because of distortion of the transducer diaphragm when subjected to thermal shock. It was possible to negate this effect by protecting the diaphragm with a laminated heat-shield of silicon asbestos. Dynamic calibration, in the shock tube, showed that the response of the transducer of 10^6 lbf $in^{-2}.s^{-1}$ was 3 times that required for the present autoignition tests. Static calibration was obtained using a dead-weight testing machine.

b) The recording equipment

The output signal from the pressure transducer is amplified and displayed on one channel of a four-trace oscilloscope. Fig 4.32-1 shows that an operational amplifier simultaneously differentiates the pressure signal and dp/dt is displayed on a second trace. The axes of the oscilloscope cathode-ray-tube were found not to be orthogonal, and the traces could thus misrepresent the measured parameters in time. To avoid this, pulses from a marker generator are simultaneously superimposed on all four traces as dots of increased intensity at 1.0 ms intervals. Not only do the dots provide a means of correlating points on each trace at the same instant in time, but also they provide an internal time-standard on each record.

The sweep of the traces across the cathode-ray-tube is synchronised with the release of the compression-machine pistons by a triggering pulse from a microswitch. The switch itself is actuated by the release mechanism.

Each sweep of the traces is recorded on Polaroid transparencies. These are enlarged in the darkroom and analysed with the aid of a specially-devised film-reader. The reader gives the digital value

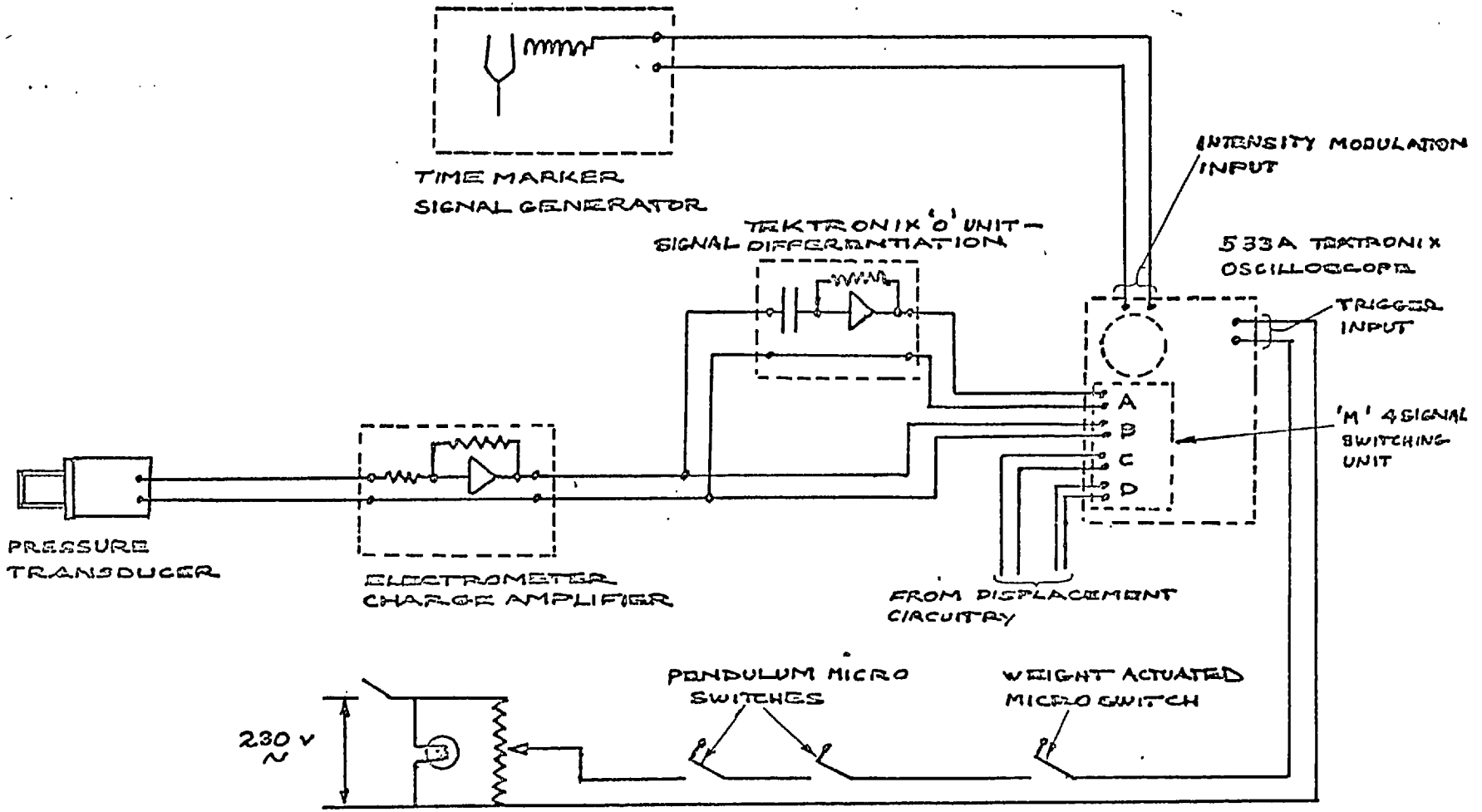

FIG. 4.32-1 SCHEMATIC DIAGRAM OF PRESSURE MEASUREMENT AND OTHER CIRCUITRY

of any point on the enlarged record to which a fine-lined cursor is moved.

c) The precision of measurement

A detailed assessment of the experimental precision in measuring the cylinder pressure has been made. The errors accounted for, as percentage error of a pressure of 300 lbf in^{-2}, are: 1. the time for the pressure within the cylinder to equalise, when a pressure rise is induced by the motion of the piston at one end of the cylinder (.4%); 2. electro-static charge leakage in the transducer-amplifier system (.005%); 3. delay in transducer response to applied pressure (.001%); 4. static calibration reproducibility (.5%); 5. film reading and optical errors (.2%).

If all the errors are unidirectional, then the maximum accumulative error in pressure measurement will be 1.1%.

4.33 The measurement of cylinder volume

a) The transducer

The linear displacement of the piston in the compression cylinder is directly related to the cylinder volume by the piston area. There are many methods available for measuring displacement. Resistive and photo-electric transducers had already been applied to the measurement of piston displacement in rapid-compression machines [52,,39]. Inductive and capacitive transducers also appeared to be suitable for the present measurement.

The resistive transducer* was chosen because, by using a potentiometric measuring technique, the output is both linear and to the same precision over the entire 14 inches of piston travel. A capacitive transducer was also constructed which could be coupled

---

* Described in Appendix D.

directly to the compression piston when the cylinder head was removed. It was thus possible to obtain, dynamically, a cross-calibration of the resistive transducer. Static calibration of both transducers was effected by measuring, with a micrometer-screw-gauge, the displacement of the compression piston in its cylinder as a function of trace deflection on the oscilloscope.

b) The circuitry

The circuit diagram, fig 4.33-1, shows the arrangement used for measuring the piston displacement by the potentiometric method. Direct-current supply is obtained by rectifying and smoothing alternating current which is itself maintained at constant voltage irrespective of small variations in mains supply. The direct current is supplied to a wire-wound resistor. A follower, mounted on the external shaft of the compression machine, picks up a voltage proportional to the piston displacement.

The voltage signal is fed on to the two remaining traces of the oscilloscope. One of these signals is amplified 2.5 times by the operational amplifier so that measuring accuracy is increased when the piston displacement from the cylinder head is smallest.

Experimental records, displaying the typical behaviour of the four traces are given in fig 5.25-1

c) The precision of measurement

The errors in displacement measurement have been assessed. At a piston displacement corresponding to a compression ratio of 30:1. The errors were as follows: 1. distortion of the piston assembly between the piston face and the measuring point at the end of the external shaft (.02%); 2. static calibration reproducibility

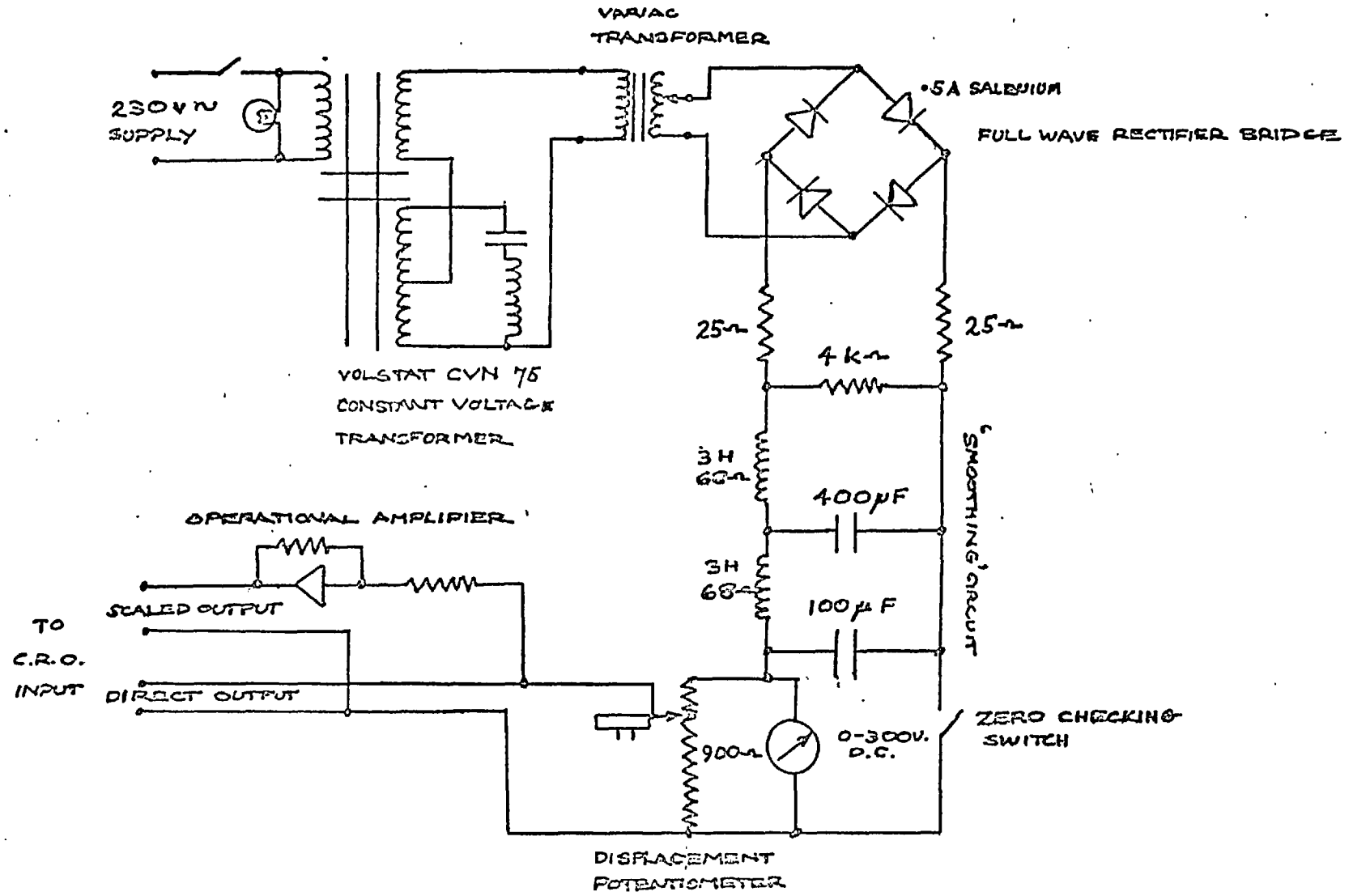

FIG. 4.33-1 DISPLACEMENT MEASURSMENT CIRCUIT DIAGRAM

(.5%); 3. backlash and follower inertia (.6%); 4. film reading and optical errors (.7%).

The maximum accumulative-error is 1.8%, reducing to .2% at maximum piston-displacement from the cylinder head.

4.34 The measurement of the pre-compression charge state

a) The method

The method of introducing the gaseous charge into the compression cylinder has been outlined in section 4.21. The composition of the mixture is determined from the partial pressure of each component as it is admitted to the cylinder, and the pressures are measured by either the mercury or the water manometer seen in fig 4.21-1. The sequence of gas admission is such that the smallest component is admitted last, and the water manometer selected to monitor its introduction, increasing the measuring precision of the pressure of both the component and the final pre-compression values.

The pre-compression temperature of the gas is always that of the cylinder walls.

b) Precision of measurement

The errors involved in the measurement of the pre-compression state of the charge were assessed: the mixture composition could be controlled to within $\pm$ 1% and the initial temperature and pressure to 0.2% and 0.1% of their respective absolute values.

4.4 The Merits of the Compression Machine for a Wide Range of Engine Research

Now that we have described the apparatus and the precision with which measurements can be made, we can discuss the advantages

of this apparatus in some of its applications. Its applications fall into two categories; the first one is specialised: an apparatus for obtaining experimental data, from which reaction kinetics can be derived on the autoignition of reacting gases; the second one is general: the study of reciprocating-engine phenomena such as: heat transfer; fluid mechanics and other engine-combustion processes not covered by (i).

4.41 Application to reaction-kinetic studies

In discussing this application we shall, for completeness, need to presuppose knowledge of later findings in Chapters 5 and 6: specifically, which variables have important effects on observed and predicted autoignition.

For obtaining results from which reaction-kinetic data can be derived, the compression machine has advantages as an experimental tool over steady-flow reactors, such as the well-stirred reactor. The advantages are:

1. In the compression machine, exact control of the mixture composition is possible for any experimental test. Additionally, we shall show that the reaction-rate constants can be determined from a knowledge of the induction-time to autoignition and that the induction-time is insensitive to mixture variations within the range of experimental error. In the reactor, however, reaction-rate constants are derived from the flame temperature which is dependent, not only upon the kinetics of the reaction and the flow rate, but also upon small variations in mixture composition.*

2. In the ignition process, the degree of mixing of reactants and products does not influence the pressure, and thus induction-

---

* See Jenkins et al. [26.].

time, in the compression machine, because pressure is an extensive property; whereas in the reactor incomplete mixing can lead to local variations in flame temperature - an intensive property; and the difficulty in choosing the representative value fromwhich to calculate the kinetic data.

3. The compression machine lends itself to the study of two-stage ignition because the density path in time is adjustable. It is possible to reduce the density as ignition begins, and the reaction will proceed more slowly; if conditions of temperature, pressure etc. are suitable, the two stages of pressure rise can be distinctly separated. Thus, we can study the influence of experimental variables on the reactions which control, and derive kinetics for, the production of the unstable intermediate-species formed during the first stage.

However, on the debit side, the compression machine cannot be made adiabatic, as can the steady-flow reactor, and heat transfer must be allowed for in any prediction of autoignition.

4.42 Application to piston-engine combustion studies

A critical examination has been made by Crease [12] of apparatus used in combustion studies. He concluded that the present apparatus was, in many ways, superior to other research tools for the study of spark-ignition and diesel-engine combustion, and suited to examining both fluid dynamic and chemical factors which affect the progress of combustion.

The outstanding superiority of the compression machine over current research-engines is the single-operating cycle, permitting control of,or freedom from, the influence of previous cycles on factors which affect the reaction chemistry: surface activity,

residual gases etc.; and those which influence the fluid mechanics: mixing of reactants and residuals, and induction swirl.

An additional asset which the present machine has is the ability to reproduce a wide range of piston motion: to simulate the density-time history experienced by the end-gas, remote from the sparking plug in a gasoline engine; or to create piston-motion as controlled by a crank-shaft and connecting-rod. Thus the density-time history to which a charge is subjected need not be removed from that of a continuously-operating engine as in the constant-volume bomb, or the rapid-compression machine.

CHAPTER 5

THE EXPERIMENTAL INVESTIGATIONS

5.1 Introduction

5.11 The purpose of the investigations

The main purpose of the experimental investigations was to obtain pressure- and density-time records of the compression to autoignition of hydrogen-oxygen-argon mixtures, over a wide range of hydrogen-oxygen mixture composition.

The inert-gas, argon, was used as diluent, in preference to nitrogen, so that we need not include N_2-O_2 reactions, known to be of importance at elevated temperatures*, in the kinetic model on which the prediction of autoignition is based.

Before the main investigations could be undertaken, some exploratory researches were necessary, and we shall discuss these now before describing the autoignition tests.

5.12 The exploratory investigations

The first part of the preliminary investigations was concerned with the development of the apparatus and its instrumentation, principally: the elimination of oscillations in the pressure and rate-of-pressure-rise records, originating from the rapid acceleration of the compression-machine pistons; and the development of the potentiometer follower so that it would maintain contact with the resistor at high wiping speeds. This development is briefly discussed in Appendix D.2.

---

* See, for example, Bulewicz [10.].

The second part was the compression of non-reacting gases in the apparatus. The results from these tests were analysed in section 3.25 and yielded a single equation for predicting the gas-wall heat-transfer (equation 3.26-1). The procedure for these tests was simple: air was admitted to the compression cylinder and time allowed for the temperature throughout the cylinder to equalise. Then, the air was compressed, monitoring the cylinder pressure and volume. The tests were conducted for a range of compression ratios* (6:1 to 30:1) and compression stroke times (30 to 60 ms). The starting pressure and temperature (14.7 lbf in^{-2} and 353°K) were maintained constant in all the tests. The present analysis has been confined to those results at the single compression-stroke time (37.5 ms) which was used for the autoignition tests.

5.2 Autoignition of hydrogen-oxygen-argon mixtures

5.21 Definitions: the 'point of ignition' and 'induction-time'

Until now we have loosely talked of autoignition, assuming that the reader would know that when a charge of reactant gas is raised to a sufficient temperature and pressure, the rate of reaction accelerates to a value where self-ignition is said to have occurred, because further rises in pressure, temperature, or both, are exhibited beyond that brought about by the raising process.

In this chapter the 'point of ignition' will be discussed and in later chapters observed and predicted 'induction-times' will be compared. These terms are now defined.

a) The point of ignition. Many methods have been used for defining the point at which the first observable sign of ignition occurs.

---

* The ratio of the maximum cylinder-volume to that at P.M.P.T.

Some definitions rely directly on observed parameters: for example, when temperature rise has reached a fixed proportion of the total rise on ignition [41.] or when, in reciprocating engines, the pressure deviates from that of the corresponding non-firing cycle. Other definitions rely on deductions made from the observed parameters: for example, a heat-release analysis of the engine pressure-record may be performed and the point at which the reaction becomes exothermic, defined as ignition. We shall adopt the former procedure and define the point of ignition from the pressure record.

On ignition, whether early or late of P.M.P.T., it was observed that the rate of pressure rise rapidly accelerated to a more constant slope. Thus, for comparing ignition over the range of experimental variables, the point of ignition is defined as when acceleration of pressure is a maximum, and when $d^3p/dt^3 = 0$.

b) The induction-time. We shall primarily refer to induction-time as a means of comparing experimental pressure records with calculated ones. Our purpose will be to obtain predicted records which reproduce the entire observed record to reaction completion, for tests in which the point of ignition is close to P.M.P.T. For these tests it is more expedient to compare their pressure records at the maximum rate-of-pressure-rise than at the point of ignition.

Therefore, the induction-time τ, is defined from the start of compression to the maximum rate-of-pressure-rise after the point of ignition. This definition facilitates the determination of the difference between observed (τ_e) and predicted (τ_p) induction-time, $\Delta\tau$, for as we shall see in section 5.2, that the time difference between observed and predicted pressures is constant for 50% of the pressure rise on ignition and there is no need to specify the maximum dp/dt precisely.

5.22 The test conditions

The motivation in using argon as diluent has been introduced. The dilution ratio in the autoignition tests was maintained at the constant argon:oxygen ratio of 79:21 by volume, thus replacing the nitrogen component of air by argon on a mole-for-mole basis. An exception to this dilution ratio was made for stoichiometric H_2-O_2 mixtures, when dilution was increased to 90:10, to prevent the magnitude of the peak cylinder-pressure rising beyond the maximum value at which the pressure transducer could safely operate.

The range of H_2-O_2 mixture composition tested was over the equivalence ratio, ϕ, of 0.05 to 2.5 of the stoichiometric value. In all the tests the compression ratio was maintained constant at 37.5 ms and the compression ratio was adjusted to give autoignition ranging from early of P.M.P.T. to later in the cycle and finally to a ratio at which ignition just failed to occur. In each test the starting pressure was 14.7 lbf in^{-2} and the starting temperature was 353°K.

Alternative specifications for the range of experimental variables could have been chosen. For example: we could have investigated autoignition at constant ignition-pressure, over the mixture range, by varying the compression-stroke time; but this would narrow the range of mixture composition which would ignite,and complicate the heat-transfer prediction; for in long compression-stroke times conduction plays a more prominent role than convection. Instead, the adopted procedure is common to engine research-practice: to operate at constant engine-speed and to vary the compression ratio to obtain ignition throughout the range of ϕ.

5.23 Selected records of experimental tests

Initially, mixtures hydrogen weak of stoichiometry were auto-ignited for which peak cylinder pressures were less than the transducer's maximum operating pressure of 1500 lbf in^{-2}. When this mixture range was fully covered tests were made for stoichiometric and richer mixtures. Thus, records of pressure- and volume-time were obtained at the equivalence ratios, ϕ = 0.05, 0.08, 0.11, 0.15, 0.25, 1.0 and 2.5. At ϕ = 0.08 a few records showed two-stage ignition which will be discussed separately in section 5.25.

In figs 5.23-1, 5.23-2 and 5.23-3 families of pressure-time records are shown for increasing compression ratio at ϕ = 0.05, 1.0 and 2.5 respectively. Also shown are the piston displacement-time records which correspond to the earliest and latest pressure records in which ignition occurred.

5.24 Discussion of results

For the case of ϕ = 0.05, fig 5.23-1, the increase in compression ratio required to advance the point of ignition in time is such that intersection of the pressure records during the expansion process does not occur. At richer mixtures (see fig 5.23-2 and 5.23-3) intersection of the pressure records occurs. We can offer a qualitative explanation as to why, at an instant of time, the pressure is reduced despite the reduced cylinder volume: the charge has been subjected to a different time history; the pressure and temperature have been higher, heat losses have increased and the extent of dissociation of the charge constituents has been altered. A quantitative explanation can only be obtained by prediction calculations made with the procedure of Chapter 2.

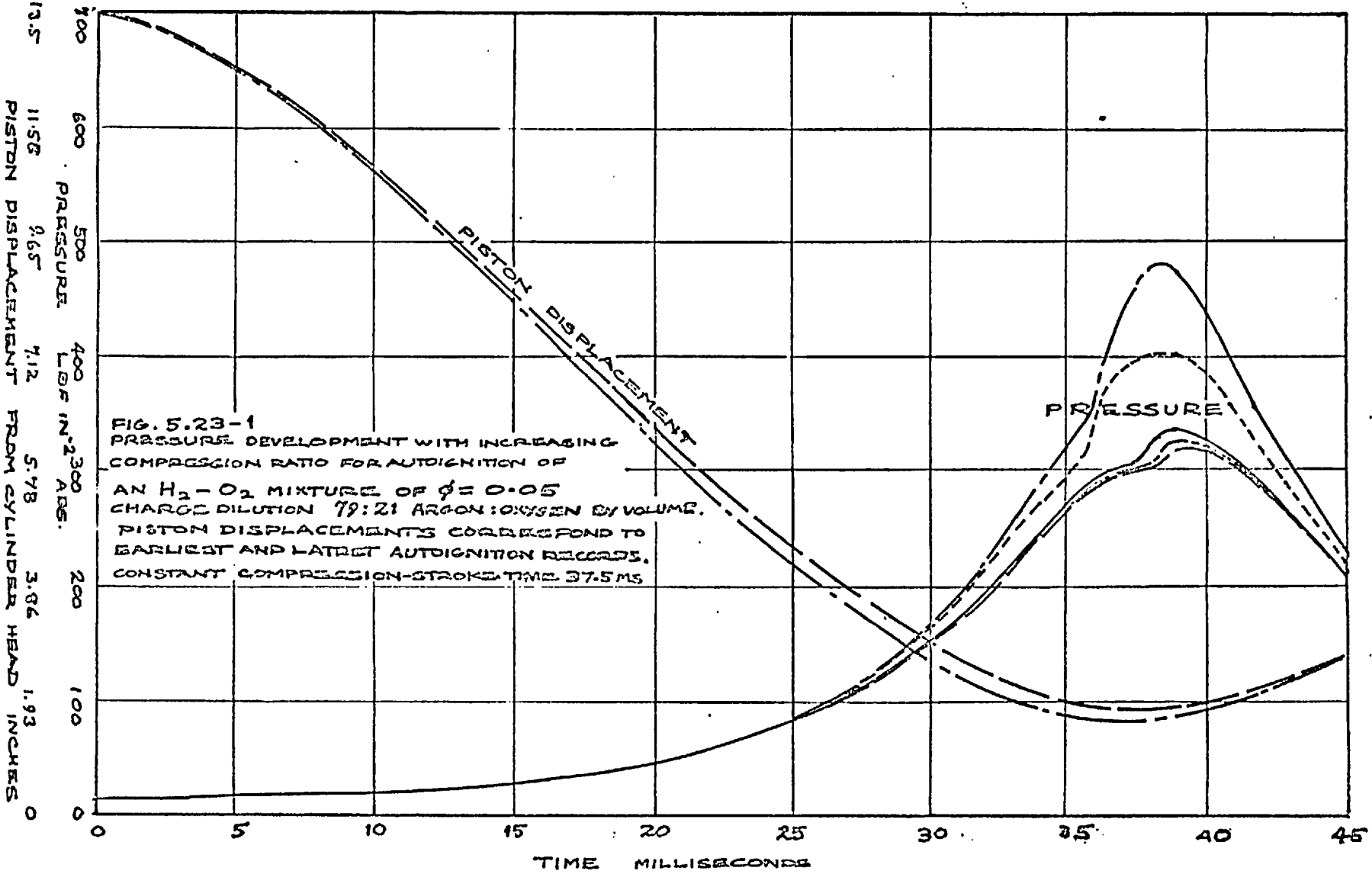

FIG. 5.23-1
PRESSURE DEVELOPMENT WITH INCREASING COMPRESSION RATIO FOR AUTOIGNITION OF AN $H_2 - O_2$ MIXTURE OF $\phi = 0.05$
CHARGE DILUTION 79:21 ARGON:OXYGEN BY VOLUME.
PISTON DISPLACEMENTS CORRESPOND TO EARLIEST AND LATEST AUTOIGNITION RECORDS.
CONSTANT COMPRESSION-STROKE TIME 37.5 MS

FIG. 5.23-2
PRESSURE DEVELOPMENT WITH INCREASING COMPRESSION RATIO FOR AUTOIGNITION OF AN H_2-O_2 MIXTURE OF $\phi = 1.0$
CHARGE DILUTION 90:10 ARGON: OXYGEN BY VOLUME
PISTON DISPLACEMENTS CORRESPOND TO THE EARLIEST AND LATEST AUTOIGNITION RECORDS.
CONSTANT COMPRESSION-STROKE TIME 37.5 MS

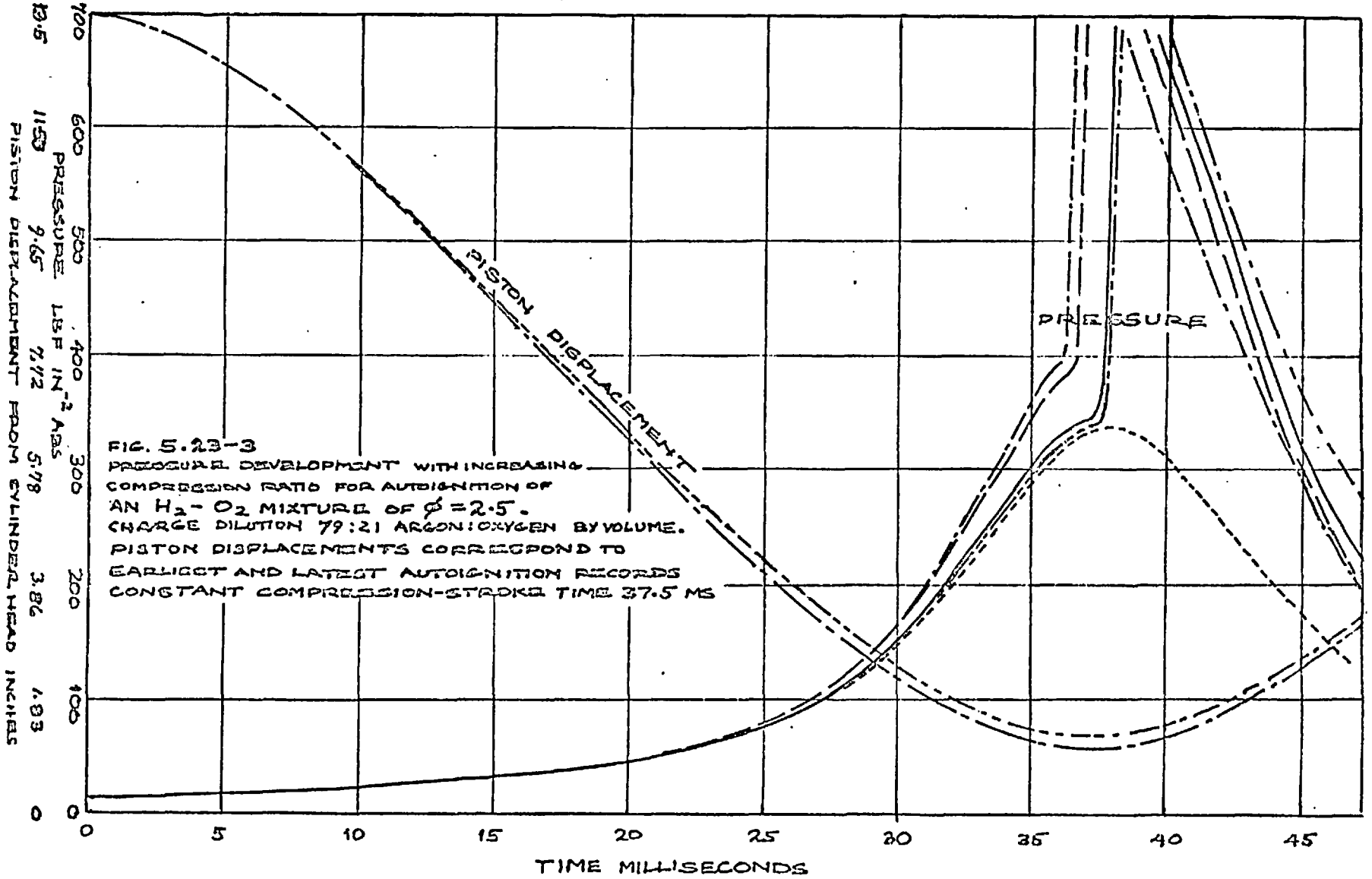

FIG. 5.23-3
PRESSURE DEVELOPMENT WITH INCREASING COMPRESSION RATIO FOR AUTOIGNITION OF AN $H_2 - O_2$ MIXTURE OF $\phi = 2.5$.
CHARGE DILUTION 79:21 ARGON:OXYGEN BY VOLUME.
PISTON DISPLACEMENTS CORRESPOND TO EARLIEST AND LATEST AUTOIGNITION RECORDS
CONSTANT COMPRESSION-STROKE TIME 37.5 MS

The results of the influence of mixture composition and compression ratio on the point of ignition are summarised in fig 5.24-1 for the constant compression-stroke time (37.5 ms).

The curves show, for $\phi = 2.5$, that the time of ignition during expansion (i.e.beyond P.M.P.T. of 37.5 ms) is not sensitive to changing compression ratio; while stoichiometric mixtures are most sensitive to compression ratio changes. At $\phi = 0.25$ ignition occurs at the lowest compression ratio; 6.3:1. However, the compression ratio location of the $\phi = 1.0$ curve is undoubtedly influenced by the increased oxygen dilution at this mixture composition. The direction of diluent influence is difficult to forecast: increased dilution with argon reduces the mean-mixture specific-heat; but reduced reactant-gas concentrations require increased temperatures to ignite them.

5.25 Two-stage autoignition of hydrogen

Experimental studies have been made in research piston-engines of the two-stage ignition of hydrocarbon fuels, such as n-heptane.* The shape of the pressure-temperature explosion limits of hydrogen+ shows that there are three limits, and therefore hydrogen can also exhibit two-stage ignition. That is; the pressure-temperature path followed by the reactant gas passes beyond the second limit, leading to ignition; the resultant rise in pressure and temperature causes the path to pass out of the limit and through the extinction region until the third limit is reached and re-ignition occurs. The chemical explanation of the second explosion limit is in the formation of hydroperoxyl (HO_2) and the third limit by the formation of

---

* See, for example, Downs and Wheeler [13.].

+ See, Lewis and von Elbe [34.] page 29.

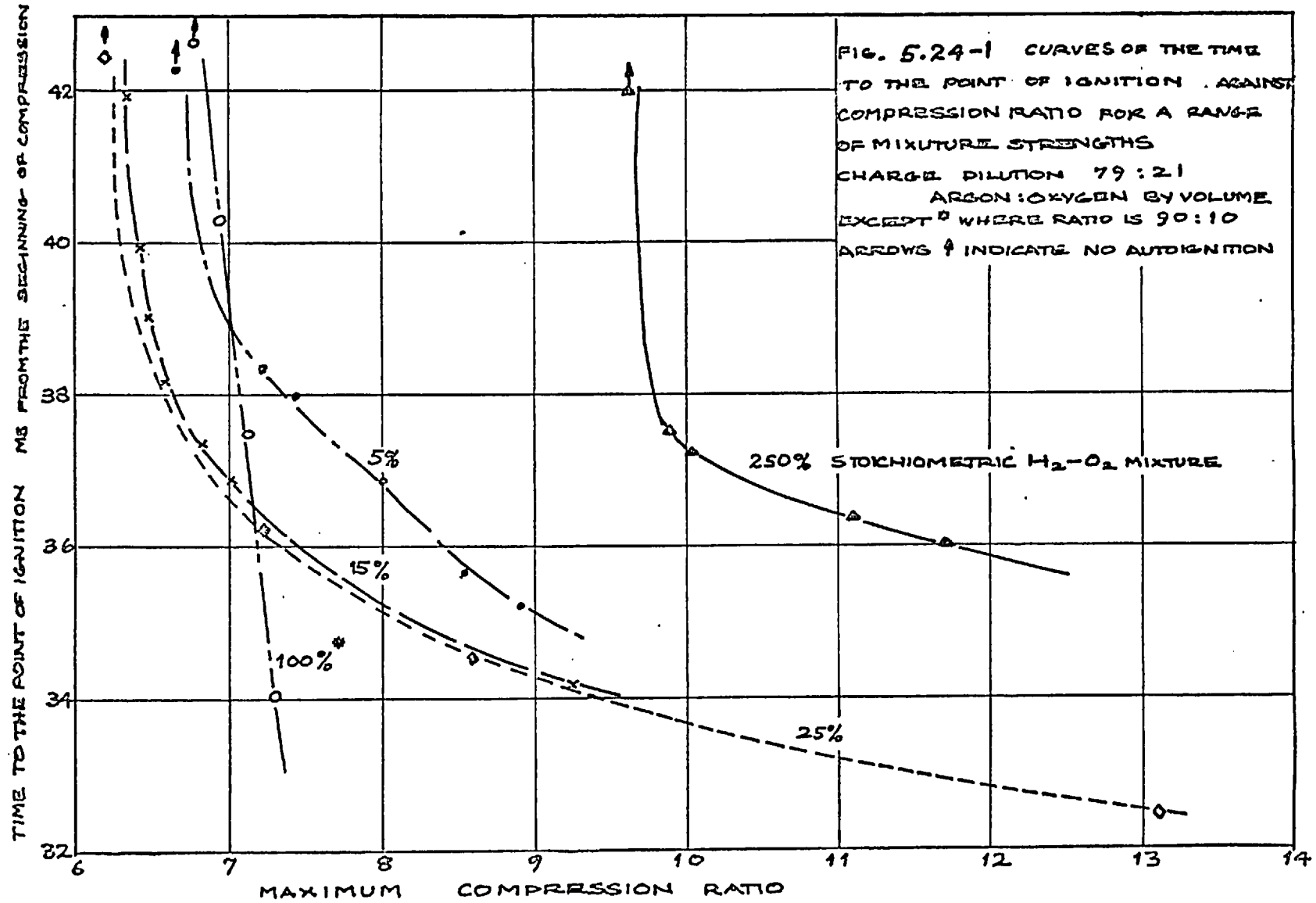
FIG. 5.24-1 CURVES OF THE TIME TO THE POINT OF IGNITION AGAINST COMPRESSION RATIO FOR A RANGE OF MIXUTURE STRENGTHS
CHARGE DILUTION 79 : 21
ARGON : OXYGEN BY VOLUME
EXCEPT * WHERE RATIO IS 90 : 10
ARROWS ↑ INDICATE NO AUTOIGNITION
250% STOICHIOMETRIC H_2–O_2 MIXTURE
5%
15%
25%
100%*
TIME TO THE POINT OF IGNITION MS FROM THE BEGINNING OF COMPRESSION
MAXIMUM COMPRESSION RATIO
42
40
38
36
34
32
6
7
8
9
10
11
12
13
14

H_2O. Lewis and von Elbe [34.] show the upper bound to the second limit 8 lbf in^{-2} abs* and 850°K for a stoichiometric mixture. These limits represent the results obtained for infinite induction times. When induction-times are shorter the limits will be shifted. It is accepted+ that HO_2 formation is important at higher pressures than 8 lbf in^{-2} abs in the temperature range 700 to 900°K.

The author believes that the results now described, show the first experimental observations made of the two-stage ignition of hydrogen.

Fig. 5.25-1(a) presents a typical experimental record of cylinder pressure, rate of pressure rise and piston displacement as functions of time, for the 'normal' single-stage ignition of hydrogen at $\phi = 0.08$. Fig 5.25-1(b) shows that increasing the compression ratio further resulted in two distinct-stages of ignition; most clearly seen in the dp/dt record. The state of the charge at the point of ignition of the first stage was calculated, from the record, to be p = 267 lbf in^{-2} abs and T = 891°K.

The density-time path needed to separate out the two stages of ignition proved to be critical: a further eight tests giving auto-ignition within $\pm$ 2ms of the record shown demonstrated only normal ignition. However, by increasing the compression-stroke time from 37.5 ms to 43 ms, reproducible, but less distinct, two-stage ignition records were obtained having pressures in the range 271 to 273 lbf in^{-2} abs and temperatures of 896 to 899°K at the point of ignition.

It is possible that the range of mixture composition at which two-stage ignition can be obtained, could be extended by varying other parameters such as the pressure or temperature at the start of compression. In this way it may be possible to obtain sufficient

---

* 100 lbf in^{-2} ≡ .688 MN m^{-2}

+ See Fristrom and Westenberg [20.].

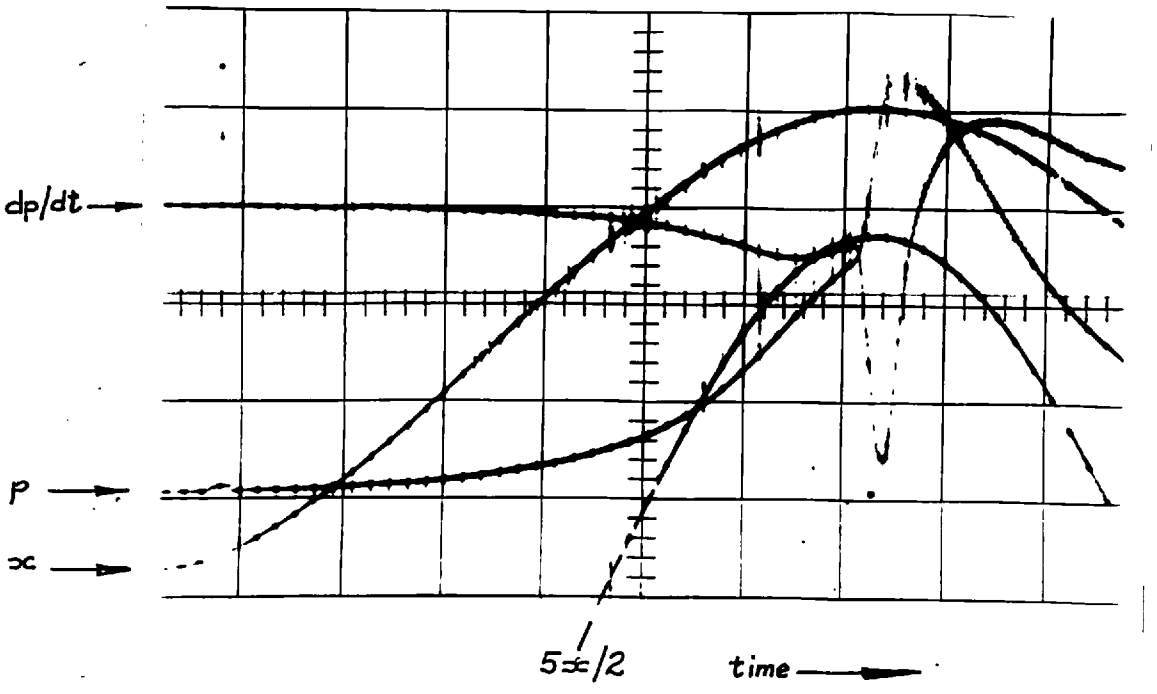

a) Single-stage ignition.

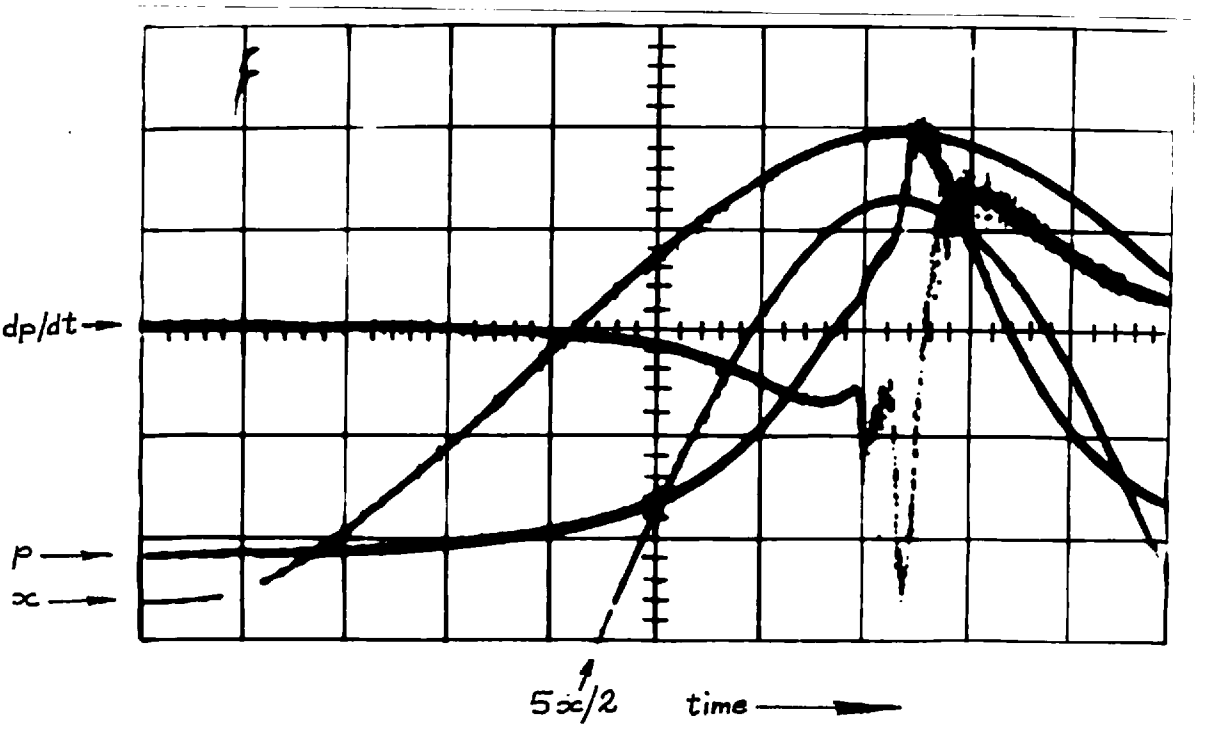

b) Two-stage ignition.

Fig 5.25-1 Oscillographs of autoignition of a $\phi = 0.08$ H_2-O_2 mixture. p = pressure; dp/dt = rate of pressure rise; x = piston displacement.

results to study the ignition kinetics of the first-stage reactions involving the species HO_2 and H_2O_2, about which there are few published results.

5.3 Comparison of results with those in other apparatus

We shall conclude the presentation of the experimental results by comparing them with the few results of H_2-O_2 autoignition available in the literature.

Klat [32.] has published information on the autoignition of hydrogen in a motored piston-engine. His results were obtained in a C.F.R. engine, and show that the onset of hydrogen-air ignition occurred at a compression ratio, r, of 14.8:1 for the conditions: $\phi = 0.2$; intake pressure 14.7 lbf in^{-2} abs and temperature 72°C at an engine speed of 900 revs min^{-1}. Knowing that the engine volumetric-efficiency was 76% we can calculate that, for an argon-diluted charge, the same temperature at ignition would be obtained at r = 7.1:1. By interpolating the present results in fig 5.24-1 the limit of ignition at $\phi = 0.2$ may be seen to be 6.4:1. We have already pointed out* that there may be parameters in research engines which cannot be controlled, but which can influence engine autoignition results. These must be the main cause of the discrepancy between the limiting compression ratios.

It is possible to compare the present experimental results with those obtained in two other apparatus; the rapid-compression machine and the constant-volume bomb; by determining the third explosion limit in each apparatus. This is specified by extrapolating results of temperature vs. induction-time, at fixed pressures, to find the temperature at infinite induction-time.

---

* In section 4.42.

Fig 5.3-1, curve 1, shows the third explosion limit as derived by Jost [27.] in his rapid-compression machine for stoichiometric hydrogen-air mixtures. Lewis and Elbe's results (curve 2) were obtained for stoichoimetric hydrogen-oxygen reactants in a 7.4 cm diameter bomb.

To obtain the explosion limit for the compression-machine tests for H_2-O_2-Ar mixtures at $\phi = 1.0$, it is necessary to note that the cylinder pressure approximates (within 5%) to constant pressure for 2.5 ms on each side of P.M.P.T., in a late or non-igniting test.* Now, Jost's results show that at 860°K and at induction-times greater than 5 ms, induction-time is asymptotic with pressure. Thus the pressure and temperature at the explosion limit correspond to those at the point of ignition in the test for which 40 ms elapse to the point of ignition. These values are plotted as point 3 on fig 5.3-1.

There is a measure of agreement between the present result and the curves 1 and 2 on fig 5.3-1. It would be expected that the non-uniform pressure during the 5 ms before ignition, in the presented result, together with effect of diluting the charge with argon will tend to give too high a value of temperature for the explosion limit.

---

* See fig 5.23-2.

FIG. 5.3-1 CURVES OF HIGH PRESSURE REGIONS OF THIRD EXPLOSION LIMIT
AFTER (1) LEWIS AND VON ELBE (UNDILUTED CHARGE)
(2) JOST (CHARGE N_2 DILUTED)
3 IS LIMIT IN COMPRESSION MACHINE. TRUE LIMIT WILL BE AT LOWER TEMPERATURE DUE TO ARGON DILUTION OF CHARGE USED IN THESE TESTS

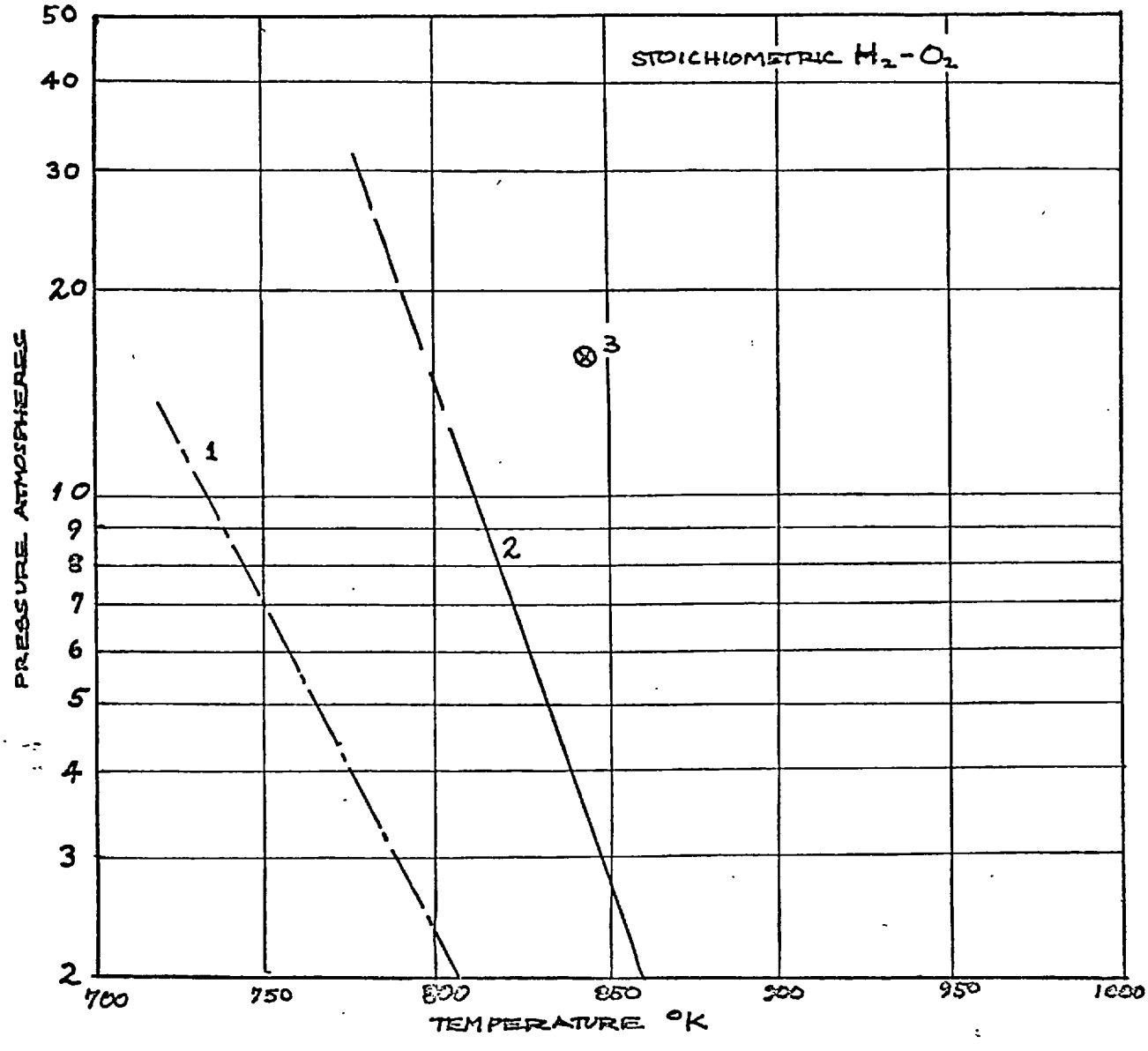

CHAPTER 6

COMPARISON OF PREDICTED AND EXPERIMENTAL PRESSURE-TIME HISTORIES

6.1 Introduction

6.11 Outline of the chapter

In this chapter we shall compare selected experimental-pressure-time records with predicted results calculated by the procedure developed in Chapter 2. We will show that the chemical-kinetic data used in the calculation procedure can influence the predicted pressure record: changes in reaction scheme selected or the reaction rate-constants alter the predicted induction-times.*

The purpose is to find which kinetic-data gives agreement between predicted and observed induction-times throughout the range of H_2-O_2 mixture composition, $\phi = 0.05$ to $\phi = 2.5$. But, we shall conclude that not any of the data tested gave the desired quantitative agreement. Nonetheless, from the results we can show whether a particular reaction ought to be included in the reaction mechanism from the effect of its inclusion on the predicted induction-times. This will enable us to establish a reaction scheme which we may use, in the next chapter, to find the rates of the reactions which do give agreement between predicted and observed induction-times.

6.12 The records selected for comparison

The experimental tests selected for comparison with the predicted records were confined to those having induction-times in the range 36 to 39 ms, irrespective of mixture composition. These induction-times correspond closely to the time to P.M.P.T. (the point of maximum piston-travel) when the density is approximately

---

* Already defined in section 5.21.

constant, and the sensitivity of induction-time to changes in control parameters such as kinetic-data or experimental variables is least affected by changing density: when ignition is late in the test (e.g. 42 ms), the density is rapidly decreasing and small changes in control parameters cause large changes in induction-time; whereas for early ignition (e.g. 32 ms) the converse is true.

Predicted results have been calculated for many combinations of input data: kinetic data, ϕ, T_o, p_o and r. For consistency throughout this chapter, we shall present the details of comparison between predicted and observed results for one mixture, $\phi = 0.15$, and will only refer to the comparative induction-times of other mixtures; thus avoiding the presentation of excessive amounts of data.

6.13 The procedure for comparison

In section 5.12 we defined the induction-times τ. This is the parameter we shall use to compare the predicted- and experimental-pressure records. We shall examine the difference between observed and predict. induction-times, Δt, and seek that combination of reaction-kinetic data which makes $|\Delta\tau|$ less than .1 ms throughout the range of mixture composition. $\Delta\tau$ is measured at the maximum rate of pressure rise. For ease of inspection of the records presented it will frequently be found sufficient to measure $\Delta\tau$ as the difference between the time on each record when the pressure, on ignition, has reached 25% of the total ignition pressure rise.

6.14 The kinetic data used for predicting pressure-time histories

It is appropriate to recall the kinetic data which was proposed as the basis for the first prediction calculations: only reactions of the species H_2, O_2, H, O, OH and H_2O should be considered; the chain-

reaction should consist of reactions I to V*; and we should assign to these the rate constants of the present survey (Appendix C) or those of Jenkins et al. [26.].

Table 6.14-1 summarises the combinations of reactions which were eventually tested.

6.2 Comparisons Made for a Range of Kinetic Data

6.21 The five reaction scheme

From the scheme of reactions I to V it is plain to see that unless input values are given to radical concentrations as well as reactants, reaction cannot proceed because there is no initiation reaction: a reaction involving only reactant species on one side of the equation. In the input data arbitrary concentrations were assigned to H, O and OH, the values being calculated for chemical equilibrium at 600°K.

Much of the development and testing of the computer programme was carried out with the five reaction scheme and the kinetic data from reference [26.]. The sensitivity of the induction-time, τ_p, was investigated to control parameters such as: the length of the integrating time-step, Δt; and to experimental parameters such as: T_o and ϕ. Typical effects of the adjustment of T_o and ϕ on the predicted pressure are shown in fig 6.21-1.

The effects of varying T_o by 5% above and below the experimental value of 353°K show that 7% changes in τ_p result; whereas changing ϕ to 0.10 and 0.20 from the experimental $\phi = 0.15$, causes only small changes (0.75%) in τ_p. From the experimental-pressure record the induction-time, τ_e, may be deduced and it is apparent that τ_e is greater than τ_p at the same T_o and ϕ. The difference, $\Delta\tau$ is 4.4 ms

---

* See table 3.42-1.

TABLE 6.14-1 DETAILS OF REACTION MODELS

IDENTIFICATION No. OF REACTION	H_2	O_2	H	O	OH	H_2O	HO_2	H_2O_2	M	MODEL USES REACTIONS INDICATED ✓ 5	6	7	9	13	TOTAL No. OF REACTIONS IN MODEL
I	1		(1)		1	(1)				✓	✓	✓	✓	✓	
II		1	1	(1)	(1)					✓	✓	✓	✓	✓	
III	1		(1)	1	(1)					✓	✓	✓	✓	✓	
IV				1	(2)	1				✓	✓	✓	✓	✓	
V			1		1	(1)			1 (1)	✓	✓	✓	✓	✓	
VI		(1)		2					1 (1)			✓	✓	✓	
VII	(1)		2						1 (1)			✓	✓	✓	
VIII			1	1	(1)				1 (1)				✓	✓	
IX	1	1			(2)						✓		✓	✓	
X		1	1				(1)		1 (1)					✓	
XVI		(1)					2	(1)						✓	
XVII					(2)			1	1 (1)					✓	
XVIII			1		(1)	(1)		1						✓	

KEY.

UNBRACKETED FIGURES DENOTE THE STOICHIOMETRIC COEFFICIENTS OF THE REACTANTS
BRACKETED FIGURES DENOTE THE STOICHIOMETRIC COEFFICIENTS OF THE PRODUCTS

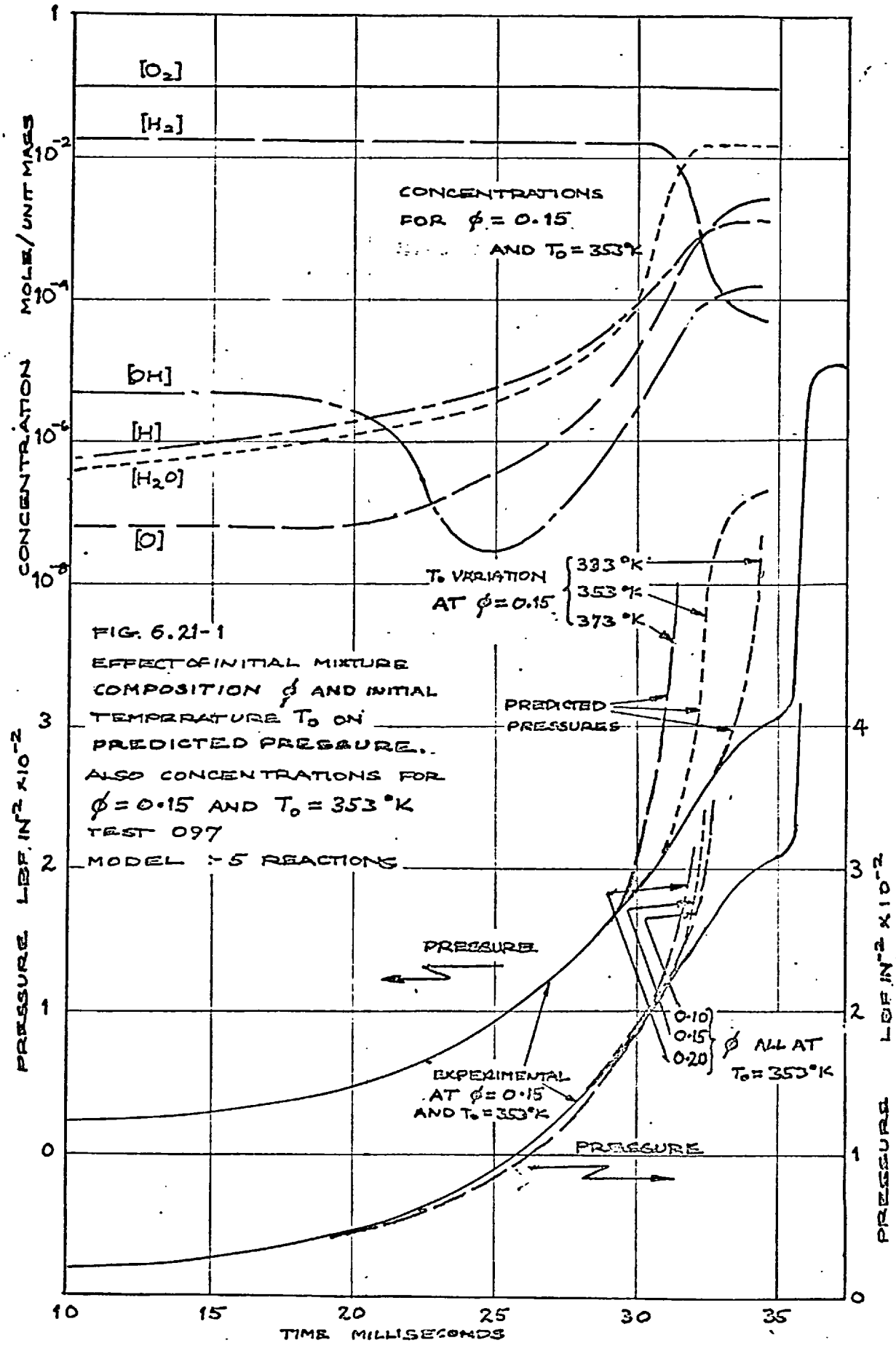

FIG. 6.21-1
EFFECT OF INITIAL MIXTURE COMPOSITION ϕ AND INITIAL TEMPERATURE T_0 ON PREDICTED PRESSURE.
ALSO CONCENTRATIONS FOR $\phi = 0.15$ AND $T_0 = 353\,^{\circ}K$
TEST 097
MODEL :- 5 REACTIONS

(11.6% of τ_e).

The upper half of fig 6.21-1 gives the concentrations predicted for the starting conditions of the experimental test. Large variations in radical concentrations do not occur until the charge temperature has risen above the equilibrium temperature (600°K) selected arbitrarily for their initial concentrations. Predictions made for other values of the initial concentrations showed a negligible effect on τ_p.

Predictions were also made at other equivalence ratios, but at no value throughout the range $\phi = 0.05$ to $\phi = 2.5$ was $\Delta\tau$ zero.

6.22 The influence of initiation reactions on the induction-time

The contribution to the induction-times, predicted from the five reaction scheme with alternative initiation reactions, was assessed. Firstly, reaction IX was added to I to V. The predicted-pressure record on fig 6.22-1 shows that $\Delta\tau$ is reduced to 2.5 ms (6.6%). If initial radical concentrations, as in 5.21, are included in the input data at the start of integration, then $\Delta\tau$ is 2.6 ms (6.9%).

Shown on fig 6.22-1, as well as the concentration profiles, is the combustion-energy release-rate. This exothermic rate of heat-release is plotted on a $\log_{10}$ scale, and in consequence does not show the small (about 30 ft lbfs^{-1}) endothermic energy absorbed at 27 to 30 ms, prior to the main heat-release.

Secondly, reactions VI and VII for the dissociation of hydrogen and oxygen were added to reactions I to V to initiate the chain. Fig 6.22-2 demonstrates that with this scheme $\Delta\tau$ is reduced further to 2.1 ms (5.6%).

The 'troughs'* in the concentrations [O] and [OH] at 28 ms are a result of limitations in the reaction model: with a simple reaction

---

* Also apparent in fig 6.21-1.

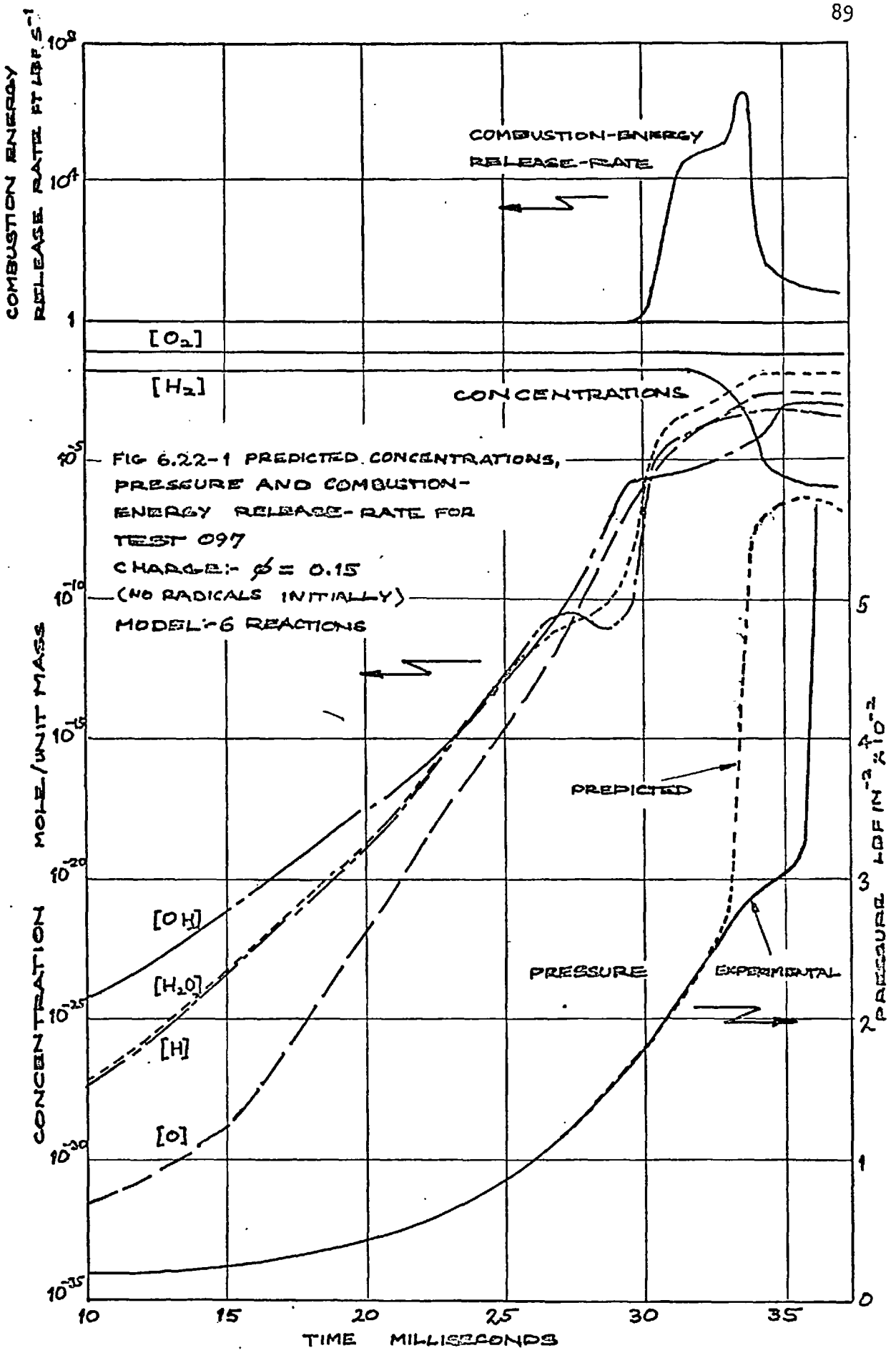
COMBUSTION ENERGY RELEASE RATE FT LBF S⁻¹
COMBUSTION-ENERGY RELEASE-RATE
[O₂]
[H₂]
CONCENTRATIONS
FIG 6.22-1 PREDICTED CONCENTRATIONS, PRESSURE AND COMBUSTION-ENERGY RELEASE-RATE FOR TEST 097
CHARGE:- ϕ = 0.15
(NO RADICALS INITIALLY)
MODEL:-6 REACTIONS
CONCENTRATION MOLE/UNIT MASS
PREDICTED
[OH]
[H₂O]
[H]
[O]
PRESSURE
EXPERIMENTAL
PRESSURE LBF IN⁻² X 10⁻²
TIME MILLISECONDS

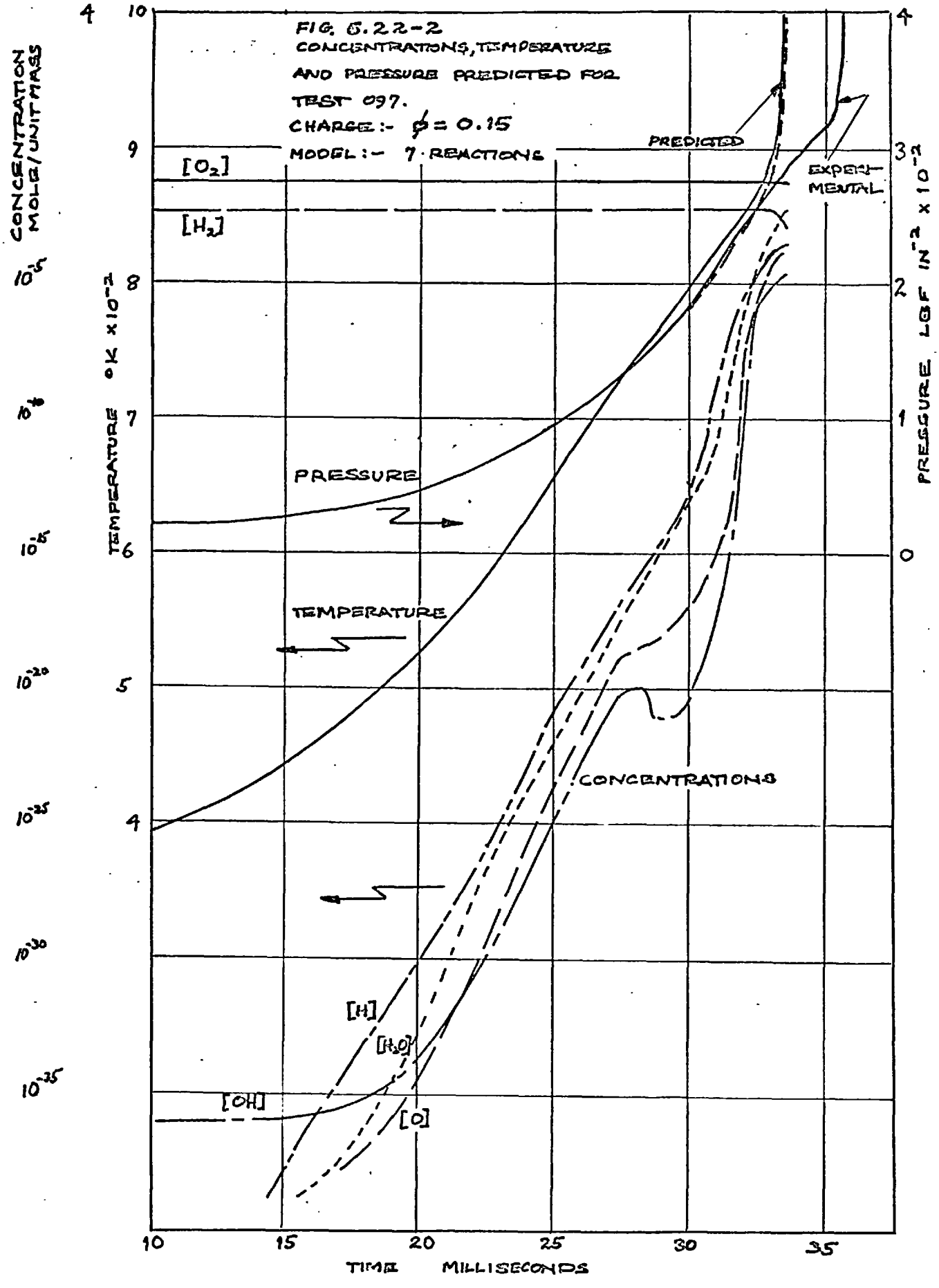
FIG. 6.22-2
CONCENTRATIONS, TEMPERATURE AND PRESSURE PREDICTED FOR TEST 097.
CHARGE:- $\phi = 0.15$
MODEL:- 7 REACTIONS
PREDICTED
EXPERIMENTAL
$[O_2]$
$[H_2]$
PRESSURE
TEMPERATURE
CONCENTRATIONS
$[H]$
$[H_2O]$
$[OH]$
$[O]$
CONCENTRATION MOLE/UNIT MASS
TEMPERATURE °K x 10^{-2}
PRESSURE LBF IN^{-2} x 10^{-2}
TIME MILLISECONDS
10
15
20
25
30
35
4
5
6
7
8
9
10
0
1
2
3
4
10^{-5}
10^{-10}
10^{-15}
10^{-20}
10^{-25}
10^{-30}
10^{-35}

model, some reactions proceed sufficiently rapidly to deplete the system of certain species, and there is a time delay before a mechanism, with a small number of reactions, can compensate for their loss.

6.23 The 9 reaction model

In the same way as the initiation reactions were added, reaction VIII was added to the five reaction scheme and its importance proven by changing τ_p in tests of 1.0 equivalence ratio. Therefore, it was concluded that any scheme for the species H_2, O_2, H, O, OH and H_2O ought to include all the reactions I to IX.

Concentration, pressure and temperature profiles predicted from these nine reactions are plotted in fig 6.23-1, for the same $\phi = 0.15$ test as in previous figures. The difference between predicted and observed induction time $\Delta\tau$ is now 1.9 ms (5.0%).

The predicted concentration curves are free from sudden troughs with the more complex model. It is interesting to note that for the first 30 ms of the induction period [H] and [H_2O] follow each other closely, indicating that the reaction is proceeding by the equation

$$2H_2 + O_2 \rightarrow 2H_2O + 2H \qquad 5.23\text{-}1$$

and that [O] and [OH] may be regarded as steady-state intermediate compounds.

As with the simpler reaction models, there was no agreement between predicted (τ_p) and observed (τ_e) induction-time at other mixture strengths. For example, at $\phi = 0.05$ $\Delta\tau$ was 0.9 ms (2.4%) and at $\phi = 2.5$, τ_p was late of τ_e, $\Delta\tau = -1.9$ ms (5%).

Similar comparisons were made between τ_p and τ_e using the rate-constant data from the present survey instead of that from reference [26.]. The extreme values of $\Delta\tau$, throughout the mixture range, were 1.8 ms (4.8%) at $\phi = 0.15$ and -0.2 ms (0.5%) at $\phi = 2.5$, representing

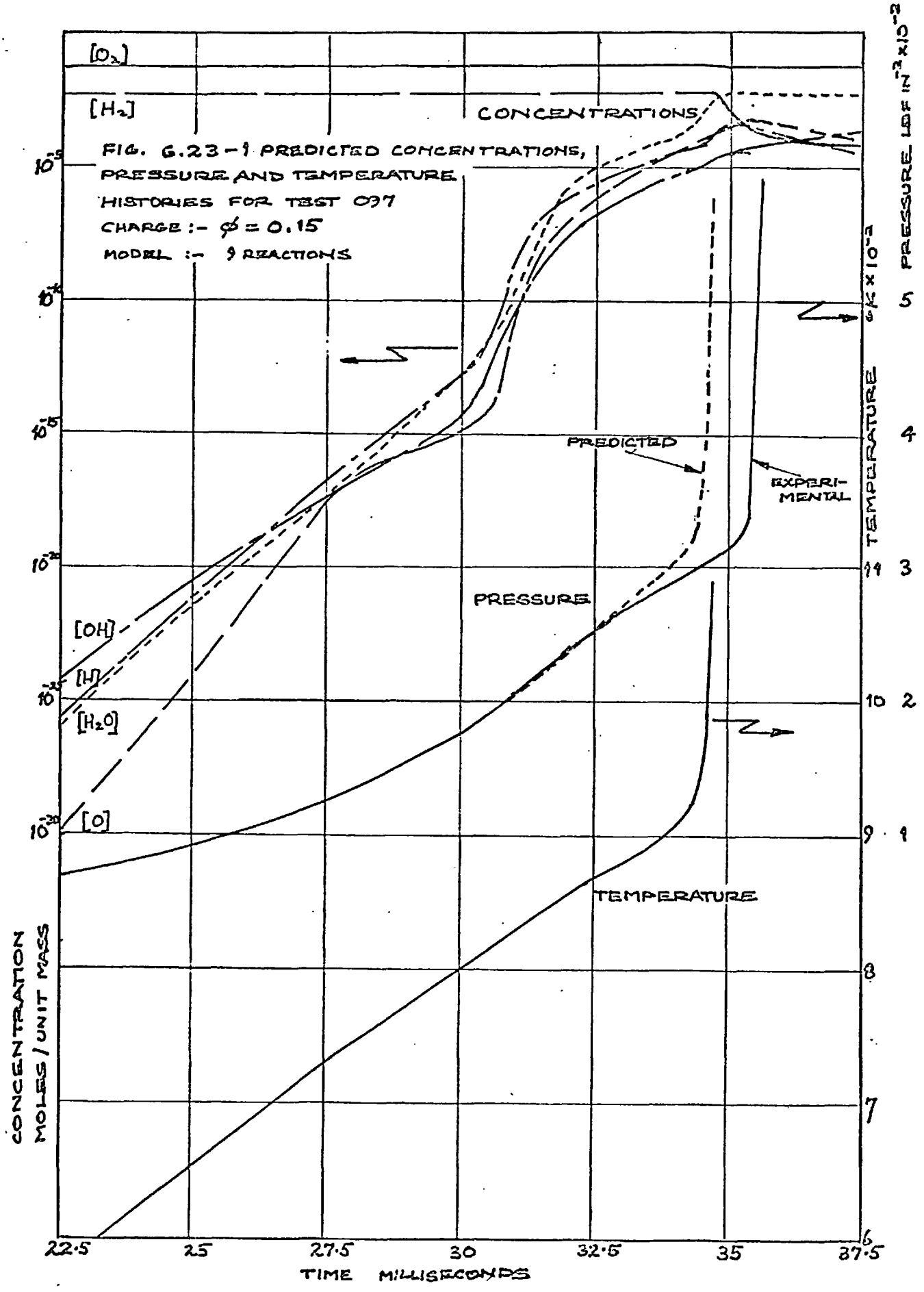
[O₂]
[H₂]
CONCENTRATIONS
FIG. 6.23-1 PREDICTED CONCENTRATIONS, PRESSURE AND TEMPERATURE HISTORIES FOR TEST 097
CHARGE :- φ = 0.15
MODEL :- 9 REACTIONS
PREDICTED
EXPERI-MENTAL
PRESSURE
[OH]
[H]
[H₂O]
[O]
TEMPERATURE
CONCENTRATION MOLES / UNIT MASS
TEMPERATURE °K x 10⁻³
PRESSURE LBF IN⁻² x 10⁻²
TIME MILLISECONDS
22·5
25
27·5
30
32·5
35
37·5

better agreement than with the data previously used.

6.24 A scheme for including reactions of HO_2 and H_2O_2

Thus far we have ignored possible reactions for the species HO_2 and H_2O_2, although they are probably of importance for a limited range of equivalence ratio at ignition temperatures up to 900°K.

Table 3.42-1 listed eleven reactions involving HO_2 and H_2O_2, but for most of these there are, at best, few reported values for their rate constants. However, Baldwin [3.] proposed a simplified scheme in which reactions X, XVI, XVII and XVIII were most important for these species. In Appendix C rate constants of these four reactions have been obtained from the limited data available.

These four reactions for HO_2 and H_2O_2 were added to the nine reaction scheme and their effect on the predicted induction-time determined.

6.25 The results with the 13 reaction model

Fig 6.25-1 shows predicted concentrations, pressure, temperature and combustion-energy release-rates for a $\phi = 0.15$ mixture. The predictions are based on rate constants from reference [26.] for reactions I to IX and values from the present survey for the remaining reactions. $\Delta\tau$ may be seen as 1.1 ms (3.0%), whereas with only nine reactions it was 0.9 ms (2.4%) for the test shown. At other values of ϕ throughout the mixture range, $\Delta\tau$ was changed by approximately the same amount.

6.3 Conclusions

In this chapter we have seen that the induction-time, τ_p, deduced from the predicted pressure-time history, may be influenced by the kinetic data on which the prediction calculations are based.

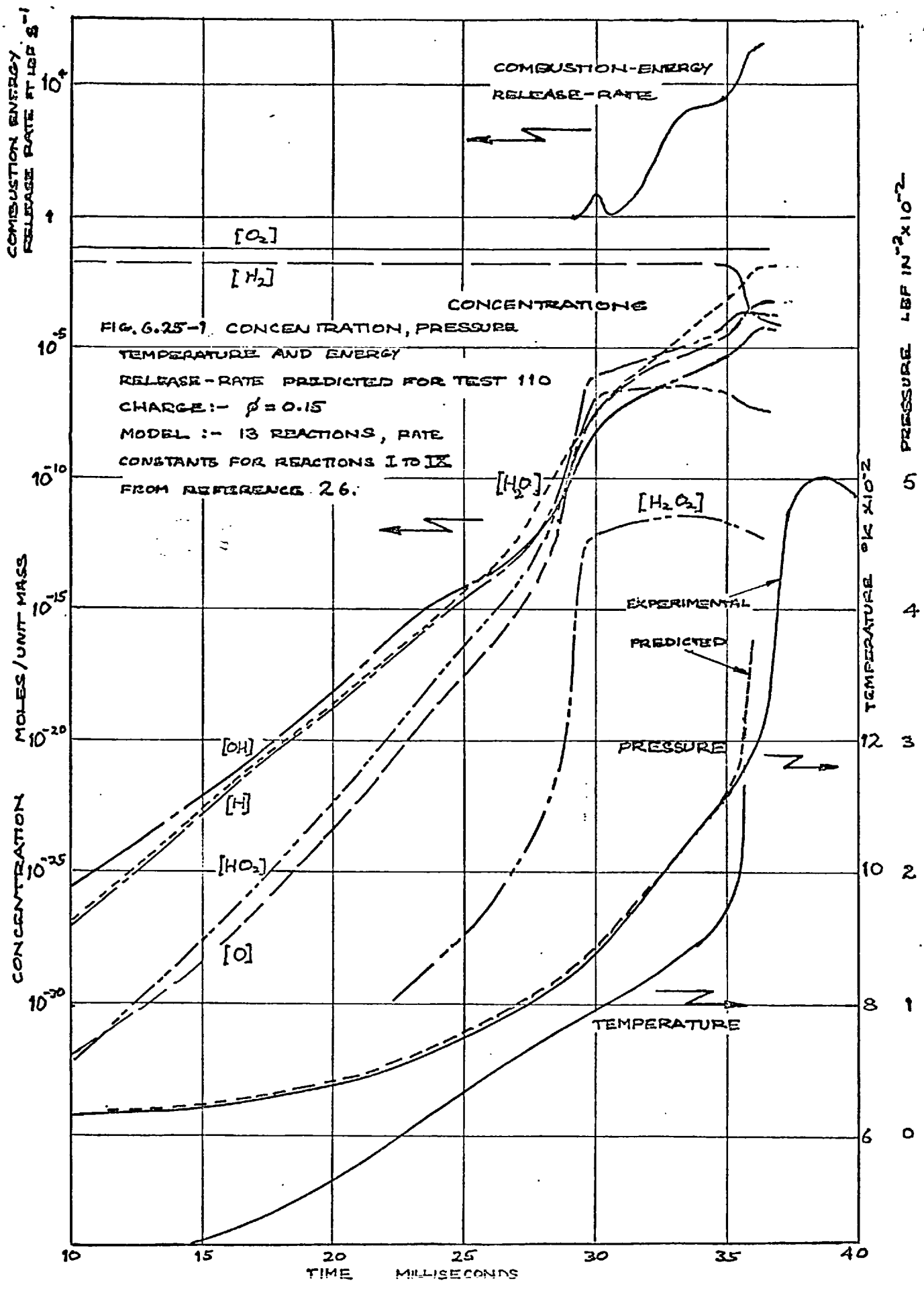

FIG. 6.25-1 CONCENTRATION, PRESSURE TEMPERATURE AND ENERGY RELEASE-RATE PREDICTED FOR TEST 110
CHARGE:- $\phi = 0.15$
MODEL :- 13 REACTIONS, RATE CONSTANTS FOR REACTIONS I TO IX FROM REFERENCE 26.

When considering reactions of the species H_2, O_2, H, O, OH and H_2O we found that reactions VI to IX ought to be added to the model of reactions I to V which we used at the outset, since each of the additional reactions altered τ_p at some mixture strength within the range $\phi = 0.05$ to 2.5. Changing the rate constants from the data of Jenkins et al. [26.] to that obtained in Appendix C gave reduced differences between predicted and observed induction-times at most mixture strengths.

Next, including reactions XI, XVI, XVII and XVIII for the species HO_2 and H_2O_2 demonstrated only small changes in τ_p, despite the relative uncertainty, when compared to reactions I to IX, of the rate-constant data.

It was concluded that reactions I to IX predominantly controlled the reaction mechanism of the ignition of hydrogen and oxygen over the range of experimental conditions at present considered. However, neither of the available sets of rate constants could be used to predict induction-time in quantitative agreement with the experimental results. Therefore, we conclude that these rate constants, which have in general been derived at pressures of 1 atmosphere or less, are no longer pertinent to autoignition at the present elevated pressures: 10 to 25 atmospheres. To obtain the desired quantitative agreement we shall need to find, in the next chapter, a new set of rate constants.

CHAPTER 7

THE EFFECTIVE RATE-CONSTANTS

7.1 Introduction

7.11 The procedure for rate constant adjustment

In the last chapter we demonstrated the need for a new set of rate constants for reactions I to IX*, which would enable the prediction pressure-time histories in agreement with experimental observations.

The strategy, by which this kinetic data may be derived, is simple in principle: experimental pressure-time records are obtained for a wide range of test conditions; with the help of a suitable digital-computer programme, rate constants are then calculated which, when applied, predict the observed results within a specified tolerance.

In execution, this strategy is difficult to effect: in the forward rate of each of the nine reactions we can relax both activation energy and pre-exponential constants, in which case we must perform a search in space of 18 dimensions for their desired values. Such a search, even if possible, may lead to rate constants which contradict the accepted values, unless many experimental results are surveyed.

The present strategy is more modest; the activation energies, obtained by the survey in Appendix C, are assumed to be correct. Only the pre-exponential factors are altered. The method of pre-exponential factor (hereinafter implied in rate constant) adjustment is an iterative procedure: guided by the sensitivity, through-

---

* See table 3.42-1.

out the experimental range of mixture composition, of the predicted induction-time, τ_p, to changes in the forward rate of each reaction in turn, the rates of influential reactions are systematically adjusted to minimise $\Delta\tau$ - the difference between observed and predicted induction-times. With the adjusted values, the τ_p's are re-calculated over the mixture range. If any $\Delta\tau$ is non-zero, the sensitivities are again computed and adjustments made, until $\Delta\tau$ is zero for all mixture compositions.

In addition to being guided by the sensitivity calculations any adjustment to a rate constant was checked for compatibility with the evidence of the rate-constant survey, see Appendix C. For example, there are only two reported values; for the third-body collision-efficiency of argon in reaction VII; we have taken the rate constant for a bimolecular third-body, M, instead. Adjustment of the rate of this reaction in the direction indicated by the M=argon points is considered consistent.

7.12 The experimental tests on which the data adjustment is founded

Initially, adjustment of the rate constants was made for the tests identified as 110, 160 and 131, whose respective equivalence ratios were ϕ = 0.15, 1.0 and 2.5. By considering only three tests, the amount of computer time required for the initial stages of adjustment was reduced. Then for the final adjustment we included in the procedure the remaining equivalance ratios at which experimental results had been obtained.

All the tests, used in the adjustment procedure, were selected to have experimental induction-times, τ_e, occurring within $\pm$ 0.5 ms of the P.M.P.T. of 37.5 ms, when the influence of changing density on induction-time is minimised.

7.13 The kinetic data adjusted and the terminology

In section 6.24, we saw that the set of rate constants from the present survey gave the least variation in $\Delta\tau$ over the mixture range. These were the rate constants which were adjusted, and their original values were called the reference values. With this data the values of $\Delta\tau$ obtained were 1.8, -0.3 and -0.2 ms for tests 110, 160 and 131 respectively. By adjusting the rate of reaction 11 by x 1/4. the values of $\Delta\tau$ become 0.0, -0.3 and -0.4 ms. This starting point for the major data adjustment is called the standard data. Starting with the standard data, rather than the reference data, has the advantage of bringing the values of $\Delta\tau$ close to zero, so that changes in $\Delta\tau$ become more nearly linear with rate-constant adjustment and systematic adjustment can therefore be made more swiftly.

The reaction rates, which make the values of $\Delta\tau$ zero* at all mixture strengths, are defined as the effective reaction-rate constants.

7.2 Rate Constant Adjustment

7.21 The sensitivity of induction-time to standard-data adjustment

At each stage in the adjustment of the rate constants towards the effective values, the forward rates of each of the nine reactions are altered independently by factors in the range $\pm$ 5. The induction-times computed with these rates lead to a curve of τ_p vs. adjustment-factor for each reaction.

Figure 7.21-1 shows, for three equivalence ratios, the effect on the relative induction-times $\Delta\tau_s^+$ of adjustment of reaction 11 from

---

* In practice, $\Delta\tau$ in the range $\pm$ .1 ms was sufficiently close to zero, being comparable with the experimental tolerance on τ_e.

+ $\Delta\tau_s$ is defined as the difference between τ_p calculated with adjusted rate data and τ_p calculated with the standard data.

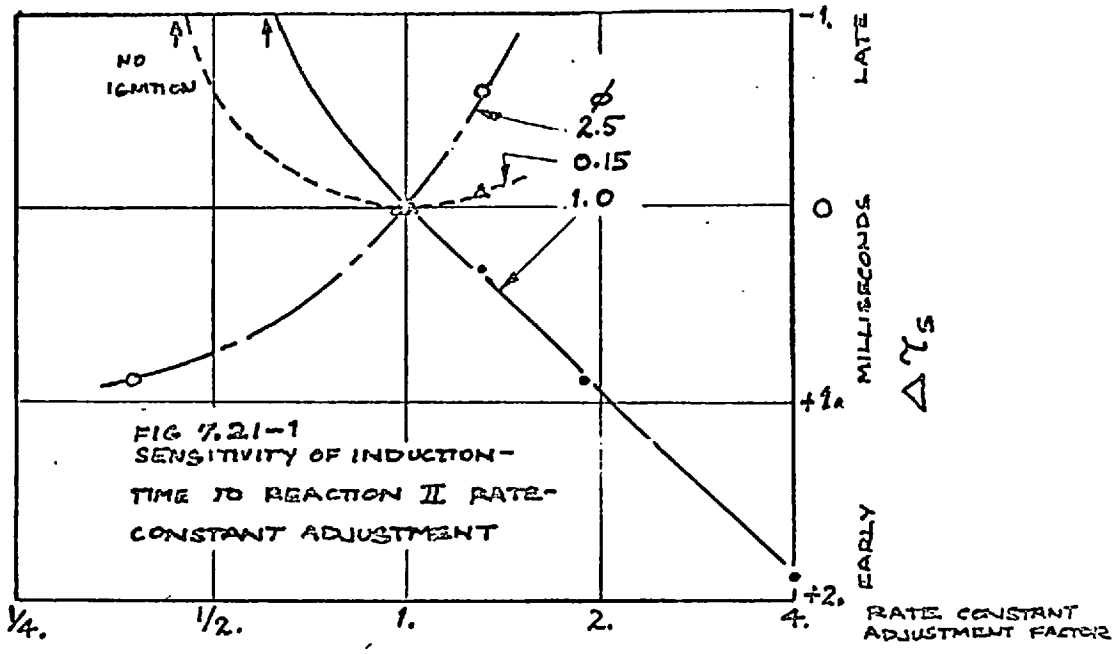

FIG 7.21-1
SENSITIVITY OF INDUCTION-TIME TO REACTION II RATE-CONSTANT ADJUSTMENT

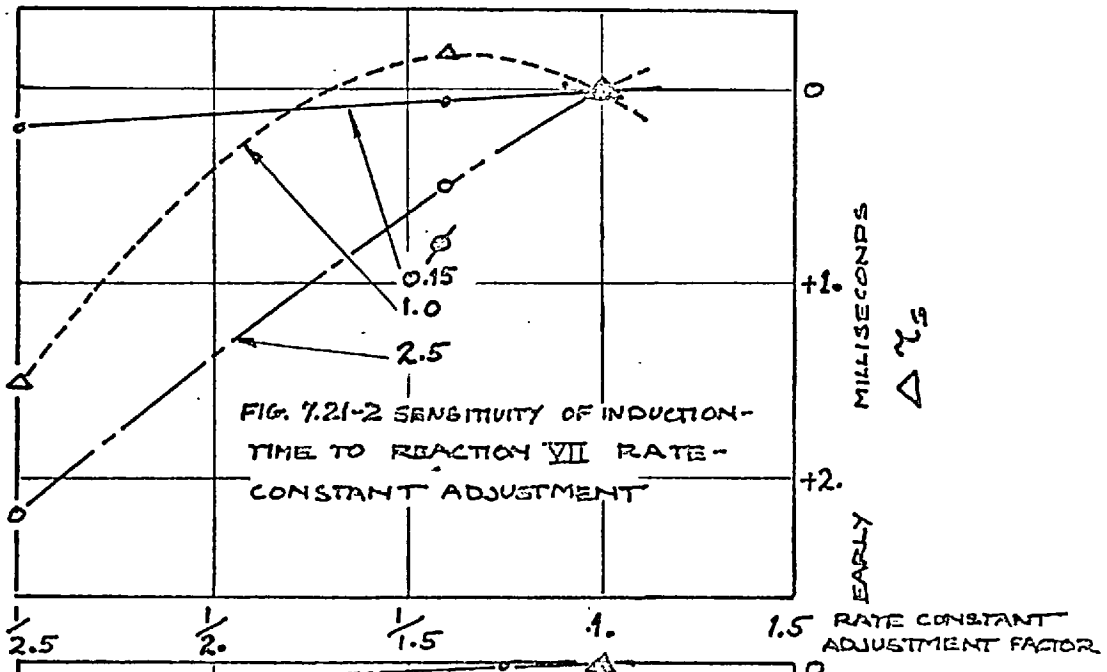

FIG. 7.21-2 SENSITIVITY OF INDUCTION-TIME TO REACTION VII RATE-CONSTANT ADJUSTMENT

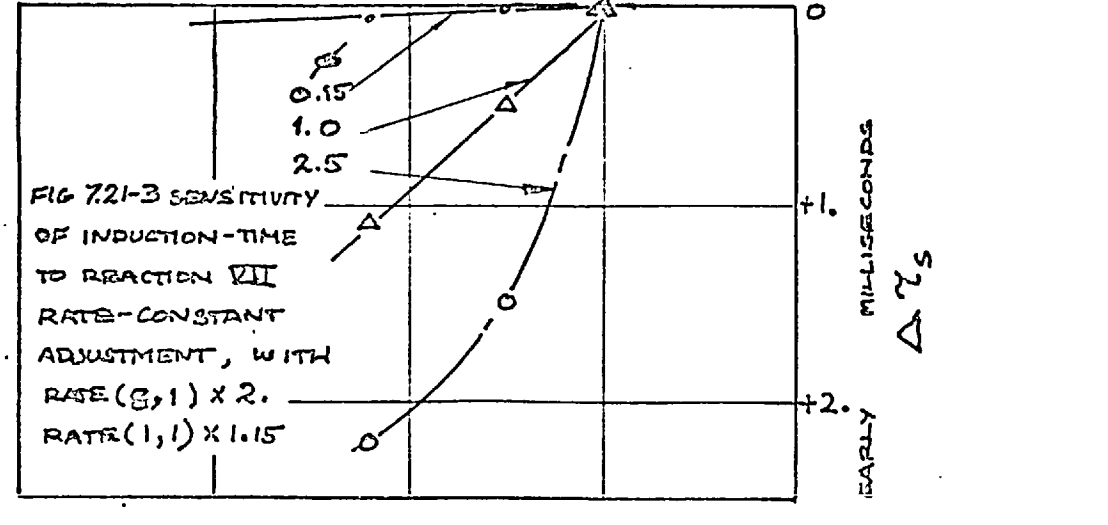

FIG 7.21-3 SENSITIVITY OF INDUCTION-TIME TO REACTION VII RATE-CONSTANT ADJUSTMENT, WITH
RATE(8,1) X 2.
RATE(1,1) X 1.15

its standard value. The next two figures demonstrate how the sensitivity curves are altered, for reaction VII, when other reactions assume: firstly their standard data, fig 7.71-2; and secondly adjustments from their standard values (VIII x 2. anx I x 1.15). It is apparent that the adjustment of additional reactions has re-shaped the effects of adjustment on $\Delta\tau_s$. Thus clearly demonstrating why, when any reaction is adjusted to minimise $\Delta\tau$, we need to recompute the new induction-time sensitivity values for the remaining reactions.

In fig 7.21-4, a cross plot of $\Delta\tau_s$ vs. adjustment-factor is shown, for a factor of x 1/2.5. The effects, for each reaction, of adjustment on $\Delta\tau_s$ throughout the equivalence-ratio range may be gauged.

7.22 One step in the overall procedure of rate-constant determination

We can now illustrate, with the aid of figs 7.21-1 to 7.21-4, one step in the procedure of minimising $\Delta\tau$. We recall at ϕ = 2.5, $\Delta\tau$ was -0.4 ms. Fig 7.21-4 indicates that τ_p at rich mixtures is predominantly controlled by reaction VIII. This was confirmed by cross-plots at other adjustment factors. On fig 7.21-2 we can see that at ϕ = 2.5 a factor of x 1/1.4 gives the value of $\Delta\tau_s$ = 0.4 ms, sufficient to negate $\Delta\tau$ at this equivalence ratio. By such an adjustment the values of $\Delta\tau$ are altered to -.2 ms and -.2 ms at ϕ = 0.15 and 1.0 respectively, which we must proceed to eliminate in the next stage of adjustment.

7.23 The effective rate-constants

By systematic adjustment as exemplified above, only one set of values for the rate constants was found which gave agreement between

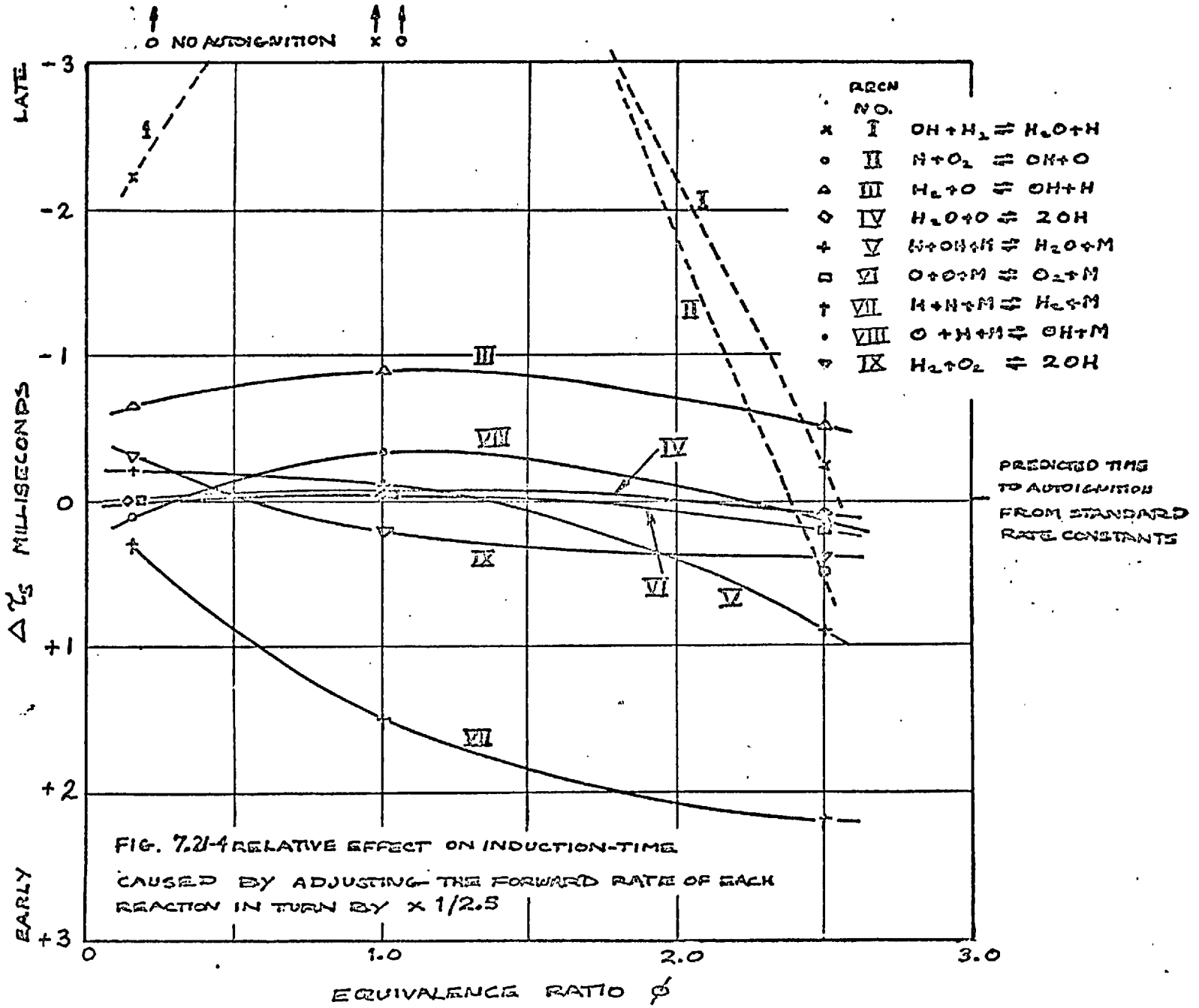

FIG. 7.21-4 RELATIVE EFFECT ON INDUCTION-TIME CAUSED BY ADJUSTING THE FORWARD RATE OF EACH REACTION IN TURN BY × 1/2.5

experimental and predicted-induction times at six values of mixture composition throughout the range ϕ = 0.05 to 2.5. Table 7.23-1 shows the final adjusted values - the effective rate-constants of the forward reaction. F is the factor by which the reference data has been multiplied to obtain the tabulated values. Also tabulated are the fitted equilibrium constants used for calculating the backward reaction rates.

From the table it is apparent that adjustments were necessary to all reaction rates except those of IV, VI and IX. The precision of adjustment varies from reaction to reaction. For example: adjustment of III by x 1/1.1 represents a change in induction time of only 0.1 ms at ϕ = 1.0 and 2.5, whereas the same adjustment to reaction VII corresponds to a change in τ_p of 0.8 ms at ϕ = 2.5.

Fig 7.23-1, 7.23-2 and 7.23-3 present the results predicted from the effective rate-constants at ϕ = 0.05, 1.0 and 2.5 respectively. The figures give the following predicted information: the concentration-time profiles for the species H_2, O_2, H, O, OH and H_2O; the temperature-time history; and computed and experimental pressure-time records.

Peak pressure agreement between computed and predicted pressure is not as good as before and during autoignition. This is largely attributed to errors in experimental mixture strength, which result in negligible effect on induction-time, but influence the combustion-pressure rise.

7.24 Some conclusions about the effective rate-constants

We have called the derived values effective rate-constants for two reasons:

TABLE 7.23-1 'FITTED' EQUILIBRIUM-CONSTANTS AND 'EFFECTIVE' FORWARD-REACTION-RATE CONSTANTS FOR 9 REACTIONS AND 'FITTED' CONSTANTS FOR 4 FURTHER REACTIONS

Reaction rate given by $k_f = A\ T^B \exp(-E/RT)$ $(cm^3\ mole^{-1})^{n-1}\ s^{-1}$ where n is the reaction order.

Adjustment factor F is the value by which the 'reference' 'A' has been multiplied to obtain the tabulated 'A'.

Equilibrium constant is given by $K_C = A_C T^{B_C} \exp(-C/T)$.

Reaction	k_f				K_C		
Number	A	B	E	F	$\text{Log}_e A_C$	B_C	C
I	0.174 E-02	0.508 E 01	0.1215 E 04	1.15	-0.21752E 01	0.79933E-01	-0.76905E 04
II	0.42 E 14		0.1617 E 05	1/3.7	0.58294E 01	-0.38762E 00	0.86348E 04
III	0.24 E 07	0.206 E 01	0.5630 E 04	1/1.1	0.67190E 00	0.19000E-01	0.92919E 03
IV	0.83 E 14		0.1810 E 05		0.28471E 01	-0.60933E-01	0.86197E 04
V	0.37 E 17		0.1600 E 04	2.0	-0.55144E 01	-0.12152E.01	-0.59791E 05
VI	0.24 E 15		-0.660 E 03		-0.84967E 01	-0.88857E 00	-0.59806E 05
VII	0.555 E 15		-0.1531 E 04	1/1.4	-0.33392E 01	-0.12952E 01	-0.52101E 05
VIII	0.16 E 17		-0.2780 E 04	3.	-0.26673E 01	-0.12762E 01	-0.51172E 05
IX	0.256 E 12		0.4330 E 05		0.65013E 01	-0.36862E 00	0.95639E 04
	'Fitted' values for HO_2, H_2O_2 reactions						
X	0.55 E 18		0.1280 E 05		-0.47324E 01	-0.100535E 01	-0.23530E 05
XVI	0.457 E 15		0.1345 E 05		-0.23949E 01	0.92585E -01	-0.21327E 05
XVII	0.32 E 19		0.4320 E 04		0.15022E 02	0.25412E 00	0.25850E 05
XVIII	0.434 E 17		0.1610 E 05		0.95074E 01	-0.96114E 00	-0.33941E 05

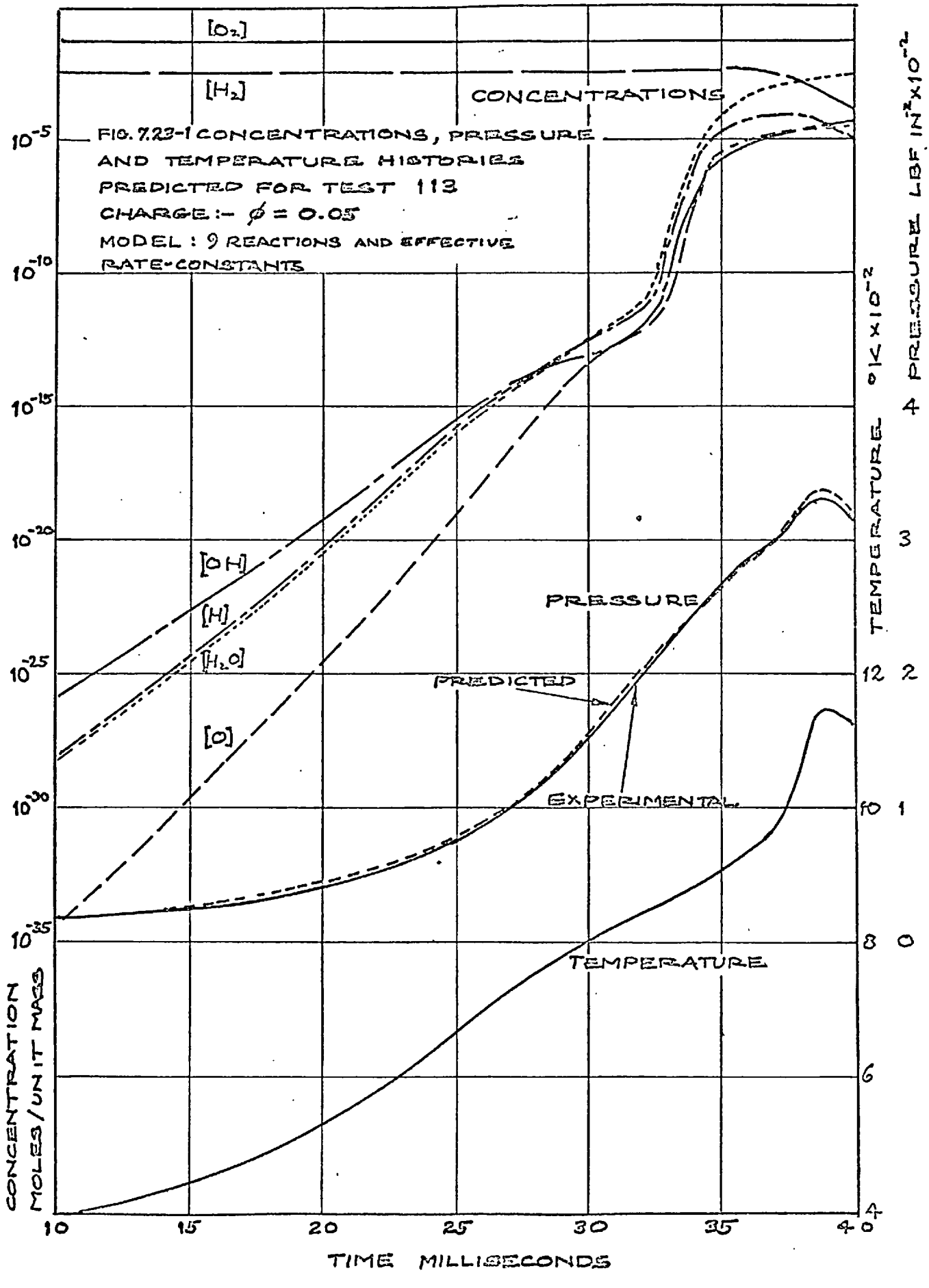
[O2]
[H2]
CONCENTRATIONS
FIG. 7.23-1 CONCENTRATIONS, PRESSURE AND TEMPERATURE HISTORIES PREDICTED FOR TEST 113
CHARGE:- φ = 0.05
MODEL : 9 REACTIONS AND EFFECTIVE RATE-CONSTANTS
[OH]
[H]
[H2O]
[O]
PRESSURE
PREDICTED
EXPERIMENTAL
TEMPERATURE
CONCENTRATION MOLES/UNIT MASS
TEMPERATURE °K x 10⁻²
PRESSURE LBF IN⁻² x 10⁻²
TIME MILLISECONDS
10⁻⁵
10⁻¹⁰
10⁻¹⁵
10⁻²⁰
10⁻²⁵
10⁻³⁰
10⁻³⁵
10
15
20
25
30
35
40
4
6
8
10
12
0
1
2
3
4

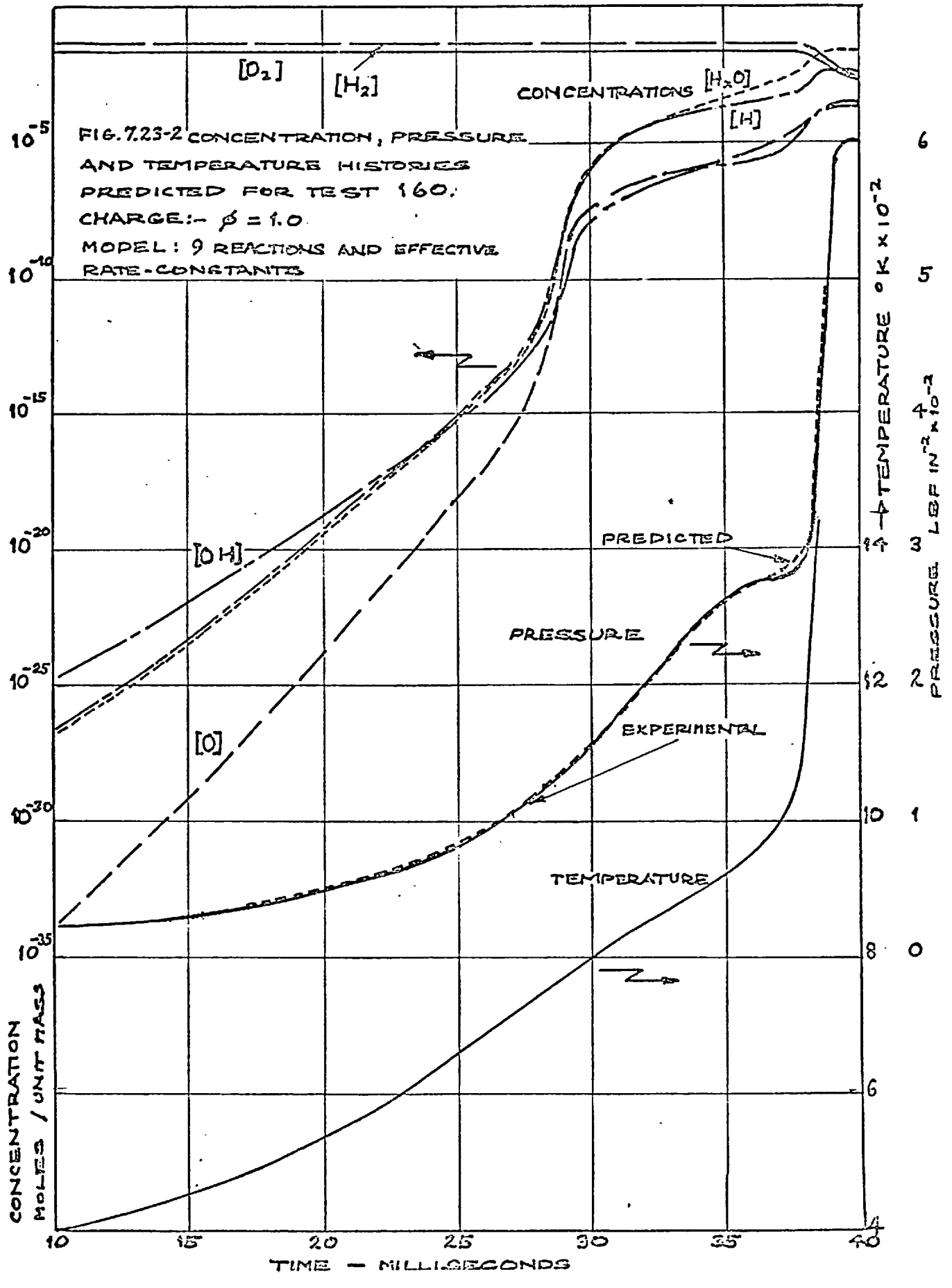
FIG. 7.23-2 CONCENTRATION, PRESSURE AND TEMPERATURE HISTORIES PREDICTED FOR TEST 160.
CHARGE:- ϕ = 1.0
MODEL: 9 REACTIONS AND EFFECTIVE RATE-CONSTANTS
[O2]
[H2]
CONCENTRATIONS
[H2O]
[H]
[OH]
[O]
PREDICTED
PRESSURE
EXPERIMENTAL
TEMPERATURE
CONCENTRATION MOLES / UNIT MASS
TEMPERATURE °K x 10-2
PRESSURE LBF IN-2 x 10-2
TIME — MILLISECONDS
10-5
10-10
10-15
10-20
10-25
10-30
10-35
10
15
20
25
30
35
40
6
5
4
3
2
1
0

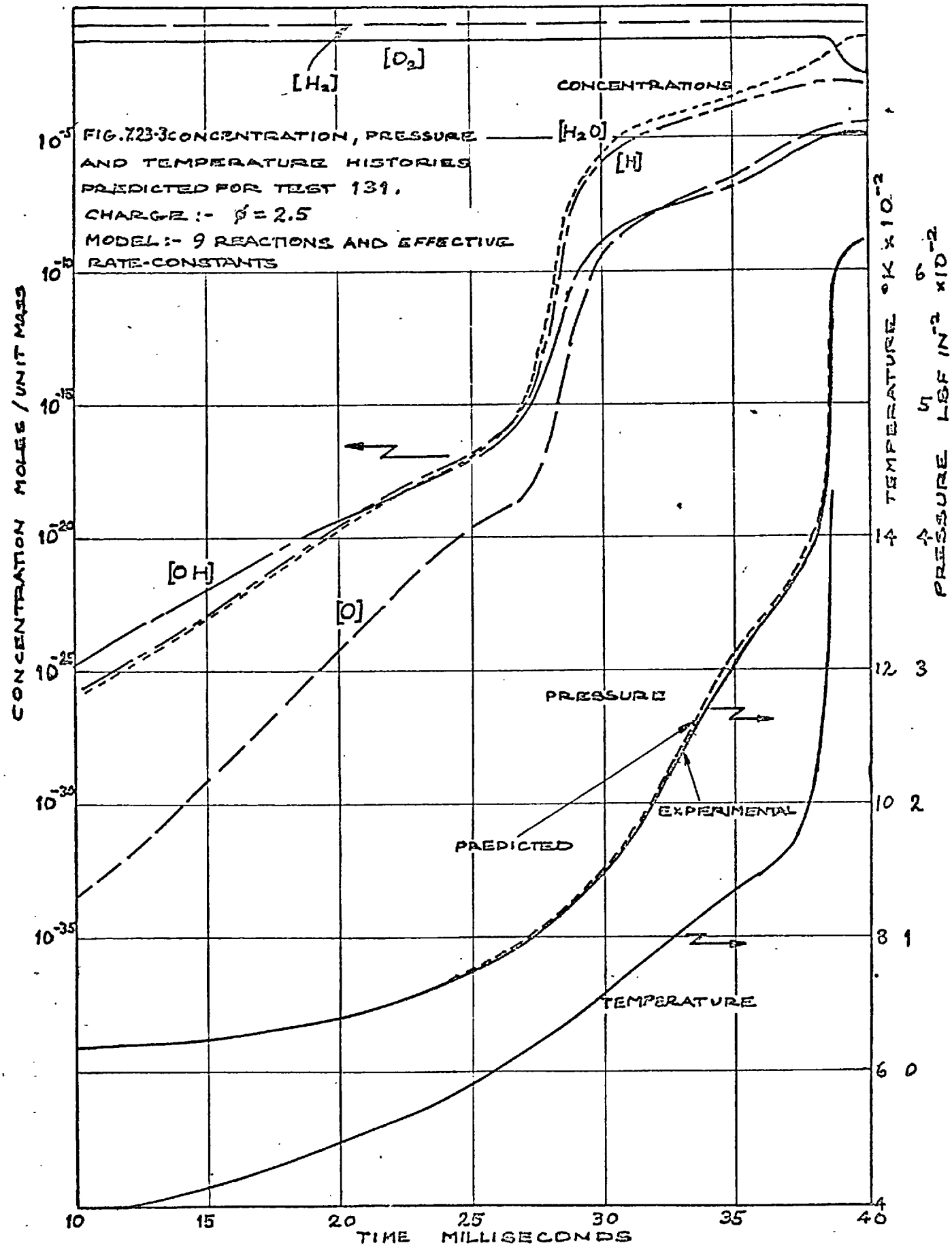
FIG. 7.23-3 CONCENTRATION, PRESSURE AND TEMPERATURE HISTORIES PREDICTED FOR TEST 131.
CHARGE :- $\phi = 2.5$
MODEL :- 9 REACTIONS AND EFFECTIVE RATE-CONSTANTS
CONCENTRATIONS
$[H_2]$
$[O_2]$
$[H_2O]$
$[H]$
$[OH]$
$[O]$
PRESSURE
TEMPERATURE
EXPERIMENTAL
PREDICTED
CONCENTRATION MOLES / UNIT MASS
10^{-5}
10^{-10}
10^{-15}
10^{-20}
10^{-25}
10^{-30}
10^{-35}
TEMPERATURE °K x 10^{-2}
PRESSURE LBF IN^{-2} x 10^{-2}
14
12
10
8
6
6
5
4
3
2
1
0
4
10
15
20
25
30
35
40
TIME MILLISECONDS

1. The nine-reaction model does not account for all known reactions of the H_2-O_2 system: others which have not been investigated may be important; especially those of the species HO_2 and H_2O_2.

2. The reaction rates were derived for a small range of experimental conditions. More experimental tests are required to confirm that the constants are applicable to a wider range of density-time histories and equivalence ratios.

Nonetheless, the effective rate-data does provide, for the first time, rates of reactions applicable to pressures in the range 10 to 25 atmospheres at temperatures in the range 875 to 1200°K. Additionally, the rate values, provided they are used with the kinetic model for which they were derived, will have application to the prediction autoignition in less simplified piston-engines.

7.3 The significance of reactions for HO_2 and H_2O_2

7.31 Introduction

In section 6.25 we conducted a preliminary investigation of the effect on induction-time of adding four reactions (X, XVI, XVII, and XVIII) for the species HO_2 and H_2O_2 to the nine-reaction model. Again we use this mechanism, but with the effective rate-constants for the first nine reactions, to assess the influence of the additional reactions on the predicted results.

7.32 Discussion of the results

The results demonstrated that the four additional reactions had small effects on predicted induction-times, depending upon mixture composition. At $\phi = 2.5$, $\Delta\tau$ was still zero, as may be seen in fig 7.32-1. While at $\phi = 1.0$, τ_p was advanced by 0.3 ms and at $\phi = 0.15$, $\Delta\tau = -0.2$ ms. The results at $\phi = 0.08$ and 0.05 were contrary to the

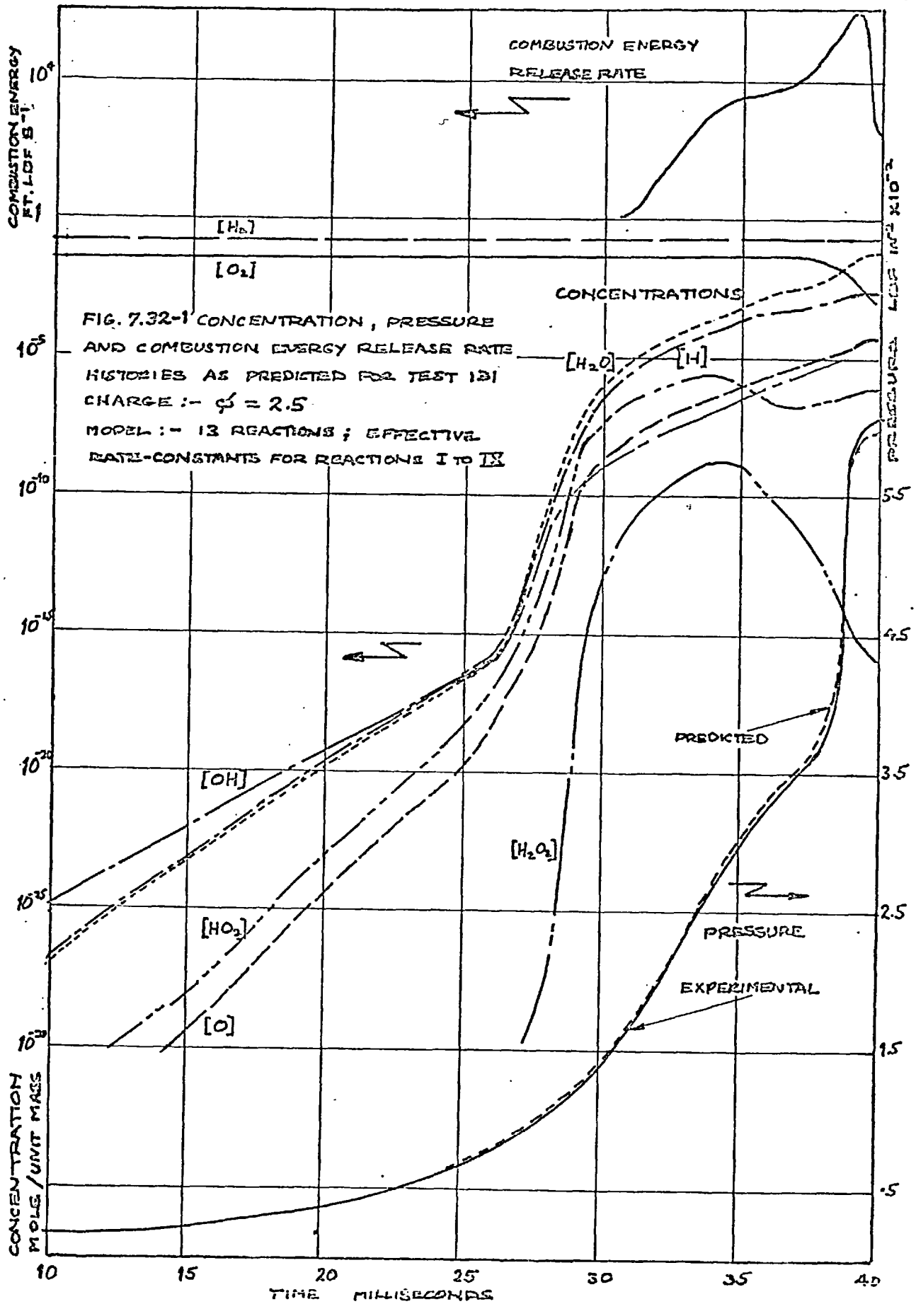

FIG. 7.32-1 CONCENTRATION, PRESSURE AND COMBUSTION ENERGY RELEASE RATE HISTORIES AS PREDICTED FOR TEST 131
CHARGE :- $\varphi = 2.5$
MODEL :- 13 REACTIONS; EFFECTIVE RATE-CONSTANTS FOR REACTIONS I TO IX

last mentioned, having $\Delta\tau$ = 0.3 and 0.2 ms respectively.

From the inconsistent affects at weak mixtures it was deduced that away from rich mixtures the reactions are of greatest significance. Confirming this deduction is another result: fig 7.32-2 shows predicted results at ϕ = 0.08. In the rate of combustion-energy release there are two peaks, whereas in the previous figure for ϕ = 2.5 only a single peak was in evidence. Two peaks were also evident to a lesser extent at ϕ = 0.05 and 0.15, demonstrating that the prediction of a two-stage pressure rise is feasible. In the particular record shown the first peak does not reach sufficient magnitude to cause a detectable variation in the pressure record; but for shorter induction-times it is probable that the first-stage energy release will be greater.

This evidence is in direct agreement with the experimental observation of two-stage ignition at ϕ = 0.08 reported in section 5.25. Two points are noteworthy about the peroxide concentration profiles: 1. the hydrogen peroxide, $[H_2O_2]$, profile in figs 7.23-1 and -2 confirms the shape of peroxide concentrations, sampled during auto-ignition of a hydrocarbon fuel in a reciprocating engine, as reported by Downs and Wheeler [13.]. 2. the depression of the $[HO_2]$ concentration at 32 ms is similar to depressions in [OH] concentration, which were noted earlier in section 6.2, for the 5 and 6 reaction schemes. As the reaction model increased in complexity so the depressions disappeared. We can infer that the scheme of four reactions for the species HO_2 and H_2O_2 is not sufficiently complex to describe the mechanism in its entirety.

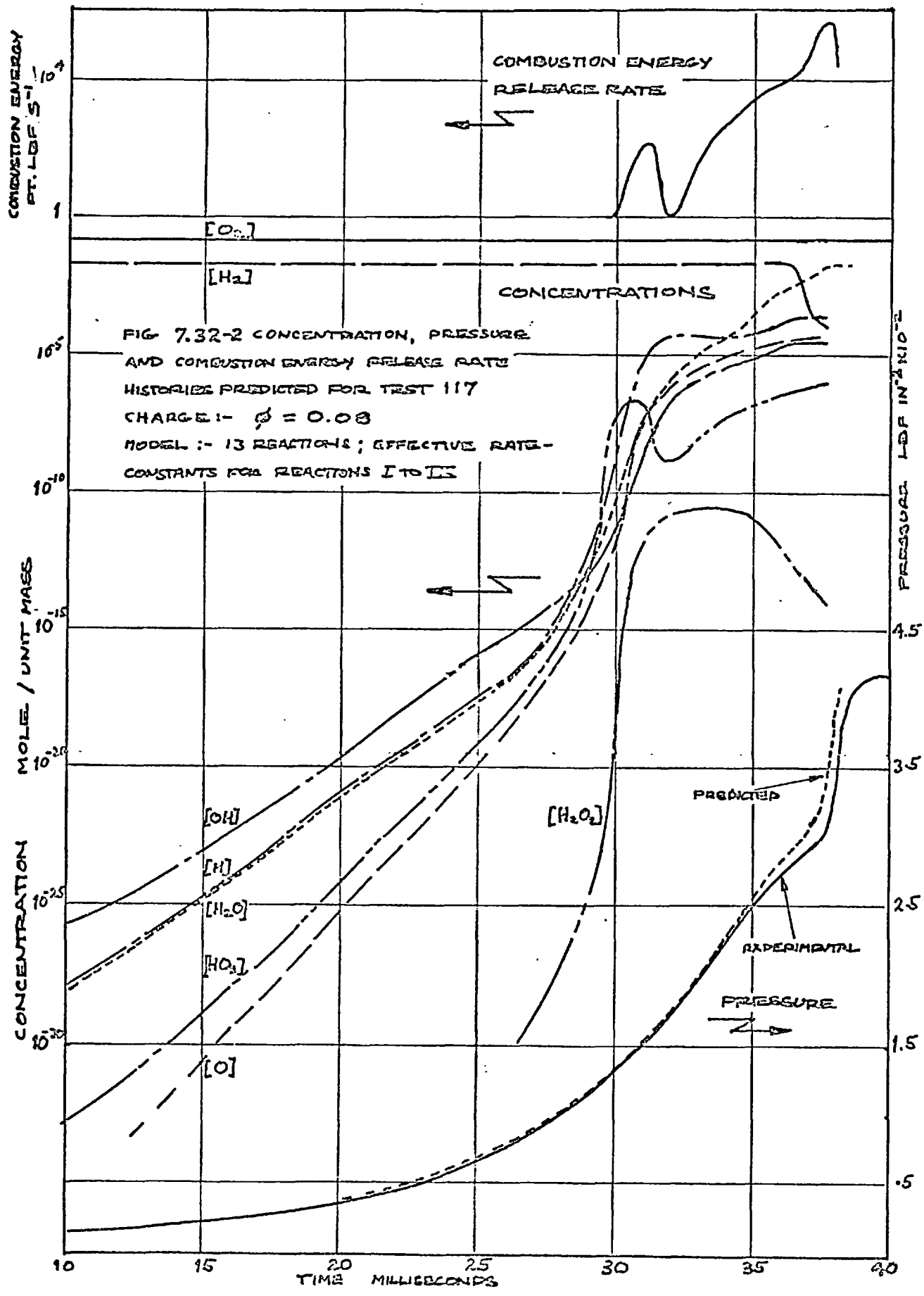

FIG 7.32-2 CONCENTRATION, PRESSURE AND COMBUSTION ENERGY RELEASE RATE HISTORIES PREDICTED FOR TEST 117
CHARGE :- $\phi = 0.08$
MODEL :- 13 REACTIONS ; EFFECTIVE RATE-CONSTANTS FOR REACTIONS I TO IX

7.33 Conclusions about the 13 reaction model

Application of the model demonstrated that the addition of four reactions for HO_2, H_2O_2, to the nine reaction scheme causes changes in induction-times up to 0.8%. No attempt has been made to derive effective reaction-rates for the additional reactions: there is evidence that the reaction model is still incomplete; and the foundation of the reaction rates is uncertain as there are few indications in the literature of values for the activation energies of the four reactions.

If work on these reactions is to be pursued, it would appear to be profitable to obtain more experimental results of two-stage ignition, before proceeding to establish reaction rate-constants.

CHAPTER 8

CONCLUDING REMARKS

8.1 Principal Results of the Present Study

The main objectives of this study, started in section 1.2, have been achieved. It has proved possible to predict for a piston-in-cylinder system, autoignition of hydrogen in agreement with results observed in a compression machine. However, this agreement was only obtained when values, different from those reported in the literature,were evolved for the kinetic data used in the prediction procedure. More specifically, the achievements of the present study were the following:

1. The solution was obtained for up to 10, simultaneous, non-linear differential equations, governing the progress of reaction in a gaseous system subjected to a prescribed density-change. A computer programme was written to solve the equations and predict the time dependence of parameters such as: pressure, temperature, species concentration and energy-release rates.

2. A compression machine was constructed in which engine-combustion phenomena may be studied with greater control over experimental parameters than in current research-engines. The single operating-cycle of the machine and its variable piston-motion are of considerable advantage: not only in obtaining autoignition results from which reaction kinetics can be derived; but also in many other areas of diesel and gasoline-engine combustion research.

3. Hydrogen-oxygen-argon mixtures were autoignited over the mixture range ϕ = 0.05 to 2.5.

4. A method was established for predicting the observed gas-to-wall heat-transfer in the compression machine.

5. An extensive survey of reported H_2-O_2 kinetic-data has been made. Plausible reaction models have been postulated and 'best' values for rate constants of 13 reactions have been calculated by statistical methods.

6. Comparisons were made between experimental and predicted induction-times leading to autoignition, throughout the range of mixture composition. When the predicted induction-times were calculated from the 'best' values for the rates of the individual reactions in various chain-reaction models, only qualitative agreement could be obtained between predicted and observed induction-times. To obtain quantitative agreement, it was necessary to derive the effective reaction-rates for a model containing nine reactions, of proven importance, for the species H_2, O_2, H, O, OH, and H_2O. These reaction-rates contribute to the knowledge of the kinetics of the H_2-O_2 reaction in the unexplored pressure range of 10 to 25 atmospheres at temperatures in the range 850 to 1200°K.

7. The kinetic model was extended to include four reactions for the species HO_2 and H_2O_2. Induction-times predicted with the model were only altered by small amounts, up to 0.8%. At weak mixtures, two-stage-energy release was indicated in accord with the experimental evidence of two-stage ignition for a narrow band of operating conditions.

8.2 Recommendations for future work

The value of the experimental and computational techniques in establishing chemical-kinetic data has been demonstrated. These

techniques form the foundations on which other kinetic studies could be based:

1. An extended experimental study of the two-stage ignition region of hydrogen could enable us to evaluate critically the importance, in the reaction mechanism, of plausible reactions of the species HO_2, H_2O_2; and to derive rate constants for the important reactions.

2. An increased understanding of the reactions of CO [7., 9., 62] should permit the investigation of the kinetics of H_2-O_2-CO mixtures,by the presently reported technique. Ultimately, it is hoped to extend experimental study and prediction of autoignition to hydrocarbon fuels: some details of the reaction kinetics of methane are already available [3., 14]. The prediction of methane autoignition would be an advance of considerable practical significance: it would be possible to determine which of the controlling variables influence the formation of harmful intermediate products of combustion, and indicate a way of reducing these polluants in the exhaust gas.

3. A similar study of the autoignition of H_2-O_2-N_2 mixtures would enable us to predict the formation of the oxides of nitrogen, and to investigate ways of reducing their concentrations in the exhaust gas.

Both the compression machine and the computational technique can also have independent application in future work:

4. Already, in the compression machine, some information has been obtained on the heat transfer from a rapidly-compressed gas to its surrounding walls. Extending this work to a wider range of experimental variables should lead to a better understanding of heat transfer in piston engines.

5. The computer programme is readily adaptable to the prediction of autoignition in other reciprocating engines: an obvious application is the prediction, from the presently-derived kinetic-data, of the autoignition of hydrogen in a motored engine.

REFERENCES

1. ANNAND, W.J.D. "Heat transfer in the cylinders of reciprocating internal combustion engines" Proc. I. Mech.E. 177, 1963, p. 973.
2. ANNAND, W.J.D. and ABAYZID, O.M. "Self ignition of propane-air mixtures in a supercharged, motored reciprocating engine." Proc. I. Mech. E. 181, 1967, 1, 20.
3. BALDWIN, R.R., NORRIS, A.C. and WALKER, R.W. "Reactions of methane in a slowly reacting hydrogen-oxygen mixture." 11th Symposium on Combustion, 1967, p. 889.
4. BASCOMBE, K.N. "Calculation of ignition delays in the hydrogen-air system." Combustion and Flame, 11, 1967, p. 2.
5. BASCOMBE, K.N. "Reaction kinetics of the H-O-N system." Aeronautical Research Council report, 1964.
6. BENSON, S.W. "Foundations of chemical kinetics." McGraw-Hill, 1960.
7. BRABBS, T.A. and BELLES, F.E. "Recombination of CO and O at high temperatures." 11th Symposium on Combustion, 1967, p. 125.
8. BROKAW, R.S. "Analytic solutions to the ignition kinetics of the hydrogen oxygen system." 10th Symposium on Combustion, 1965.
9. BROKAW, R.S. "Ignition kinetics of the carbon monoxide-oxygen reactions" 11th Symposium on Combustion, 1967, p. 1063.
10. BULEWICZ, E.M. Discussion contribution on kinetics of hydrogen-air flow systems. 9th Symposium on Combustion, 1962, p. 239.
11. CARSLAW, H.S. and JAEGER, J.C. "Conduction of heat in solids." Oxford, Clarendon Press, 1959.
12. CREASE, A.B. "A universal apparatus for reciprocating engine combustion." Unpublished final year report, Imperial College, London, 1966.

13. DOWNS, D. and WHEELER, R.W. "Recent developments in 'knock' research." Proc. I. Mech. E. (AD) 1952, p. 89.

14. DIXON-LEWIS, G. and WILLIAMS, A. "Some observations of the combustion of methane in pressurised flames." 11th Symposium on Combustion, 1967.

15. EICHELBERG, G. "Some new investigations on old combustion engine problems." Engineering, London, 148, 1939, p. 463.

16. EICHENBERGER, L.C. "Methods for dynamic pressure calibration of pressure transducers." NBS Monograph 67, p. 1.

17. ELSER, K. "Der instationäre wärmeubergang in diesel-motoren." Mitt. Inst. Thermodyn. Zurich, 1954, No.15, p. 19.

18. Engineering News, Sept. 23, 1965, Article 177. "Displacement transducers."

19. FALK, G. "The ignition temperature of hydrocarbon-oxygen mixtures." J. Am. Chem. Soc. 1907, 29, p. 1536.

20. FRISTROM, R.M. and WESTENBERG, A.A. "Flame structure." McGraw-Hill, 1965, p. 379.

21. Ditto. p. 67.

22. HAVEMANN, H.A. "Development of a compression apparatus." J. Ind. Inst. Sc., 37, 1955, 67.

23. HILSENRATH, J. et al. "Tables of the thermal properties of gases." NBS Circular 564, 1965.

24. HOLT,R.B. and OLDENBERG, O. "Spectroscopy of the role of H_2O_2 in the thermal combination of H_2 and O_2." Phys. Rev. 71, 1947, p. 479.

25. JANAF Thermochemical Tables. Dow Chemical Co., Midland, Michigan, 1963.

26. JENKINS, D.R., SPALDING, D.B. and YUMLU, V.S. "The combustion of hydrogen and oxygen in a steady flow stirred reactor." Thornton

Res.Centre Report TRCP 1224.

27. JOST, W. "Knock Reaction." 9th Symposium on Combustion, 1962, p. 1018.

28. KARIM, G.A., KLAT, S.R. and MOORE, N.P.W. "Knock in dual fuel engines." Proc. I. Mech. E. 181; 1967, 1, 20.

29. KARIM, G.A. "Application of elementary chemical kinetics to engine calculations." Proc. Symposium on Combustion in S.I. Engines, Cranfield, 1965.

30. KARIM,G.A. and WATSON, H.C. "Analytical expressions for some tabulated thermodynamic properties of the H-O-N system." Imperial College Report TN/C/2, 1967.

31. KHAN,M.A. "A critical survey of the rate constants of elementary steps in the high temperature flame of hydrogen and oxygen." Thornton Res. Centre Report TRCP 1191, 1965.

32. KLAT,S.R. "Combustion mechanisms in dual fuel engines." Ph.D. Thesis, London, 1965, p. 239.

33. KNIGHT, B.E. Discussion contribution to paper by Annand, W.J. Proc. I. Mech. E., 177, 36, 1963.

34. LEWIS, B. and VON ELBE, G. "Combustion, Flames and Explosions." Academic Press Inc. 1951.

35. MARQUARDT Report, "Literature survey of the H-O-N system." AD 297457, 1962.

36. McCRACKEN, D.T. and DORN, W.S. "Numerical methods and Fortran programming." J. Wiley, 1966.

37. MILKINS, E.E. M.Sc. Thesis, London, 1967.

38. MOMTCHILOFF, I.N., TABACK, E.D. and BUSWELL, K.F. "Kinetics in hydrogen air flow systems." 9th Symposium on Combustion, 1962, p.220.

39. NG.H. "Investigation of the ignition of hydrocarbon-air mixtures in an adiabatic compression machines." Ph.D. Thesis, London, 1963.

40. OVERBYE, V.D. et al. "Unsteady heat transfer in engines." Trans. S.A.E. 69, 1961, p. 461.

41. PERGAMENT, H.S. Hypersonic Ram Jet Conference. AIAA-ASME Preprint No. 63113, 1963.

42. PRATT,N.H. "Some chemical reaction rate data for gas dynamic studies." Ministry of Aviation ARC 25163, 1963.

43. PUN, W.M. and SPALDING, D.B. "The procedure for predicting velocity and temperature --." Imperial College, Mech. Eng. Dept. Report No. SF/TN/11.

44. REID,R.C. and SHERWOOD, T.K. "The properties of gases and liquids." McGraw-Hill, 1966.

45. RYABININ, Yu. N. "Gases at high temperatures and pressures." Pergamon Press, 1961.

46. SCHEUERMEYER, M. and STEIGERWALD. "Die messung des zundveruges verdichter kraftstuff-luftgemischenzur untersuchung der klopsneigung." MTZ, 1943, p. 229.

47. SCHMIDT, F.A.F. "The internal combustion engine." Chapman and Hall,1965, p. 34.

48. SCHWEPPE, J.L. "Methods for dynamic calibration of pressure transducers." NBS Monograph 67, p. 81.

49. SEMENOV, N.V. "Some problems of chemical kinetics and reactivity." Pergamon Press, 2, 1958, p. 84.

50. SPALDING, D.B. private communication to G.A. Karim. 1961.

51. SPALDING, D.B., JENKINS, D.R. and YUMLU, V.S. "Combustion of hydrogen and oxygen in a steady flow adiabatic stirred reactor." 11th Symposium on Combustion, 1967, p. 779.

52. TAYLOR, C.F. et al. "Ignition of fuels by rapid compression." Trans. S.A.E., 1950, p. 232.

53. TAYLOR, C.F. Discussion contribution. Proc. I. Mech. E., 177, 36, 1963.

54. TEICHMAN, H. "Die selbstentzundung von kohlenwasserstoffluftgemischen und das klopfen im ottomotor." Z. Elektrochemie, 1941, 47, p. 299.

55. TIZARD, T. and PYE, D.R. "Experiments on the ignition of gases by sudden compression." Phil. Mag. 1922, 49, p. 6.

56. THOMPSON, D. et al. "A Fortran program to calculate the flow field and performance of an axially symmetric de Laval nozzle." NASA report, 1964, TND 2579.

57. VARGA, R.S. "Matrix iterative analysis." Prentice-Hall International, London, 1962.

58. WATSON,H.C. Unpublished annual report, Imperial College, 1964.

59. WATSON, H.C. Discussion contribution. Proc. I. Mech. E., 181, 1967,1, 20.

60. WOLFSHTEIN, M. Private communiction to author. 1968.

61. YATES, D.A. "Knock and autoignition characteristics of fuel mixtures." Unpublished work.

62. YUMLU,V.S. Paper to be published.

63. YUMLU,V.S. Private communication, February 1967.

NOMENCLATURE

Symbol	Meaning	Equation of first mention
A	surface area	2.22-3
A	pre-exponential factor	2.22-15
B	temperature exponent	2.22-15
C_p	specific heat at constant pressure	B.3-6
C_v	specific heat at constant volume	2.22-5
CO	carbon monoxide	
E	activation energy	2.22-15
H	energy of reaction	
H	atomic) hydrogen	
H_2	molecular)	
H_2O	water	
HO_2	hydroperoxyl	
H_2O_2	hydrogen peroxide	
J	Joule's constant	B.3-6
K	equilibrium constant	2.22-16
M	mass of charge	2.22-13
M	third body species	
N	number of reactions	2.22-20
Nu	Nusselt's number	3.25-1
N	atomic) nitrogen	
N_2	molecular)	
NO	nitric oxide	
O	atomic) oxygen	
O_2	molecular)	
OH	hydroxyl	

Symbol	Meaning	Equation of first mention
P.M.P.T	point of maximum piston travel	
Pr	Prandtl's number	3.25-1
Q	heat transferred	2.22-1
R	gas constant	B.3-3
Re	Reynold's number	3.25-1
$\mathcal{R}$	universal gas constant	2.22-6
S	species	2.22-13
T	temperature	2.22-5
U	internal energy	2.22-5
V	cylinder volume	2.22-10
W	work	2.22-1
W_m	molecular weight	2.22-19
a	order of reaction	
f	function of	2.22-7
g	total number of reactants	2.22-13
h	total number of products	2.22-13
i	i th species	
j	j th reaction	
k	thermal conductivity	3.25-2
k	reaction rate	2.22-15
m	mass fraction	2.22-14
n	number of species	
p	pressure	2.22-6
r	compression ratio	3.25-2
s	clearance length	
t	time	2.22-7
x	piston displacement	2.22-3

Symbol	Meaning	Equation of first mention
y	an argument	2.33-3
α	surface heat transfer coefficient	B.3-9
α_{sub}	stoichiometric coefficient	2.22-13
γ	specific heat ratio	B.3-6
ε	density-time index	F.4-1
μ	viscosity coefficient	3.25-2
ρ	density	2.22-3
σ	concentration	2.22-4
ϕ	equivalence ratio	
Δ	incremental value	
$\Delta\tau$	$\tau_e - \tau_p$	
τ_e, τ_p	experimental and predicted induction times	

SUBSCRIPTS

A,B,C,D	of species A,B,C,D
R	reference
P	product
M	of species M
a	atomic
b	backward
c	concentration
e	equilibrium
f	forward
n	a number
p	partial pressure
q	molecular species

Symbol	Meaning
r	reactants
t	total
w	wall
0	initial
1	driving chamber
2	retarding chamber
3	compression cylinder

SUPERSCRIPTS

$\cdot$	w.r.t. time
$'$	first differential
$_{,}^{1\ 11}$	previous values of
$'''$	per unit volume
$\bar{}$	mean

APPENDIX A

THE COMPUTER PROGRAMME FOR THE SOLUTION OF THE REACTING-SYSTEM EQUATIONS

A.1 Introduction

A.11 The requirements of the programme

This programme provides the link between the numerical procedure formulated in Chapter 2 and the practically-useful predictions made in Chapters 6 and 7.

The present programme has been written to comply with the specific needs of predicting the time dependence of cylinder pressure and other parameters in the compression apparatus. However, with small modifications, the programme can be applied to predicting the time-dependence of the same variables in other systems which are subjected to prescribed density-changes.*

A.12 Outline of the contents

The programme consists of a main routine and seven subroutines. The important features of each routine are described: what purpose they fulfil; and what their principles of organisation are.

Before describing the programme the Fortran names used and their meanings are listed. After the description computation time is discussed and a user's guide presented. At the end of the Appendix the programme is listed and a sample data deck provided.

A.2 Conventions and Symbols used in the Programme

System boundary. The conventions adopted for describing the boundaries of the considered system are the same as used in the deri-

---

* In, as yet, unreported work the programme has been adapted to predicting autoignition in a motored engine.

vation of equations and specified in fig 2.21-1: the location of the piston in the cylinder is X; the surface area of the cylinder is SAREA.

Independent variable. The independent variable, time, is TIM.

Dependent variables. The array MF(I) is used for the species concentrations, numbered from I = 1, JSPENO, where JSPENO is the total number of considered species. Each of the integers from 1 to JSPENO is assigned to an individual species. The dependent variable for pressure at each integration step N is PC(N) and for temperature is TEMP1. The combustion-energy release-rate is TERM2 of the energy-conservation equation; while TERM4 represents the heat-transfer rate to the cylinder surfaces, and TERM1 and TERM3 are the work and internal-energy components respectively.

Other important symbols are listed below.

List of important FORTRAN names

Fortran Name	Meaning	Symbol	Units of input/ output variables
A	time-interval multiplying-factor		
C	specific-heat coefficient	C	CHU $mole^{-1} deg^{-1}$
CEQ(i,j)	equilibrium constants for reaction	K_C	$(ft^3 lb.mole^{-1})^{a-1}$ sec^{-1}
CS(i,j)	equilibrium constant for species		
DELTAP	finite pressure-increment	Δp	$lbf\ in^{-2}$
DELTAX	finite displacement-increment	Δx	in
DIFMF(i)	incremental concentration	$\Delta\sigma$	$lb.mole\ lbm^{-1}$
DIFMFS, DIFMFT, DIFMFK, DIFMFU	storage locations of concentration increments		

Fortran Name	Meaning	Symbol	Units of input/ output variables
DT	incremental temperature	ΔT	°C
DTS,DS,Z	storage locations for DT		
DTRA,DTRB	time-interval ratios		
EQUN	energy-conservation equation		
EQUNS,Y	storage locations for equation 6.10		
F	2nd iterative 'guess' temperature-interval multiplying-factor		
IRECN	total number of reactions	N	
II	time-loop integer-count		
IY	designates cause of programme failure		
ICON	experimental data-fitting control		
JSPENO	total number of species	n	
JCON	Type I iteration count, also Type II count for DIFMF root iteration		
KON	Type II count for temperature iteration		
KTEST	output control integer		
LCUT	count check on DIFMF convergence		
LTEST	failure-to-converge-stop control		
MAX2	see fig A-2		
MF(i)	species concentration	σ	lb.mole lbm^{-1}
MF1	concentration at beginning of time step		
MSTEP	Type II iteration procedure control		
MTEST	controls evaluation of EQUN at convergence		
NA	total number of experimental data points		

Fortran Name	Meaning	Symbol	Units of input/ output variables
NC) ND)	displacement-calibration change-over points		
NTEST	excess-iterations stop-control		
PA	beginning) of step pressure for		
PB	end) a time increment		
PC	calculated pressure		$lbf\ in^{-2}$
PCALF	pressure) calibration factors:		
PCT	crosstalk) see fig A-2		
PM	average-of-step pressure for a time increment		
POLYB	coefficients of fitted polynomials		
POLY2) POLY3)	displacement calibration coefficients		
PP(i)	partial pressure		$lbf\ in^{-2}$
P3	combustion-cylinder pressure	p	$lbf\ in^{-2}$
Q	heat flux	Q	ft lbf
RATE(j,L)	reaction rate		
L=1	forward)	k_{fj})	$(ft^{1}lb.mole^{-1})^{a-1}$
2	backward)	k_{bj})	sec^{-1}
3	forward)		$(cm^{3}lb.mole^{-1})^{a-1}$
4	backward)		sec^{-1}
RATENT(j)	net reaction-rate	$\dot{m}'''_j$	$sec^{-1}ft^{-3}$
RCOMP	compression ratio		
ROE	density	ρ	$lbm\ ft^{-3}$
ROEO	initial density		$lbm\ ft^{-3}$
RI	universal gas constant	R	$CHU\ lb.mol^{-1}{}^{\circ}C^{-1}$
TEMP1	temperature at beginning of time increment		

Fortran Name	Meaning	Symbol	Units of input/ output variables
TERM1	work) terms of		
TERM2	combustion release) energy		ft.lbf sec^{-1}
TERM3	internal energy) conservation		
TERM4	heat transfer) equation		
TEMINT	temperature increment	ΔT	°C
TIM	time of calculation	t	m sec
TIME	experimental-data-point time		m sec
TIMINT	time increment	Δt	m sec
TITLE	title		
TEMP1	absolute temperature	T	°K
TOMASS	total mass	w	lbm
TSTORE	time-interval storage-location		
UR(i)	heat of formation above 298.15°K	u_{Ri}	Kcal $gm.mole^{-1}$
VA	beginning) of step velocity		
VB	end) for a time incre-		
VM	average) ment		
VEL	velocity	V_P	in sec^{-1}
WM(i)	molecular weight	W	lb.mole lbm^{-1}
X	piston displacement	x	in
XA	beginning) of step piston dis-		
XB	end) placement for a		
XM	average) time increment		
ZERO1) ZERO2) ZERO3)	see fig A-2		

Species identification numbers

i	Species	i	Species
1	H_2	7	OH
2	O_2	8	NO
3	A or N_2	9	H_2O
4	H	10	HO_2
5	O	11	H_2O_2
6	N		

A.3 The Programme Description

A.31 The main routine

Its function. The main routine of the programme performs three major tasks:

1. to coordinate the use of the subroutines
2. to solve the differential equations
3. to control the output of the relevant parameters as integration proceeds.

The flow path. A simplified flow diagram for the main routine is given in fig A.31-1. This shows the organisation of the sub-routines. The actual flow path is more complex than the simplified one shown because: 1. the two iterative procedures TYPE I and TYPE II run in parallel as seen in fig 2.33-1; 2. TYPE II iteration is a two-stage process. Thus there are three possible flow paths in any time increment loop.

Choice of the solution procedure. The rapidity of convergence of TYPE I iteration governs the choice which of the two procedures is used: if convergence is not achieved after 5 iterations with TYPE I, TYPE II is adopted. Thereafter, every 5 time increments the TYPE I

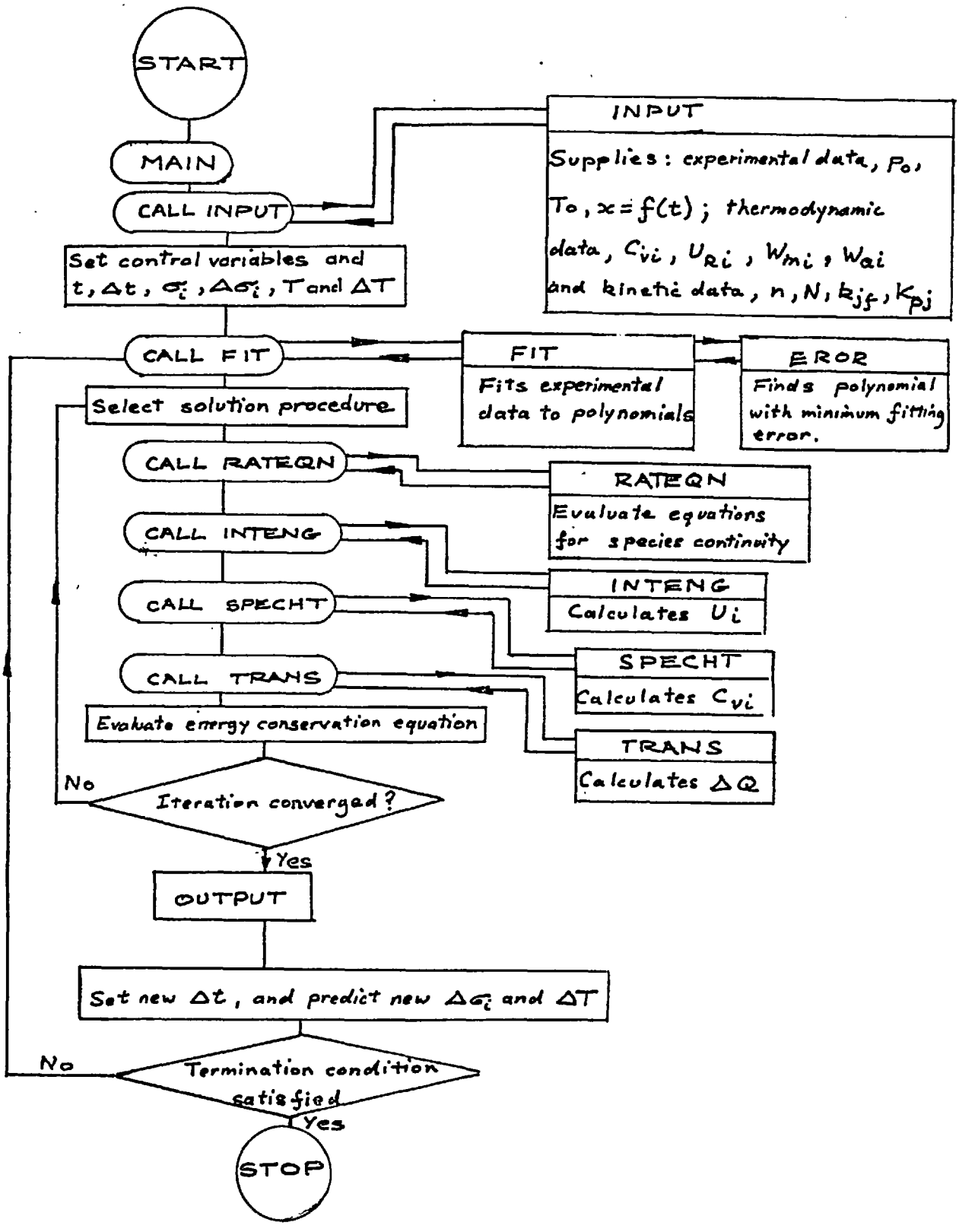

Fig A.31-1 Simplified flow diagram of computer programme showing the organisation of subroutines

procedure is again tried.

Time increment control. The need to control the length of the time increment TIMINT arises as follows: during the initial stages of compression both rate of temperature rise and reaction rates are small; but on ignition these rates become large; if computation time is to be minimised, largest time-steps should be taken when the rates of charge are smallest. Control of TIMINT by relating it to the rate of change of H_2O concentration proved to be insufficiently responsive, leading to temperature overshoot of up to 100°C. TIMINT adjusted to give values of temperature increments, TEMINT, of approximately $\pm$ 5°C gave the best compromise between prediction precision and computing time: 10°C increments reduced the computing time by one third and only marginally affected the induction-times predicted; but with increments of 20°C the values of induction-time were altered by about 0.5%. An upper bound of 0.5 ms was placed on TIMINT.

Exits from the programme. There are three possible exits from the programme:

1. the normal STOP at the end of integration.

2. an exit when the mass fraction of any species becomes greater than unity - always as a result of erroneous input data.

3. if convergence is not obtained. Normally the incremental variables have to satisfy the convergence requirement of 2%, if the number of iterations exceeds 20 in any time increment, the convergence condition is relaxed to 10%, but if this high limit is used more than 5 times in the overall integration procedure or is not satisfied the exit facility will be taken and the details of the concentration increments leading to failure printed out.

A.32 Subroutine INPUT

This subroutine is concerned with reading all the input data and

converting it into a standard form for acceptance by the main routine.

Conversion of experimental data. Experimental records of piston displacement are converted into length units by calibration curves. These curves are read in as the arrays POLY2(I) and POLY3(I), for direct and scaled displacements respectively. The arrays represent coefficients of polynomial expressions which have been fitted to the calibration curves. The zeros of each of the experimental parameters are read by the programme: ZERO1, ZERO2 and ZERO3 are defined by fig A.32-1 as is the internal standard MAX2 and the cross-talk factor PCT. Experimental pressure data is converted by the calibration factor PCALF.

The actual piston-displacement X(I) and pressure P3(I) records are read in as digital values at increments of time, TIME(I). The total number of time points isNA, while the data points at which the use of the scaled displacement begins is NC and ends is ND.

The experimental data input is concluded by reading the initial pressure PO, temperature TO and the partial pressures PP(I) of each component species I.

Thermodynamic data. The required thermodynamic data is read in as: CP(I,JCF), the JCF coefficient of a polynomial expression for the molar-specific-heat at constant pressure of the species I; UR(I), the heat of formation of each species; and WM(I) the molecular (or atomic) weight of each species.

Kinetic data. The forward rates of each reaction are read in by the coefficients CK(IR,IC). IR takes a value for the number of the reaction in the kinetic model. The number of the last reaction is IRECN. IC takes a value from 1 to 3, 1 corresponds to A, 2 to B and 3 to E/R in the Arrhenius equation when written as

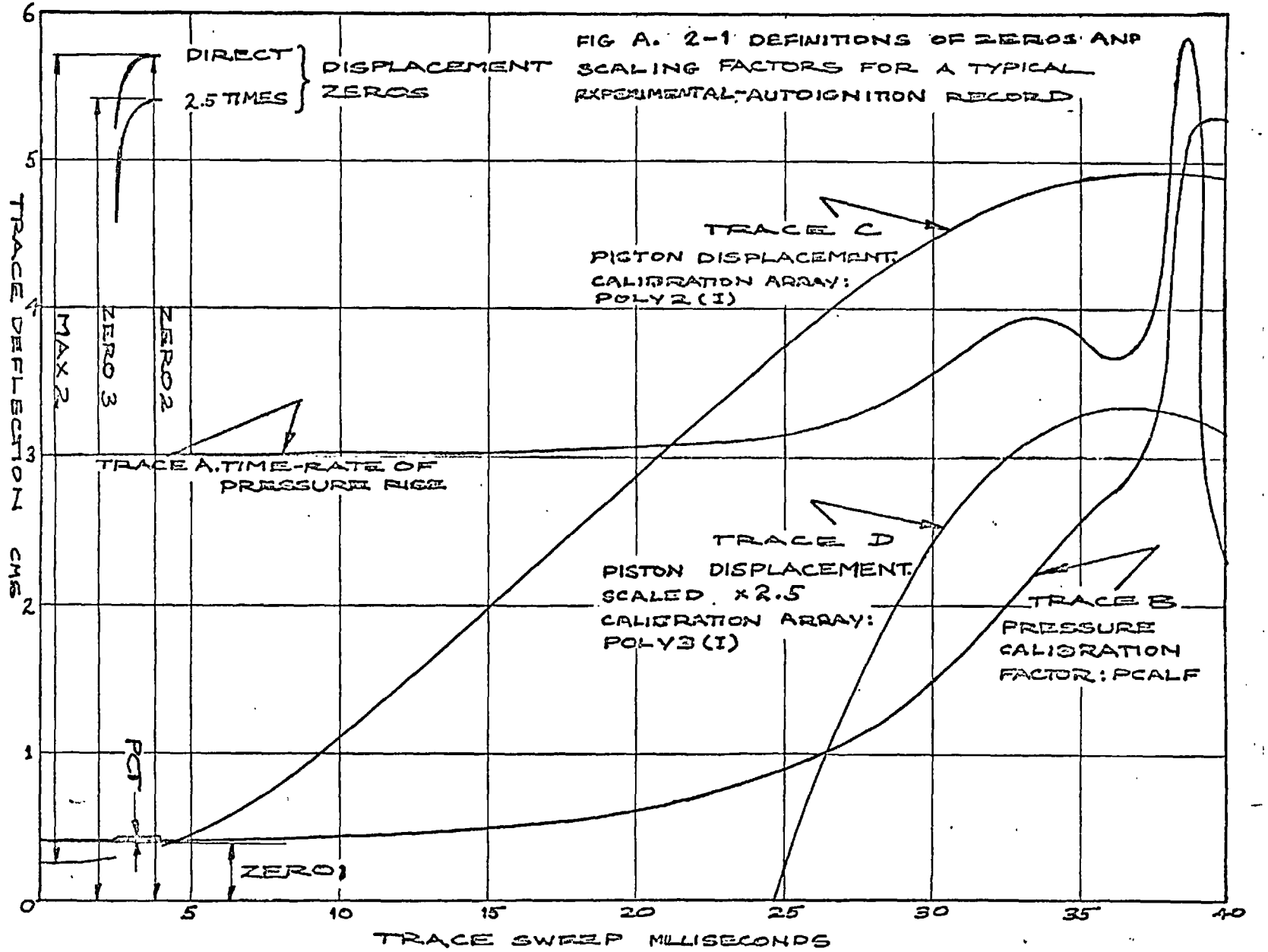
FIG A. 2-1 DEFINITIONS OF ZEROS AND SCALING FACTORS FOR A TYPICAL EXPERIMENTAL AUTOIGNITION RECORD
DIRECT
2.5 TIMES
DISPLACEMENT ZEROS
TRACE C
PISTON DISPLACEMENT
CALIBRATION ARRAY: POLY2(I)
MAX 2
ZERO 3
ZERO 2
TRACE A. TIME-RATE OF PRESSURE RISE
TRACE D
PISTON DISPLACEMENT SCALED ×2.5
CALIBRATION ARRAY: POLY3(I)
TRACE B
PRESSURE CALIBRATION FACTOR: PCALF
PCT
ZERO 1
TRACE DEFLECTION CMS
TRACE SWEEP MILLISECONDS
0
1
2
3
4
5
6
5
10
15
20
25
30
35
40

$$k_{jf} = e^{A_T B} e^{-E/RT} \quad . \qquad \text{A.32-1}$$

Similarly, the equilibrium constants are read in as CS(I,JCF) - the constants of an Arrhenius expression fitted to the equilibrium constants for the formation of each species I. To convert these to the equilibrium constant of each reaction CEQ(IR,JCF) the equations of each reaction need to be written into the subroutine.

Initial programme values. The routine concludes by calculating the initial concentrations MF(I) of each species, the initial density ROEO and the total system mass TOMASS.

A.33 The other subroutines

RATEQN. The function of this subroutine is to evaluate the finite-difference equations of atomic and molecular continuity. It requires that these equations should be written into it for each reaction model used.

SPECHT. This routine evaluates the mean-mixture specific-heats by the method outlined in section 3.32.

INTENG. Subroutine INTENG evaluates the mean-mixture internal-energy and computes the combustion-energy release resulting from changes in the species concentrations as reaction proceeds.

TRANS. This subroutine evaluates the gas-to-wall heat-transfer as defined by equation 3.26-1. We have shown that this equation is only applicable beyond the maximum Reynolds number of the compression stroke. The piston displacement at which this maximum number is exceeded is controlled in the routine by the divisor of XF. XF represents the maximum piston-displacement in the cylinder.

FIT and EROR. Subroutine FIT fits the experimental p and x to polynomial expressions of time. These expressions provide a means of smoothing, and interpolating between, data points.

The procedure used is to fit, by the method of least squares, an array of six consecutive data points. Three of the points are selected to be in advance of and three in retard of the time TIM at which integration is proceeding. As TIM exceeds the TIME of the 4th data point a new set of points are taken: point one is dropped and the 7th data point added to the array.

The function of subroutine EROR is to find the order of polynomial in the range 2 to 4 which is the best fit to the data, i.e. the fitting errors are minimised. The coefficients of the optimum order of polynomial are returned to the main routine.

A.34 Normal output

In a normal sequence of output from the programme, subroutine INPUT, prints the data as read in and converted.

Whenever FIT fits a new set of polynomial coefficients details of the order of the polynomial; the location amongst the six fitted points of the maximum error and the percentage value of this error.

On completion of each integration step in the programme, the temperature increments leading to convergence are written out. Once every five steps, a block of detailed output is written:

1. the first line lists the parameters: t, x; the experimental and calculated values of p; T, and the number of iterations to convergence.
2. the second and third lines consist of the species concentrations σ_i.
3. the fourth line of the block represents the four terms of the energy-conservation equation 2.22-12 in ascending order.
4. lastly details of the rates-of-reaction are written: the net reaction-rate $\dot{m}'''$; and the forward and backward rate-constants, k_{jf} and k_{jb}.

A.4 Computation time

The total computer time for the prediction of a complete auto-ignition test, from the beginning of compression to the end of expansion, is dependent upon many factors. The most important are:

1. the experimental density-time history on which prediction is based.

2. the mixture strength and dilution of the charge: the number of integrating steps taken is dependent upon the temperature rise on ignition.

3. the number of species and reactions in the kinetic model.

Typically, the programme, when run on an IBM 7090 computer, will perform 2000 iterations per minute. The total computer time for a $\phi = 0.05$ mixture and a nine reaction kinetic model was 3.6 minutes. For the same kinetic model, the time taken to predict the pressure-time history of a stoichiometric mixture was 5 minutes.

A.5 User's Quick Reference Guide

The details given so far and the listing which follows complete the presentation of the information necessary for the user to proceed. The information which he needs to provide is listed below:

A. On data cards.

1. Title.

2. The coefficients of polynomial expressions for the conversion of piston-displacement readings.

3. The experimental constants.

4. The total number of input data points NA, the NCth and NDth points at which change of displacement calibration occurs.

5. Time, pressure and displacement points.

6. The total number of species and their specific heats.

7. The number of reactions and their forward reaction-rates.

8. The equilibrium constants for the reaction of formation of each species.

9. The molecular weights of each species.

10. Energy of formation of each species.

11. The partial pressures of each species.

B. Programme adjustments.

1. In INPUT the equations for the calculation of the equilibrium constant of each reaction.

2. In RATEQN the net-rate equations and atomic and molecular continuity equations should be written.

3. The value of piston displacement at which maximum Reynolds number is attained is required in TRANS.

PROGRAMME XII

AUTOIGNITION PREDICTING PROGRAMME

```
$IBFTC MAIN12  DECK
       REAL MF,MF1,MAX2
       COMMON    POLY2(10),POLY3(10),TIME(200),P3(200),X(200),XT(200),RA1
      1EP(200),VEL(200),CP(20,10),CK(20,3),CEQ(20,3),POLY(10,10),POLYXB(1
      20),POLYPB(10),POLYVB(10),POLYRB(10),RATE(20,4),RATENT(20),R(20),U
      320),CV(20),DT(100),EQUN(100),PP(20),WM(20),MF1(20),PC(1000),MF(20)
      4,DIFMF(20),CS(20,3),TITLE(12),UR(20),
      5TO,R1,PO,NA,NC,JSPENO,IRECN,SIGMA6,ROE,TOMASS
       DIMENSION DTS(100),EQUNS(100)
       DIMENSION DIFMFS(20,100),Y(100),Z(100)
       DIMENSION DS(20),FX(20,40)
       DIMENSION TSTORE(1000),DIFMFT(20,2),DIFMFK(20,40)
       DIMENSION DIFMFU(20,50)
       CALL INPUT
C
C  DISPLACEMENT,VELOCITY AND STARTING PARAMETERS
       SIGMA=0.
       A=1.
       LTEST=1
       MTEST=0
       NTEST=0
       F=.9
       KTEST=0
       MSTEP=0
       I1=1
       TIM=0.
       TIMINT=0.5
   50  TIM=TIM+TIMINT*A
       CALL FIT(TIM,TIME,X,POLY,M,NA,ICON,TIMINT)
       IF (ICON .EQ. 0) GO TO 55
       NXB=M+1
       DO 51 I=1,NXB
   51  POLYXB(I)=POLY(M,I)
       CALL FIT(TIM,TIME,P3,POLY,M,NA,ICON,TIMINT)
       NPB=M+1
       DO 52 I=1,NPB
   52  POLYPB(I)=POLY(M,I)
       CALL FIT(TIM,TIME,RATEP,POLY,M,NA,ICON,TIMINT)
       NRB=M+1
       DO 53 I=1,NRB
   53  POLYRB(I)=POLY(M,I)
       CALL FIT(TIM,TIME,VEL,POLY,M,NA,ICON,TIMINT)
       NVB=M+1
       DO 54 I=1,NVB
```

```
   54 POLYVB(I)=POLY(M,I)
   55 XB=POLYXB(1)
      DO 56 I=2,NXB
   56 XB=XB+POLYXB(I)*TIM**(I-1)
      PB=POLYPB(1)
      DO 57 I=2,NPB
   57 PB=PB+POLYPB(I)
      VB=POLYVB(1)
      DO 58 I=2,NVB
   58 VB=VB+POLYVB(I)*TIM**(I-1)
C
C  INITIAL GUESS AT TEMINT
      IF(TIM .GE. (TIMINT+.05)) GO TO 59
      TEMINT=T0/150.
      TEMP1=T0
      XA=X(4)
      VA=0.
      GO TO 60
   59 IF(TIM .GT. 5.) GO TO 60
      TEMINT=TEMP*((XA/XB)**(1.37-1.)-1.)
   60 JCON = 1
      ROE=TOMASS/(XB*3.142*1.006/1728.)
      VM=(VA+VB)/2.
      XM=XB-VM*TIMINT*.001/2.
      IF(FLOAT(NTEST/5) .NE. FLOAT(NTEST)/5.) GO TO 607
   61 TEMP=TEMP1+TEMINT/2.
      IF(JCON .LE. 2) GO TO 63
      JCON2=JCON-2
      DO 62 J=1,JSPENO
      IF(KTEST .NE. 1) GO TO 62
      DIFMF(J)=(DIFMFS(J,JCON2)+DIFMF(J))/2.
   62 MF(J)=MF1(J)+DIFMF(J)*TIMINT/(1000.*2.)
   63 CONTINUE
      CALL RATEQN(TEMP,MSTEP)
      IF(MSTEP .NE. 2) GO TO 73
      DO 308 J=1,JSPENO
  308 FX(J,JCON)=DIFMF(J) - DIFMFS(J,JCON)
      GO TO 200
C  EQUATION 8
C  TERM 1
   73 SIGMA1=0.
      DO 76 IS=1,JSPENO
   76 SIGMA1=SIGMA1+MF(IS)
      TERM1=TOMASS*R1*1400.*TEMP*VM*SIGMA1/XM
C  TERM 2
      TERM2=0.
      DO 75  IS=1,JSPENO
      CALL INTENG(IS,CP,R1,TEMP,U,I1,UR)
   75 TERM2=TERM2+U(IS)*DIFMF(IS)
```

```
      TERM2=TERM2*TOMASS*1400.
C
C  TERM 3
      SIGMA2=0.
      DO 77 IS=1,JSPENO
      CALL SPECHT(IS,CP,R1,TEMP,CV,I1)
   77 SIGMA2=SIGMA2+CV(IS)*MF(IS)
      TERM3=(SIGMA2*TOMASS*TEMINT/TIMINT)*1000.*1400.
C
C  TERM 4
      PM=ROE*MF1(3)*RT*TEMP*1400./144.
      CALL TRANS(XM,TEMP,VM,ROE,TO,DELTAQ,X(4))
      TERM4=DELTAQ
C
      EQUNA=TERM1+TERM2+TERM3+TERM4
      IF(NSTEP .EQ. 1) GO TO 291
      IF(MTEST .EQ. 2) GO TO 200
      KTEST=0
      IF(MTEST .NE.  1) GO TO 187
      MTEST=0
      EQUN(JCON)=EQUNA
      EQUNS(JCON)=EQUN(JCON)
      DTS(JCON)=DT(JCON)
      GO TO 86
C
C  FINDING A BETTER TEMPERATURE INCREMENT
  187 IF (JCON .NE. 1) GO TO 79
      JCON=2
      EQUN(2)=EQUNA
      TEMINT=TEMINT*F
      GO TO 61
   79 IF (JCON .NE. 2) GO TO 80
      EQUN(1)=EQUNA
      DT(1)=TEMINT
      DT(2)=TEMINT/F
      DT(3)=(EQUN(2)*F-EQUN(1))*DT(2)/(EQUN(2)-EQUN(1))
      TEMINT=DT(3)
      JCON=3
      DTS(1)=DT(1)
      DTS(2)=DT(2)
      EQUNS(1)=EQUN(1)
      EQUNS(2)=EQUN(2)
      GO TO 61
   80 EQUN(JCON)=EQUNA
      EQUNS(JCON)=EQUN(JCON)
      DTS(JCON)=DT(JCON)
      IF (ABS(EQUN(JCON-2))-ABS(EQUN(JCON-1)))81,82,82
   81 EQUN(JCON-1)=EQUN(JCON-2)
      DT(JCON-1)=DT(JCON-2)
   82 DT(JCON+1)=(DT(JCON)*EQUN(JCON-1)-DT(JCON-1)*EQUN(JCON))/(EQUN(JC
     1N-1)-EQUN(JCON))
```

XII CONTD. - 3

```
      JCON=JCON+1
      TEMINT= DT(JCON)
      TEST=ABS(TERM1)*.005
      IF(EQUN(JCON-1) .GE. -TEST .AND. EQUN(JCON-1) .LE. TEST) GO TO 186
      IF(JCON .GT. 7) GO TO 83
      IF(ABS(EQUNS(JCON-1)-EQUNS(JCON-2)) .GE. 2.) GO TO 183
  301 WRITE(6,188)LTEST
  188 FORMAT(8H FAILTYP I2)
      WRITE(6,122)TEMP1,(DTS(I),EQUNS(I),I=1,JCON)
      JCON=1
      LTEST=LTEST+1
      IF(LTEST .GT. 2) GO TO 83
  183 IF(LTEST .LT. 5) GO TO 61
      WRITE(6,226)(DTS(I),EQUNS(I),I=1,JCON)
  226 FORMAT(12H STOP AT 226 (4(1XE13.5,1XF10.3)))
      STOP
   83 WRITE(6,84)I1,(EQUNS(I),DTS(I),I=1,6)
   84 FORMAT(22H EXCESSIVE ITERATIONS I3,12HTH INCREMENT/(10(1XF10.5)))
C    RELAXING DIFMF ONLY BY USING NEWTON-RAPHSON
C    ------------------------------------------
  607 NTEST=NTEST+1
      KTEST=0
      KON=0
      TEMINT=TS*.98
      DO 256 J=1,JSPENO
      DIFMF(J)=DS(J)
  256 DIFMFS(J,3)=DIFMF(J)
  228 JCON=3
      MSTEP=2
      GO TO 61
  200 IF(JCON.NE. 3) GO TO 311
      JCON = 4
      DO 310 J=1,JSPENO
      DIFMF(J)=(DIFMF(J) + DIFMFS(J,3))/2.
  310 DIFMFS(J,4)=DIFMF(J)
      GO TO 61
  311 LCUT=0
      PERCNT=.02
      IF(JCON .GT. 20) PERCNT=.03
      IF(JCON .GT. 25) PERCNT=.1
      DO 241 J=1,JSPENO
      LCHEK=0
C                                CONVERGENCE TEST
      IF(ABS(DIFMFS(J,JCON-1)-DIFMFS(J,JCON)).GT. PERCNT*ABS(DIFMFS(J,JC
     1ON))) LCHEK=1
  241 LCUT=LCUT+LCHEK
      IF(LCUT .GT. 0)GO TO 245
  323 KON=KON+1
      DO 805 J=1,JSPENO
      DIFMF(J)=DIFMFS(J,JCON)
```

```
  805 DIFMFU(J,KON)=DIFMF(J)
      MSTEP=1
      GO TO 61
  291 Y(KON)=EQUNA
      Z(KON)=TEMINT
      IF(KON .EQ. 1) GO TO 242
      IF(Y(KON).GE. -TEST .AND. Y(KON) .LE. TEST) GO TO 251
      IF(KON.EQ. 2) GO TO 282
      ZIC=(Z(KON-2)+Z(KON-1)+Z(KON))/3.
      IF(ABS(ZIC-Z(KON-1)) .LE. .002*ABS(TEMINT) .AND. ABS(ZIC-Z(KON)) .
     1LE. .002*ABS(TEMINT)) GO TO 251
      IF(ABS(Y(KON-2))-ABS(Y(KON-1)))281,282,282
  281 YA=Y(KON-2)
      ZA=Z(KON-2)
      GO TO 283
  282 YA=Y(KON-1)
      ZA=Z(KON-1)
  283 TEMINT=(Z(KON)*YA-ZA*Y(KON))/(YA-Y(KON))
      IF(KON+1 .GT. 40) GO TO 247
      IF(KON  .GT. 20) TEMINT=(TEMINT+Z(KON))/2.
      GO TO 250
  242 TEMINT=TEMINT/.98
  250 DO 312 J=1,JSPENO
      DIFMFK(J,KON)=DIFMFS(J,JCON)
      DIFMFS(J,3)=DIFMFK(J,KON)-(DIFMFK(J,KON)-DIFMFK(J,KON-1))*TEMINT/Z
     1(KON-1)
  312 DIFMF(J)=DIFMFS(J,3)
      GO TO 228
  245 JCON =JCON+1
      JCON1=JCON-1
      JCON2=JCON-2
C                       LONG PERIOD INSTABILITY CORRECTOR
      IF(JCON .NE. 30 .OR. JCON .NE. 31) GO TO 317
      GO TO 316
  317 IF(JCON .NE. 35 .OR. JCON .NE. 36) GO TO 315
  316 DO 322 J=1,JSPENO
      DIFMF(J)=0.
      DO 318 I=1,5
      L=JCON-I
  318 DIFMF(J)=DIFMF(J)+DIFMFS(J,L)
  322 DIFMF(J)=DIFMF(J)/5.
      GO TO 320
C                   NEWTON-RAPHSON PREDICTOR
  315 CONTINUE
      DO 313 J=1,JSPENO
      DIFMF(J)=DIFMFS(J,JCON1)-FX(J,JCON1)*(DIFMFS(J,JCON1)-DIFMFS(J,JCO
     1N2))/(FX(J,JCON1)-FX(J,JCON2))
      IF(ABS(DIFMF(J))-ABS(DIFMFS(J,JCON1)) .GT. 100.) DIFMF(J)=(DIFMF(J
     1)-DIFMFS(J,JCON1))*100./(ABS(DIFMF(J)-DIFMFS(J,JCON1)))+DIFMFS(J,J
     2CON1)
C                 SHORT PERIOD INSTABILITY CORRECTOR
```

XII CONTD. - 5

```
  313 CONTINUE
  320 DO 321 J=1,JSPENO
  321 DIFMFS(J,JCON)=DIFMF(J)
      IF(JCON .GT. 40) GO TO 246
      GO TO 61
246   IZ=2
      GO TO 248
  247 IZ=3
  248 WRITE(6,249) IZ,(EQUN(I),DT(I),I=3,JCON),(Y(I),Z(I),I=1,KON)
  249 FORMAT(8H FAILURE,I1 /(4(1XF10.3,1XF10.6)))
      WRITE(6,352)((DIFMFS(J,I),J=1,JSPENO),I=1,JCON)
  352 FORMAT(1H 6E13.4/1H 5E13.4)
      IF(IZ .EQ. 2) GO TO 802
      I4=1
      DO 801 I5=2,KON
      DIFM = ABS(Y(I4))-ABS(Y(I5))
      IF(DIFM .LT. 0.) GO TO 801
      I4=I5
  801 CONTINUE
      TEMINT = Z(I4)
      DO 803 J=1,JSPENO
  803 DIFMF(J)=DIFMFU(J,I4)
      GO TO 251
802   CONTINUE
      I11=I11+1
      IF(I11 .LT. 5 .AND. IZ .NE. 3) GO TO 323
      TIM=50.
      GO TO 351
  186 MTEST=1
  251 DTRA=TIMINT/TSTORE(I1)
      DTRB=TSTORE(I1)/TSTORE(I1-1)
      DO 255 J=1,JSPENO
      DIFMFT(J,2)=DIFMFT(J,1)
      DIFMFT(J,1)=DIFMF(J)
  255 DS(J)=DTRA*(DIFMF(J)*1.5-.5*DTRB*DIFMFT(J,2))
      IF(MSTEP .EQ. 1) GO TO 259
      MSTEP=0
      GO TO 61
  259 WRITE(6,122)TEMP1,(Z(I),Y(I),I=1,KON)
      KTEST=1
   86 SIGMA6=0.
      DO 87 J=1,JSPENO
      MF1(J)=MF1(J)+DIFMF(J)*TIMINT/1000.
      IF(MF1(J) .LE. 0.) MF1(J)=0.
   87 SIGMA6=SIGMA6+MF1(J)
      TEMP1=TEMP1+TEMINT
      IF(KTEST .EQ. 1) GO TO 357
      WRITE(6,122)TEMP1,(DTS(I),EQUNS(I),I=1,JCON)
  357 CONTINUE
      IF(FLOAT(I1/5) .NE. FLOAT(I1)/5.) GO TO 90
```

```
  351 CONTINUE
      PC(11)=ROE*SIGMA6*R1*TEMP1*1400./144.
      WRITE(6,88) TIN,XB,PB,PC(11),JCON,TEMP1,(MF1(J),J=1,JSPENO),MF(15)
   88 FORMAT(1H@,4(1XF10.5),1X14,1XF10.5/(6(1XE13.5)))
      WRITE(6,123)TERM1,TERM2,TERM3,TERM4,ROE,SIGMA6,(DIFMF(I),I=1,JSPEN
     10)
  123 FORMAT(5(1XE13.5)/(6(1XE13.5)))
  122 FORMAT(10(1XF10.5))
      WRITE(6,134)(RATEINT(I),I=1,IRECN)
      WRITE(6,134) (RATE(I,1),I=1,IRECN),(RATE(I,2),I=1,IRECN)
  134 FORMAT(5(1XE13.5))
   90 II=II+1
      XA=XB
      VA=VB
      IY=1
      IF(TIM .GE. TIME(NA)) GO TO 100
      IY=2
      IF(TIM .LT. -1.) GO TO 100
      IY=3
      IF(TIM .LT. 5.) GO TO 601
      TIMINT1=TIMINT
  602 CONTINUE
      TPRED=TEMINT
      IF(ABS(TPRED) .LT. 3.) TPRED=3.
      TIMINT=TIMINT*5./ABS(TPRED)
      IF(TIMINT .GT. .5) TIMINT=.5
      TS=DT(JCON-1)
      IF(MSTEP .GE. 1)TS=Z(KON)
      TSTORE(II)=TS
      TS=(1.5*TSTORE(II)-.5*TSTORE(II-1))*TIMINT/TIMNT1
      TEMINT=TS
  601 CONTINUE
      TEST=.005*ABS(TERM1)
      IF(ABS(TERM1) .LT. ABS(TERM3)) TEST=.005*ABS(TERM3)
      MSTEP=0
      LTEST=1
      MTEST=0
      F=.9
      IF(MF1(1) .GT. 1.0) GO TO 100
      GO TO 50
  100 WRITE(6,604)IY
  604 FORMAT(16H STOP AT 100 FOR ,I2)
      STOP
      END

$IBFTC DEKIN   DECK
      SUBROUTINE INPUT
      REAL MF,MF1,MAX2
      COMMON    POLY2(10),POLY3(10),TIME(200),P3(200),X(200),XT(200),RAT
     1EP(200),VEL(200),CP(20,10),CK(20,3),CEQ(20,3),POLY(10,10),POLYXB(1
     20),POLYPB(10),POLYVB(10),POLYRB(10),RATE(20,4),RATEINT(20),R(20),U(
```

XII CONTD. - 7

```
     320),CV(20),DT(100),EQUN(100),PP(20),WM(20),MF1(20),PC(1000),MF(20)
     4,DIFMF(20),CS(20,3),TITLE(12),UR(20),
     5TO,R1,PO,NA,NC,JSPENO,IRECN,SIGMA6,ROE,TOMASS
      READ(5,2)TITLE
      WRITE(6,2)TITLE
    2 FORMAT(12A6)
C
C   DISPLACEMENT CALIBRATION
      DO 3 LB=1,6
    3 READ(5,5)POLY2(LB)
      DO 4 LB=1,8
    4 READ(5,5)POLY3(LB)
    5 FORMAT(E13.6)
C
C   EXPERIMENTAL DATA
      READ(5,6)TO,R1,PO,ZERO1,ZERO2,ZERO3,MAX2,PCALF,PCT
    6 FORMAT(7F10.5/2F10.5)
      WRITE(6,7)TO,R1,PO,ZERO1,ZERO2,ZERO3,MAX2,PCALF,XF
    7 FORMAT(20H INITIAL TEMPERATUREF10.5,12HGAS CONSTANTF10.5,16HINITIA
     1L PRESSUREF10.5/5HZERO1F10.5,5HZERO2F10.5,5HZERO3F10.5,4HMAX2F10.5
     2,5HPCALFF10.5,4H XF=F10.5)
      READ(5,8)NA,NC
    8 FORMAT(2I4)
      NA=NA+3
      NC=NC+3
      DO 9 IA=4,NA
      READ(5,10)TIME(IA),P3(IA),X(IA)
   10 FORMAT(3F10.5)
      IF(IA .GT. NC) GO TO 12
      X(IA)=(30.92/MAX2)*(ZERO2-X(IA))
      XT(IA)=POLY2(1)
      DO 11 LB=2,6
   11 XT(IA)=XT(IA)+POLY2(LB)*X(IA)**(LB-1)
      GO TO 14
   12 X(IA)=(30.92/MAX2)*(ZERO3-X(IA))
      XT(IA)=POLY3(1)
      DO 13 LB=2,8
   13 XT(IA)=XT(IA)+POLY3(LB)*X(IA)**(LB-1)
   14 X(IA)=XT(IA)
    9 P3(IA)=(P3(IA)-ZERO1-PCT*(1.-X(IA)/13.5))*PCALF+PO
      DO 15 IA=1,3
      TIME(IA)=TIME(4)
      P3(IA)=P3(4)
   15 X(IA)=X(4)
      DO 16 N=2,NA
      M=N-1
      RATEP(N)=P3(N)-P3(M)
   16 VEL(N)=(X(N)-X(M))*1000./(TIME(N)-TIME(M))
```

```
      DO 17 IA=3,NA
   17 WRITE(6,18)TIME(IA),P3(IA),RATEP(IA),X(IA),VEL(IA)
   18 FORMAT(5F10.5)
C
C  SPECIFIC HEAT DATA
      READ(5,19)JSPENO
   19 FORMAT(I2)
      DO 44 JS=1,JSPENO
   44 READ(5,21)(CP(JS,JCF),JCF=1,10)
   21 FORMAT(5E13.6/5E13.6)
      WRITE(6,22)
   22 FORMAT(27HOSPECIFIC HEAT COEFFICIENTS/12H SPECIES NO.)
      WRITE(6,23)(JS,(CP(JS,JCF),JCF=1,10),JS=1,JSPENO)
   23 FORMAT(I3,10X,8E13.6/12X,2E13.6)
C
C  KINETIC DATA
      READ(5,24)IRECN
   24 FORMAT(I2)
      DO 45 IR=1,IRECN
   45 READ(5,26)(CK(IR,IC),IC=1,3)
   26 FORMAT(3E13.6)
      WRITE(6,27)
   27 FORMAT(23HOKINETIC DATA CONSTANTS/8H REC.NO.4X1HA12X1HB12X1HE)
      WRITE(6,28)(IR,(CK(IR,IC),IC=1,3),IR=1,IRECN)
   28 FORMAT(I9,3E13.6)
C
C  EQUILIBRIUM CONSTANTS
      DO 46 JS=1,JSPENO
   46 READ(5,30)(CS(JS,JCF),JCF=1,3)
   30 FORMAT(3E13.6)
      WRITE(6,31)
   31 FORMAT(22HOEQUILIBRIUM CONSTANTS/8H SPEC.NO4X1HA12X1HB12X1HE)
      WRITE(6,32)(JS,(CS(JS,JCF),JCF=1,3),JS=1,JSPENO)
   32 FORMAT(I9,3E13.6)
C  EQUILIBRIUM CONSTANTS LESS TEMPERATURE TERM DUE TO CONCENTRATION CHA
C
      DO 40 I=1,3
      CEQ(1,I)=CS(9,I)+CS(4,I)-(CS(1,I)+CS(7,I))
      CEQ(2,I)=CS(7,I)+CS(5,I)-(CS(4,I)+CS(2,I))
      CEQ(3,I)=CS(7,I)+CS(4,I)-(CS(1,I)+CS(5,I))
      CEQ(4,I)=CS(7,I)+CS(7,I)-(CS(9,I)+CS(5,I))
      CEQ(5,I)=CS(9,I)         -(CS(4,I)+CS(7,I))
      CEQ(6,I)=CS(2,I)         -(CS(5,I)+CS(5,I))
      CEQ(7,I)=CS(1,I)         -(CS(4,I)+CS(4,I))
      CEQ(8,I)=CS(7,I)-(CS(4,I)+CS(5,I))
      CEQ(9,I)=2.*CS(7,I)-CS(1,I)*CS(2,I)
      CEQ(10,I)=CS(10,I)-(CS(4,I)+CS(2,I))
      CEQ(11,I)=CS(11,I)+CS(2,I)-2.*CS(10,I)
      CEQ(12,I)=2.*CS(7,I)-CS(11,I)
      CEQ(13,I)=CS(9,I)+CS(7,I)-(CS(4,I)+CS(11,I))
C ADDITIONAL EQUATIONS HERE
   40 CONTINUE
      WRITE(6,111)
```

```
  111 FORMAT(22HOEQUILIBRIUM CONSTANTS/35H RECN NO.    A              B
     1    E )
      WRITE(6,32)(IR,(CEQ(IR,IC),IC=1,3),IR=1,IRECN)
C
C  MOLECULAR WEIGHTS
      READ(5,36)(WM(I),I=1,JSPENO)
   36 FORMAT(7F10.5/7F10.5)
      WRITE(6,37)(WM(I),I=1,JSPENO)
   37 FORMAT(9H MOL.WTS./12F10.5)
C  HEATS OF FORMATION DETAILS
      READ(5,41)(UR(I),I=1,JSPENO)
   41 FORMAT(7F10.5/7F10.5)
      WRITE(6,42)(UR(I),I=1,JSPENO)
   42 FORMAT(20HOHEATS OF FORMATION   /12F10.5)
      DO 43 I=1,JSPENO
   43 UR(I)=1000.*UR(I)
C I.E.  CHUOS  -  INPUT IN KCALS/GMOLE
C
C  CHARGE DETAILS
      READ(5,34)(PP(I7),I7=1,JSPENO)
   34 FORMAT(7F10.5/7F10.5)
      WRITE(6,35)(PP(I7),I7=1,JSPENO)
   35 FORMAT(35HOCHARGE PARTIAL PRESSURES INITIALLY/103H H2        02
     1     N2         H          O          N          OH         NO         H20
     2       HO2      H202        /12F10.5)
C  END OF INPUT
C
C  INITIAL PROGRAM VALUES
C  1) MF
      SIGMA6=0.
      DO 38 J=1,JSPENO
   38 SIGMA6=SIGMA6+PP(J)*WM(J)
      DO 39 J=1,JSPENO
      MF1(J)=PP(J)/SIGMA6
   39 MF(J)=MF1(J)
C  2. ROE
      ROE=(SIGMA6/(R1*T0*1400.))*144.
C  3) TOMASS
      TOMASS=ROE*X(4)*3.142*1.006/1728.
C
      WRITE(6,130)ROE
  130 FORMAT(5H ROE=,F10.5)
      RETURN
      END

$IBFTC RATE    DECK
      SUBROUTINE RATEQN(TEMP,MSTEP)
      REAL MF,MF1,MAX2
```

```
                                                                XII CONTD. -10
      COMMON    POLY2(10),POLY3(10),TIME(200),P3(200),X(200),XT(200),RA
     1EP(200),VEL(200),CP(20,10),CK(20,3),CEQ(20,3),POLY(10,10),POLYXB(
     20),POLYPB(10),POLYVB(10),POLYRB(10),RATE(20,4),RATEMT(20),R(20),U
     320),CV(20),DT(100),EQUN(100),PP(20),WM(20),MF1(20),PC(1000),MF(20
     4,DIFMF(20),CS(20,3),TITLE(12),UR(20),
     5TO,R1,PO,NA,NC,JSPENO,IRECN,SIGMA6,ROE,TOMASS
      SIGMA5=0.
      DO 99 J=1,JSPENO
   99 SIGMA5=SIGMA5+MF(J)
      MF(15)=SIGMA5
      LCON=LCON+1
      IF(MSTEP .NE. 2) GO TO 20
      IF (LCON .GT. 1) GO TO 21
      GO TO 22
   20 LCON=0
   22 CONTINUE
C
C  REACTION RATES
      DO 70 IR=1,IRECN
      RATE(IR,3)=CK(IR,1)+CK(IR,2)*ALOG(TEMP)-CK(IR,3)/(TEMP*R1)
      RATE(IR,4)=RATE(IR,3)-(CEQ(IR,1)+CEQ(IR,2)*ALOG(TEMP)-CEQ(IR,3)/T
     1MP)
      DO 70 J=3,4
      IF(RATE(IR,J) .LE.-70.) RATE(IR,J)=-70.
      IF(RATE(IR,J) .GE. 70.) RATE(IR,J)= 70.
      J2=J-2
      IF(RATE(IR,J)) 121,122,122
  121 RATE(IR,J2)=1./EXP(ABS(RATE(IR,J)))
  122 IF(RATE(IR,J).GE. 70.) WRITE(6,145)IR,J2
  145 FORMAT(6HORATE(I2,1H,I1,1HH) .GT. EXP(70))
      RATE(IR,J2)=EXP(RATE(IR,J))
   70 RATE(IR,J2)=RATE(IR,J2)*453.6/28316.39
      RATE(5,1)=RATE(5,1)*453.6/28316.39
      RATE(6,1)=RATE(6,1)*453.6/28316.39
      RATE(7,1)=RATE(7,1)*453.6/28316.39
      RATE(8,1)=RATE(8,1)*453.6/28316.39
      RATE(10,1)=RATE(10,1)*453.6/28316.39
      RATE(12,2)=RATE(12,2)*453.6/28316.39
   91 RATE(5,2)=RATE(5,2)*82.056*TEMP
      RATE(6,2)=RATE(6,2)*82.056*TEMP
      RATE(7,2)=RATE(7,2)*82.056*TEMP
      RATE(8,2)=RATE(8,2)*82.056*TEMP
      RATE(10,2)=RATE(10,2)*82.056*TEMP
      RATE(12,2)=RATE(12,2)/(82.056*TEMP)
      J7=IRECN+1
  141 DO 132 J2=1,2
      DO 132 J1=J7,14
  132 RATE(J1,J2)=0.
C  ADDITIONAL VOL. CHANGE TEMPERATURE MAY BE NEEDED HERE
      DO 93 J=1,2
      DO 93 IR=1,IRECN
```

XII CONTD. -11

```
   93 RATE(IR,J)=RATE(IR,J)*453.6/(1728.*2.54**3.)
   21 CONTINUE
C
      RATENT(1)=(ROE**2.)*(RATE(1,1)*MF(1)*MF(7)-RATE(1,2)*MF(9)*MF(4))
      RATENT(2)=(ROE**2.)*(RATE(2,1)*MF(2)*MF(4)-RATE(2,2)*MF(7)*MF(5))
      RATENT(3)=(ROE**2.)*(RATE(3,1)*MF(1)*MF(5)-RATE(3,2)*MF(7)*MF(4))
      RATENT(4)=(ROE**2.)*(RATE(4,1)*MF(9)*MF(5)-RATE(4,2)*MF(7)*MF(7))
      RATENT(5)=(ROE**2.)*(RATE(5,1)*MF(4)*MF(7)*MF(15)*ROE-RATE(5,2)*MF
     1(9)*MF(15))
      RATENT(6)=(ROE**2.)*(RATE(6,1)*MF(15)*MF(5)*MF(5)*ROE-RATE(6,2)*MF
     1(2)*MF(15))
      RATENT(7)=(ROE**2.)*(RATE(7,1)*MF(4)*MF(4)*MF(15)*ROE-RATE(7,2)*MF
     1(1)*MF(15))
      RATENT(8)=(ROE**2.)*(RATE(8,1)*MF(5)*MF(4)*MF(15)*ROE-RATE(8,2)*MF
     1(7)*MF(15))
      RATENT(9)=(ROE**2.)*(RATE(9,1)*MF(1)*MF(2)-RATE(9,2)*MF(7)*MF(7))
      RATENT(10)=(ROE**2.)*(RATE(10,1)*MF(4)*MF(2)*MF(15)*ROE-RATE(10,2)
     1*MF(10)*MF(15))
      RATENT(11)=(ROE**2.)*(RATE(11,1)*MF(10)*MF(10)-RATE(11,2)*MF(11)*M
     1F(2))
      RATENT(12)=(ROE**2.)*(RATE(12,1)*MF(11)*MF(15)-RATE(12,2)*MF(7)*MF
     1(7)*MF(15)*ROE)
      RATENT(13)=(ROE**2.)*(RATE(13,1)*MF(4)*MF(11)-RATE(13,2)*MF(9)*MF(
     17))
C
C       ADDITIONAL TERMS MAY BE NEEDED BELOW
C
C  MOLECULAR CONTINUNITY
C       ADDITIONAL TERMS MAY BE NEEDED BELOW
      DO 71 I=1,IRECN
   71 R(I)=RATENT(I)
      DIFMF(1)=-R(1)-R(3)+R(7)-R(9)
      DIFMF(2)=-R(2)+R(6)-R(10)+R(11)-R(9)
      DIFMF(3)=0.
      DIFMF(7)=-R(1)-R(5)+R(2)+R(3)+R(4)*2.+R(8)+2.*R(9)+2.*R(12)+R(13)
      DIFMF(6)=0.
      DIFMF(9)=-R(4)+R(1)+R(5)+R(13)
      DIFMF(10)=R(10)-2.*R(11)
      DIFMF(11)=R(11)-R(12)-R(13)
C
C  ATOMIC CONTINUITY
C  ADDITIONAL EQUATIONS HERE
      DIFMF(4)=-(2.*DIFMF(1)+DIFMF(7)+2.*DIFMF(9)+DIFMF(10)+2.*DIFMF(11)
     1)
      DIFMF(5)=-(2.*DIFMF(2)+DIFMF(7)+DIFMF(9)+DIFMF(8)+2.*DIFMF(10) +2.
     1*DIFMF(11))
      DIFMF(8)=-(2.*DIFMF(3)+DIFMF(8))
      DO 72 I=1,IRECN
   72 RATENT(I)=R(I)
C
```

```
      RETURN
      END

$IBFTC DEKU    DECK
      SUBROUTINE INTENG(IS,CP,R1,TEMP,U,I1,UR)
      DIMENSION CP(20,10),U(20),UR(20)
      TEMPR=298.
      U(IS)=(CP(IS,1)-R1)*(TEMP-TEMPR)   + UR(IS)
      DO 1 JCF=2,10
    1 U(IS)=U(IS)+CP(IS,JCF)*(TEMP**JCF-TEMPR**JCF)/FLOAT(JCF)
      RETURN
      END

$IBFTC DEKCV   DECK
      SUBROUTINE SPECHT(IS,CP,R1,TEMP,CV,I1)
      DIMENSION CP(20,10),CV(20)
      CV(IS)=CP(IS,1)-R1
      DO 10 JCF=2,10
   10 CV(IS)=CV(IS)+CP(IS,JCF)*TEMP**(JCF-1)
      RETURN
      END

$IBFTC DEKDQ   DECK
      SUBROUTINE TRANS(XM,T,VEL,ROE,TO,DELTAQ,XF)
      IF(XM .LE. XF/3.5) GO TO 2
      DELTAQ=0.
      RETURN
    2 SAREA=(2.020*3.142+3.142*2.007*XM)/144.
      ETA = 1.153*145.8*(T**1.5)/((10.**8)*1.176*(T+110.4))
      REN2=VEL*XM*ROE/(ETA*144.)
      TCOND = 0.0325*14.00*1.395*(T **.5)/((1.+245.4/((10.**(12./T ))*T
     1))*5.77*3600.)
      ALPHA=0.93*(TCOND*12./XM)*(ABS(REN2))**.65
      DELTAQ=ALPHA*(T-TO)*SAREA
      RETURN
      END

$IBFTC FITING   DECK
      SUBROUTINE FIT (TIM,TIME,DUM,POLY,M,NA,ICON,TIMINT)
      DIMENSION X(20),Y(20),YC(20),P(20),A(20,20),B(20),C(20)
      DIMENSION TERM(10)
      DIMENSION MPER(20),JI(6)
      DIMENSION TIME(100),DUM(1000),POLY(10,10)
      DATA SWITCH /.75/
C TEST 1
      I1=NA-3
      ICON=0
      IF(TIM .GE. TIME(I1)) RETURN
C TEST 2
      IF (TIM .NE. TIMINT) GO TO 199
      IF (SWITCH .LT. .8 .AND. SWITCH .GE. .7) GO TO 198
```

```
      GO TO 199
  198 N1=0
      IBAD=-1
      ITCH = 1
  199 IF (ITCH .LE. 4) GO TO 5
      IF (TIM .LE. X(4)) RETURN
      ITCH = 1
    5 ITCH = ITCH + 1
      ICON=1
C SET POLYNOMIAL DATA POINTS
      IBAD=IBAD+1
      SWITCH=FLOAT(IBAD/4) - .25*FLOAT(IBAD)
      IF(SWITCH .LT. .1 .AND. SWITCH .GE. -.1) N1=N1+1
      DO 7 I2=1,6
      I3=I2+N1
      X(I2)=TIME(I3)
    7 Y(I2)=DUM(I3)
      X(7)=X(3)
      X(8)=X(4)
      Y(7)=Y(3)
      Y(8)=Y(4)
      NUMBER=8
      MM = 4
C
C     CURVE FITTING
C
      DO 999 M=2,MM
      MX2 = M*2
      DO 13 I=1,MX2
      P(I)=0.0
      DO 13 J=1, NUMBER
   13 P(I)=P(I) + X(J)**I
      N= M + 1
      DO 30 I=1,N
      DO 30 J = 1 , N
      K = I + J - 2
      IF (K) 29,29,28
   28 A(I,J) = P(K)
      GO TO 30
   29 A(1,1) = NUMBER
   30 CONTINUE
      B(1) = 0.0
      DO 21 J= 1,NUMBER
   21 B(1) = B(1) + Y(J)
      DO 22 I= 2,N
      B(I) = 0.0
      DO 22 J= 1,NUMBER
   22 B(I) = B(I) + Y(J)*X(J)**(I-1)
      NM1 = N - 1
      DO 300 K= 1, NM1
      KP1 = K + 1
```

```
      L = K
      DO 400 I = KP1, N
      IF (ABS(A(I,K)) - ABS(A(L,K))) 400,400,401
  401 L = I
  400 CONTINUE
      IF (L - K) 500,500,405
  405 DO 410 J= K, N
      TEMP = A(K, J)
       A(K,J) = A(L,J)
  410 A(L, J) = TEMP
      TEMP = B(K)
      B(K) = B(L)
      B(L) = TEMP
  500 DO 300 I= KP1, N
      FACTOR = A(I,K) / A(K,K)
      A(I, K) = 0.0
      DO 301 J = KP1, N
  301 A(I, J) =  A(I, J) - FACTOR * A(K, J)
  300 B(I) = B(I) - FACTOR * B(K)
      C(N) = B(N) / A(N,N)
      I= NM1
  710 IP1 = I + 1
      SUM = 0.0
      DO 700 J = IP1 , N
  700 SUM = SUM + A(I, J) * C(J)
      C(I) =(B(I) - SUM) / A(I,I)
      I = I - 1
      IF (I) 800,800,710
  800 DO 900 I=1,N
  900 POLY(M,I)=C(I)
      DO 911 J=1,NUMBER
      YC(J) = C(1)
      DO 911 I=2,N
  911 YC(J) = YC(J) + C(I) * X(J)**(I-1)
      CALL ERROR(X,Y,YC,C,NUMBER,I,J,N,MPER,M)
      JI(M) = J
  999 CONTINUE
      M=2
      DO 1009 I5=3,MM
      DIF2 = ABS(MPER(M)) - ABS(MPER(I5))
      IF (DIF2) 1009,1009,1008
 1008 M=I5
 1009 CONTINUE
      WRITE(6,1010)M,JI(M),MPER(M)
 1010 FORMAT(22H ORDER OF POLYNOMIAL =,I4,3X, 9HLOCATION=I4,35H MINIMUM
     1MAXIMUM PERCENTAGE ERROR =,F9.5)
      RETURN
      END

$IBFTC ERROR    DECK
      SUBROUTINE ERROR(X,Y,U,POLY,M,K,I,N,PER,NM1)
      DIMENSION X(20),Y(20),U(20),POLY(20),ORD(20)
```

XII CONTD. -15

```
      DIMENSION PER(20),MPER(20)
C
C     COMPUTE MAXIMUM ERROR
      I = 1
      DO 29 I7=2,M
      DIF=ABS(Y(I)-U(I))-ABS(Y(I7)-U(I7))
      IF(DIF)28,28,29
   28 I = I7
   29 CONTINUE
      EROR=Y(I)-U(I)
C     COMPUTE MAXIMUM PERCENTAGE ERROR
      I=1
      DO 39 I6=2,M
      DIF1=ABS((Y(I)-U(I))/Y(I))-ABS((Y(I6)-U(I6))/Y(I6))
      IF (DIF1) 38,38,39
   38 I=I6
   39 CONTINUE
      PER(MN1)=(Y(I)-U(I))*100./Y(I)
      RETURN
      END
```

```
$DATA
   TYPICAL DATA DECK N.B. EXPERIMENTAL TIME DATA CARDS 6. TO 40. MISSIN
 0.010657E 01
 0.422682E 00
-0.407836E-03
-0.648795E-04
 0.578757E-05
-0.937870E-07
 0.010938E 01
 0.159136E 00
 0.371012E-02
-0.478222E-03
 0.234284E-04
-0.385103E-06
-0.371241E-08
 0.124838E-09
353.        1.986       14.7        0.        2519.      2416.      2519.
.2759       24.
  48  24
0.          0.          0.
1.          0.5         0.
2.          1.          3.
3.          1.5         15.
4.          2.0         47.
5.          3.          81.


41.         2262.       1447.
42.         2141.       1363.
43.         1960.       1263.
44.         1760.       1147.
45.         1558.       1020.
```

XII CONTD. -16

```
46.        1384.      875.
47.        1217.      720.
11
+0.67717 E+01+0.75962 E-03-0.13791 E-05+0.16415 E-08-0.65103 E-12
+0.84921 E-16
+0.63698 E 01+0.17998 E-02+0.15815 E-05-0.21810 E-08+0.85804 E-12
-0.11137 E-15
+0.495000E+01

+0.4968  E+01

+0.56794 E+01-0.21957 E-02+0.27335 E-05-0.16397 E-08+0.46886 E-12
-0.15100 E-16
+0.49692 E+01-0.57129 E-05+0.78368 E-08-0.25396 E-11-0.13827 E-14
+0.69541 E-18
+0.77485 E+01-0.32194 E-02+0.46180 E-05-0.22728 E-08+0.50157 E-12
-0.41704 E-16
+0.71946 E+01-0.17124 E-02+0.59265 E-05-0.46178 E-08+0.14826 E-11
-0.17222 E-15
+0.79526 E+01-0.12299 E-02+0.58635 E-05-0.35407 E-08+0.89235 E-12
-0.84303 E-16
+0.60279 E+01+0.90143 E-02-0.48245 E-05+0.12089 E-08-0.13645 E-12

+0.3254575E 01+0.351203E-01-0.489914E-04+0.402408E-07-0.188512E-10
+0.477442E-14-0.528561E-18
 9
-0.6354  E 01 0.5      E 01 0.1215  E 04
 0.3145  E 02 0.0           0.16170 E 05
 0.1466  E 02 0.2056  E 01 0.5630  E 04
+0.320499E+02 0.0          +0.101   E+05
 0.3815  E 02 0.0           0.1600  E 04
 0.2934  E 02 0.0          -0.66    E 03
 0.3396  E 02 0.0          -0.1531  E 04
 0.3725  E 02 0.0          -0.2780  E 04
 0.2627  E 02 0.0           0.43300 E 05
 0.0     E 00
 0.0     E 00
 0.0     E 00
+0.166961E 01+0.647596E 00+0.260504E 05
+0.424035E 01+0.444265E 00+0.299032E 05
+0.344119E 01+0.537791E 00+0.567265E 05
+0.325064E 01-0.104311E 00+0.478199E 04
+0.140999E 01+0.139163E-01+0.108593E 05
-0.594171E 00-0.751074E 00-0.209589E 05
-0.306231E 01-0.357665E 00+0.252016E 04
-0.852058E 01-0.622745E 00-0.182063E 05
2.016      32.0       39.944     1.008      16.000     14.08      17.008
30.008     18.016     33.008     34.016
0.0        0.0        0.0        52.102     59.559     112.965    9.330
21.580     -57.798    5.000      -25.208
0.867      2.905      10.93      0.0        0.0        0.0        0.0
0.0        0.0        0.0        0.0        0.0        0.0        0.
$EOF
```

APPENDIX B

HEAT TRANSFER ANALYSIS

B.1 The Object is to derive an equation for the overall surface-heat-transfer coefficient at the gas-wall interface of the compression-machine cylinder. The experimental measurements available to evaluate the coefficient are the pressure- and volume-time histories of a compressed non-reacting charge.

B.2 Assumptions About the System

The system considered is that bounded by the cylinder walls, the cylinder head and the moving boundary of the piston-crown, as in fig 2.21-1. It is assumed that:

1) The system is at all times homogeneous.
2) The gas obeys the ideal-gas laws.
3) There is no loss of mass from the system.
4) Gravitational and gas-motion forces may be neglected.*
5) The wall temperature is constant.
6) There is immediate pressure equalisation throughout the system.

B.3 Derivation of Equations

Conservation of energy: 1st Law of Thermodynamics

$$dQ - dW = dU \qquad \text{B.3-1}$$

which relates the heat flux Q and the work W at the system boundary to the internal energy U. The internal energy of a perfect

---

* We make this assumption knowing that the heat-transfer process is convective. Milkins [37.] has shown that the gas-motion is insufficient to make a large contribution to the energy conservation equation.

gas is related to the temperature T by its specific heat at constant volume C_v, by:

$$dU = MC_v dT \qquad \text{B.3-2}$$

From the Ideal Gas Law we have:

$$Vdp + pdV = MRdt \qquad \text{B.3-3}$$

Now the system work is given by:

$$dW = pdV \qquad \text{B.3-4}$$

Thus we may rearrange equation B.3-1 as:

$$dQ = \left(\frac{C_v}{R} + 1\right) pdV + \frac{C_v}{R} Vdp \qquad \text{B.3-5}$$

We may eliminate C_v/R from this equation by means of the specific heat ratio $\gamma = C_p/C_v$ which defines

$$\frac{C_v}{R} = \frac{1}{J(\gamma-1)} \qquad \text{B.3-6}$$

Thus we may now express equation B.3-5 as

$$dQ = \frac{1}{J(\gamma-1)} (\gamma pdV + Vdp) \qquad \text{B.3-7}$$

Now the instantaneous surface-heat-transfer coefficient α is defined by

$$\alpha = \frac{1}{A_t(T-T_w)} \frac{dQ}{dt} \qquad \text{B.3-8}$$

where A_t = the area available for heat transfer

T = the gas temperature

and T_w = the wall temperature.

By substituting equation B.3-7 in B.3-8 we have

$$\alpha = \left(\gamma p \frac{dV}{dt} + V \frac{dp}{dt}\right) / J(\gamma-1) A_t (T-T_w) \qquad \text{B.3-9}$$

B.4 Application of the final equation

Equation B.3-9 expresses the surface heat-transfer coefficient, α, in terms of known or derivable quantities.

Milkins, in his thesis [37.], has made an assessment of the accuracy with which α may be calculated. He has shown that the equation always involves the difference between the two terms γpdV and Vdp, and,as a result, the final accuracy is dependent upon the derivations of the two experimental measurememements V and p. Thus in the finite-difference procedure used in evaluating these derivatives precision is of prime importance: for example, if the procedure or experimental technique introduces a .6% phase difference in time between dp and dV, α can be in error by as much as 50%.

In the computer programme, written by the present author to evaluate the heat transfer coefficient, a numerical procedure was adopted which used smoothing of fitted experimental data to minimise errors in the derivatives. The listing of this programme may be found in Milkins's thesis.

The application of this programme to derive a single equation for predicting heat transfer in the compression machine is presented in section 3.25.

APPENDIX C

THE REACTION-RATE SURVEY

C.1 Introduction

The object of this survey was to determine the reaction-rates of all the twenty-two reactions listed in table 3.43-1 over the temperature range 300 to 2000°K.*

The survey shows that there are wide variations, from one worker to another, in the values of the rates of many reactions reported in the literature. Thus, from the survey, it was essential to establish representative values which could be used in the procedure for predicting autoignition. To this end, the reported reaction-rates have been fitted to the Arrnhenius reaction-rate expression.

C.2 The Data

The reaction-rate data was assembled from a survey of recent publications on chemical-kinetics and also made use of three existing surveys [5., 35. and 42.].

The data presented here is confined to only those 13 elementary reactions considered in the predictions made in Chapters 6 and 7. The reaction rates are plotted in figs C.3-1 through to C.3-13 as $\log_{10} k_{jf}$ to a base of $\log_{10} T$.

Following the figures, abbreviated references are listed which show the source of the points plotted on the graphs.

C.3 Data Fitting Procedure

We may recall from section 2.22b that the modified Arrhenius expression for the rate of reaction is:

---

* The range of temperature encountered in the hydrogen-autoignition tests.

$$k_{jf} = A_j T^{B_j} e^{-E_j/RT} \qquad \text{C.3-1}$$

The term T^{B_j} originates from kinetic-theory relations* which express the frequency of those molecule collisions that result in chemical reaction. The value of B_j depends upon the assumptions made in formulating the theory.

An alternative form of equation C.3-1 is frequently adopted in which $B_j = 0$ and to compensate for this the activation energy E_j is modified.

For those reactions for which much rate-constant data is available, the constants in the Arrhenius expression have been found for the two forms of the equation. A computer programme has been written to find the constants in each form of the equation. Both programmes fit the reaction-rate data to the equations by the method of least squares. Where reaction rates have been reported over a range of temperature the values fitted were those at the extremes of the range.

C.4 Discussion of the Fitted Constants

The Arrhenius expressions which result from the data fitting are listed on each figure.

Fitting reaction-rate data by statistical methods can lead to anomalies. For example: the activation energy E_j in the kinetic theory must be greater than the energy of reaction ΔH_j absorbed in an endothermic bi-molecular reaction. Inspection of reaction II reveals $E_2 = 16.17$ K cal but $\Delta H_2 = 16.7$ K cal. Although inconsistent with the theory, the value of E_2 is in agreement with Bascombe's findings [6.].

---

* See, for example Benson [6.].

Figs C.3-1 and C.3-3 for reactions I and III respectively, show that, when $B_j \neq 0$ in the Arrhenius equation, a better agreement exists between the fitted equation and the experimental data at high temperatures (in excess of 1500°C) than when $B_j = 0$. The former equations have therefore been used in the autoignition predictions.

It has been argued [21.] that the recombination reactions VI and VII should, for consistency with the kinetic theory, be fitted to equations of the form:

$$k_{jf} = AT^{-B} \qquad \text{C.4-1}$$

However, the rates of reactions VI and VII are so very nearly temperature independent that fitting to equation C.3-1 or C.4-1 leads mean curves having similar values over the temperature range 300 to 2000°K.

C.5 Conclusions

We have presented in graphical form, in figs C.3-1 to C.3-13, reported values for the rates of 13 reactions. Representative values of the variation of their rates of reaction with temperature have been obtained by fitting to equations of Arrhenius type.

To enable direct comparisons to be made between the fitted curves and the effective reaction-rates derived in the present work, the effective reaction-rates have been plotted. Also plotted is the data derived by Jenkins et al. [26.] for five reactions.

FIG. C.3-1 REACTION RATES FOR REACTION NO. I

$OH + H_2 \rightleftharpoons H_2O + H$

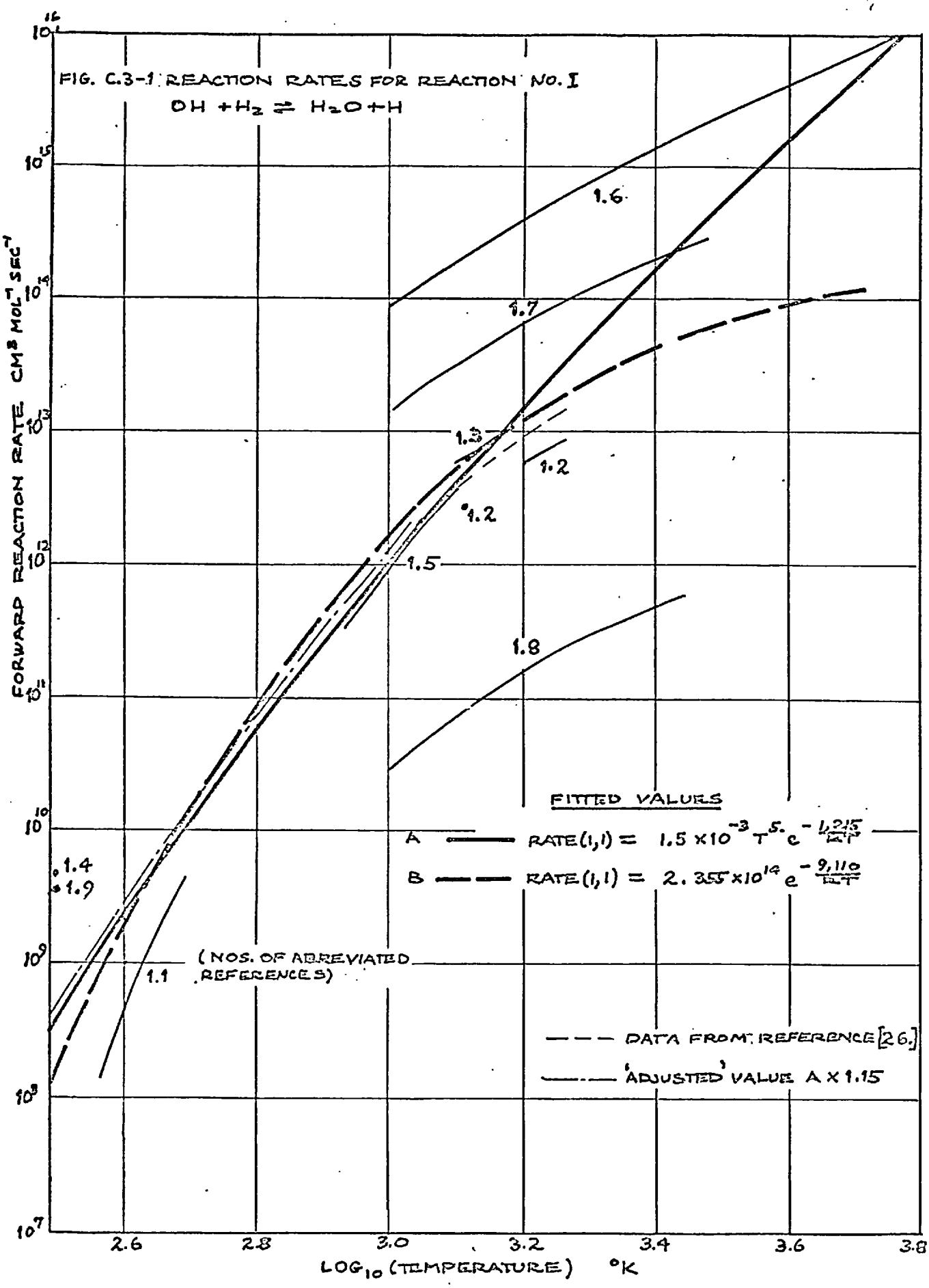

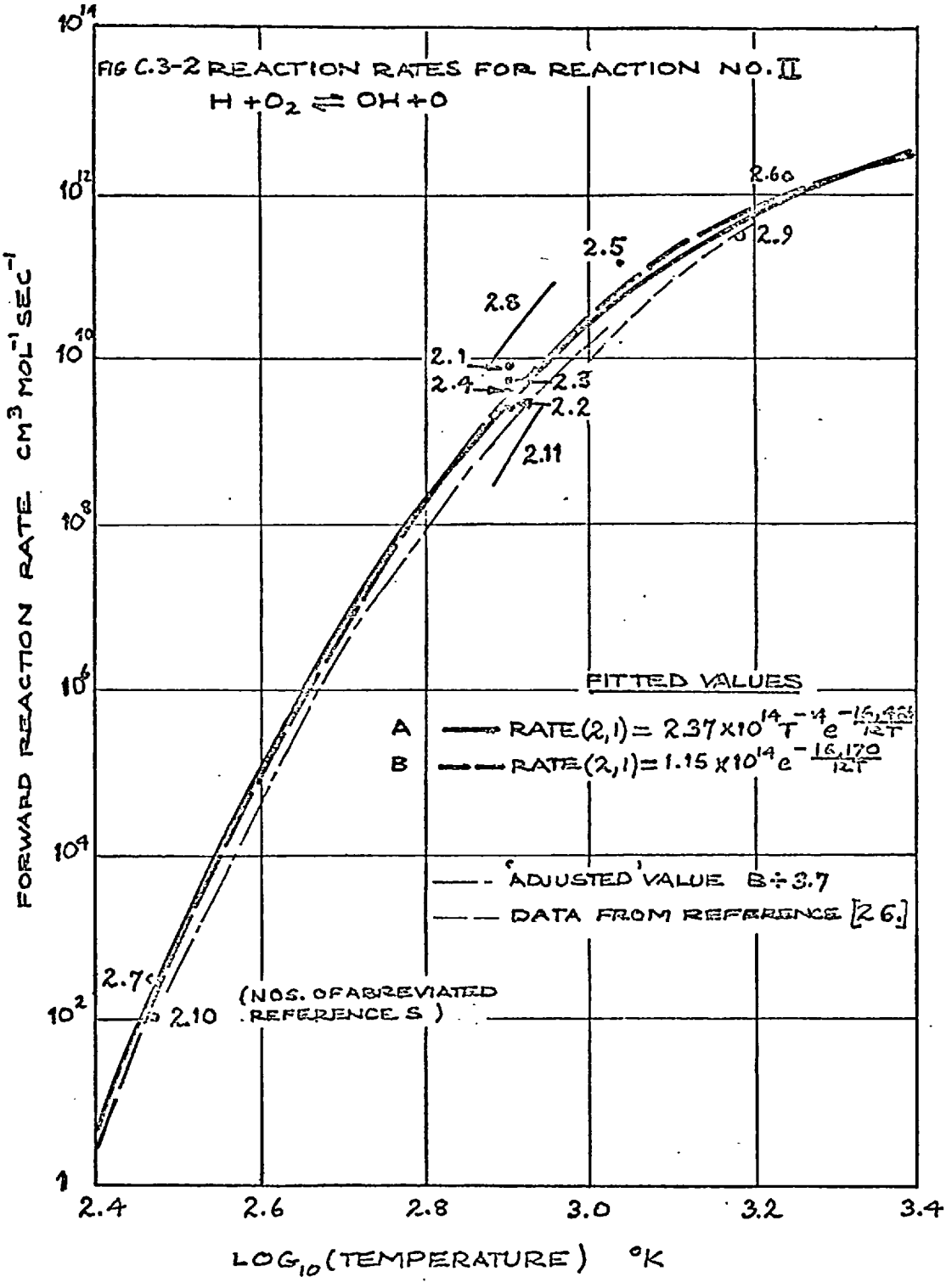
FIG C.3-2 REACTION RATES FOR REACTION NO. II
H + O2 ⇌ OH + O
FORWARD REACTION RATE CM3 MOL-1 SEC-1
LOG10 (TEMPERATURE) °K
FITTED VALUES
A RATE(2,1) = 2.37 x 10^14 T^-1.4 e^-16,444/RT
B RATE(2,1) = 1.15 x 10^14 e^-16,170/RT
'ADJUSTED' VALUE B ÷ 3.7
DATA FROM REFERENCE [26]
(NOS. OF ABBREVIATED REFERENCES)
2.60
2.9
2.5
2.8
2.1
2.4
2.3
2.2
2.11
2.7
2.10

FIG C.3-3 REACTION RATES FOR REACTION NO. III

$H_2 + O \rightleftharpoons OH + H$

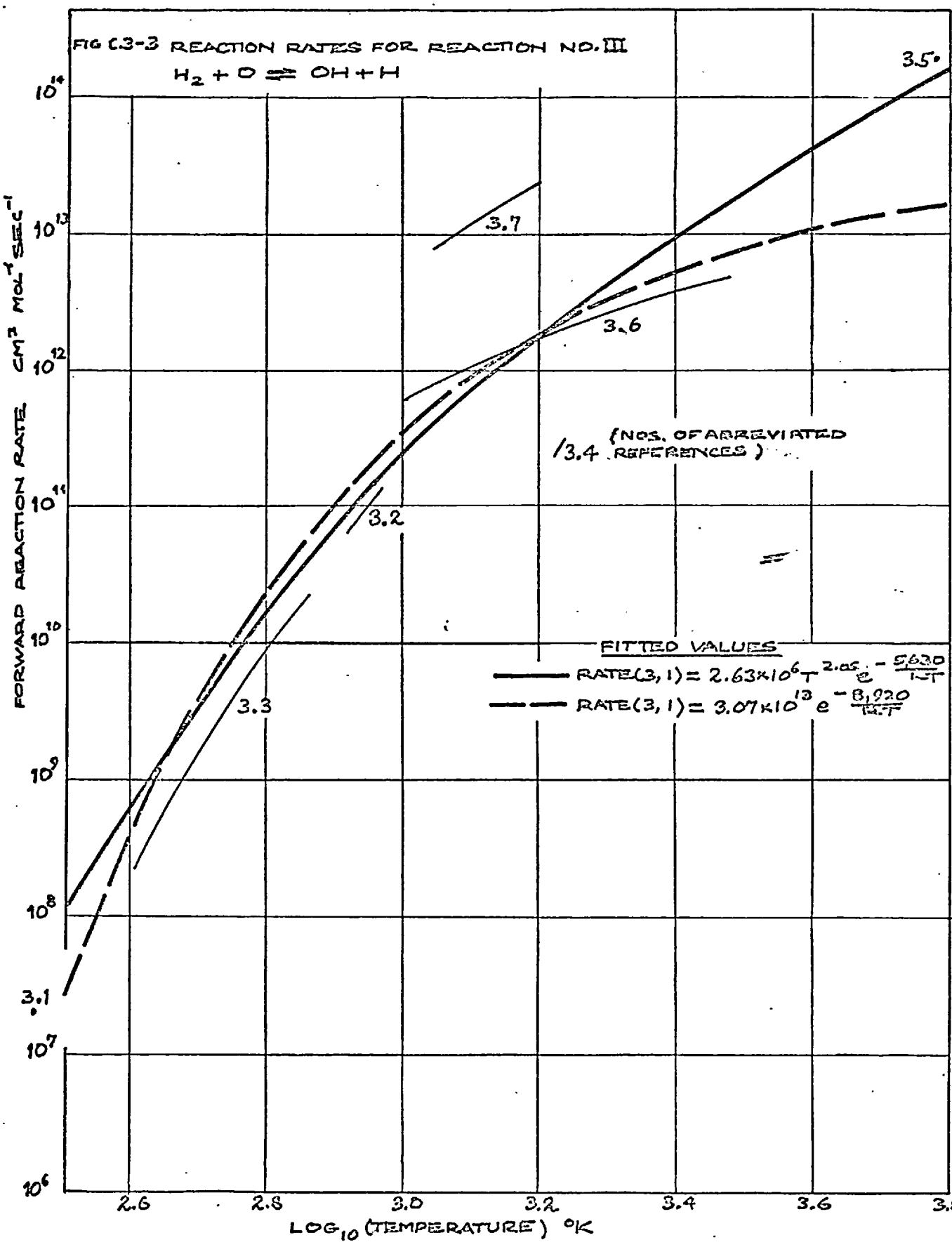

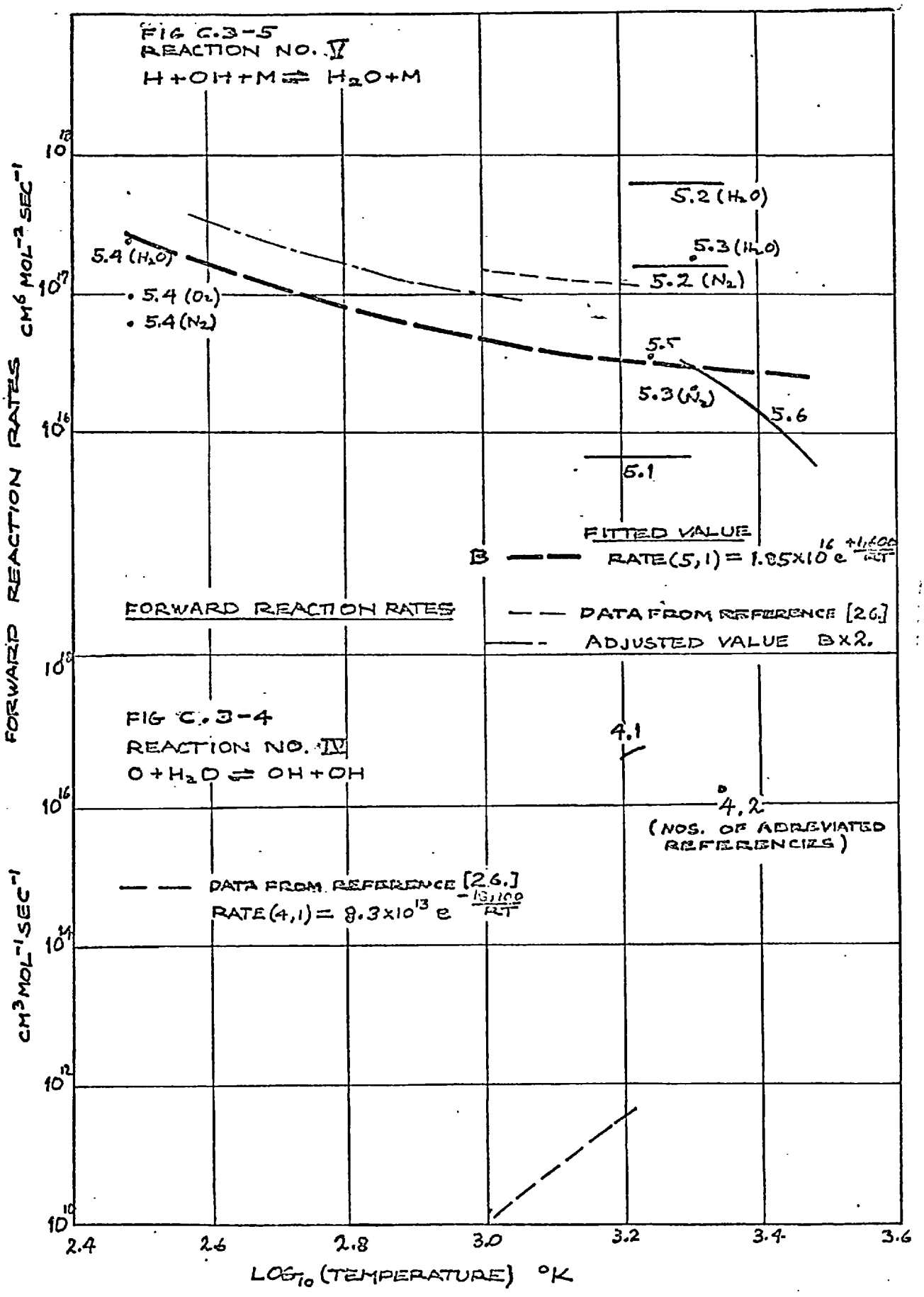
FIG C.3-5
REACTION NO. V
H+OH+M ⇌ H2O+M
FORWARD REACTION RATES CM6 MOL-2 SEC-1
5.4 (H2O)
5.4 (O2)
5.4 (N2)
5.2 (H2O)
5.3 (H2O)
5.2 (N2)
5.5
5.3 (N2)
5.6
5.1
FITTED VALUE
B
RATE(5,1) = 1.85x10^16 e^(+1,400/RT)
FORWARD REACTION RATES
DATA FROM REFERENCE [26.]
ADJUSTED VALUE B x2.
FIG C.3-4
REACTION NO. IV
O+H2O ⇌ OH+OH
CM3 MOL-1 SEC-1
4.1
4.2
(NOS. OF ABBREVIATED REFERENCES)
DATA FROM REFERENCE [26.]
RATE(4,1) = 8.3x10^13 e^(-18,100/RT)
LOG10 (TEMPERATURE) °K
2.4
2.6
2.8
3.0
3.2
3.4
3.6

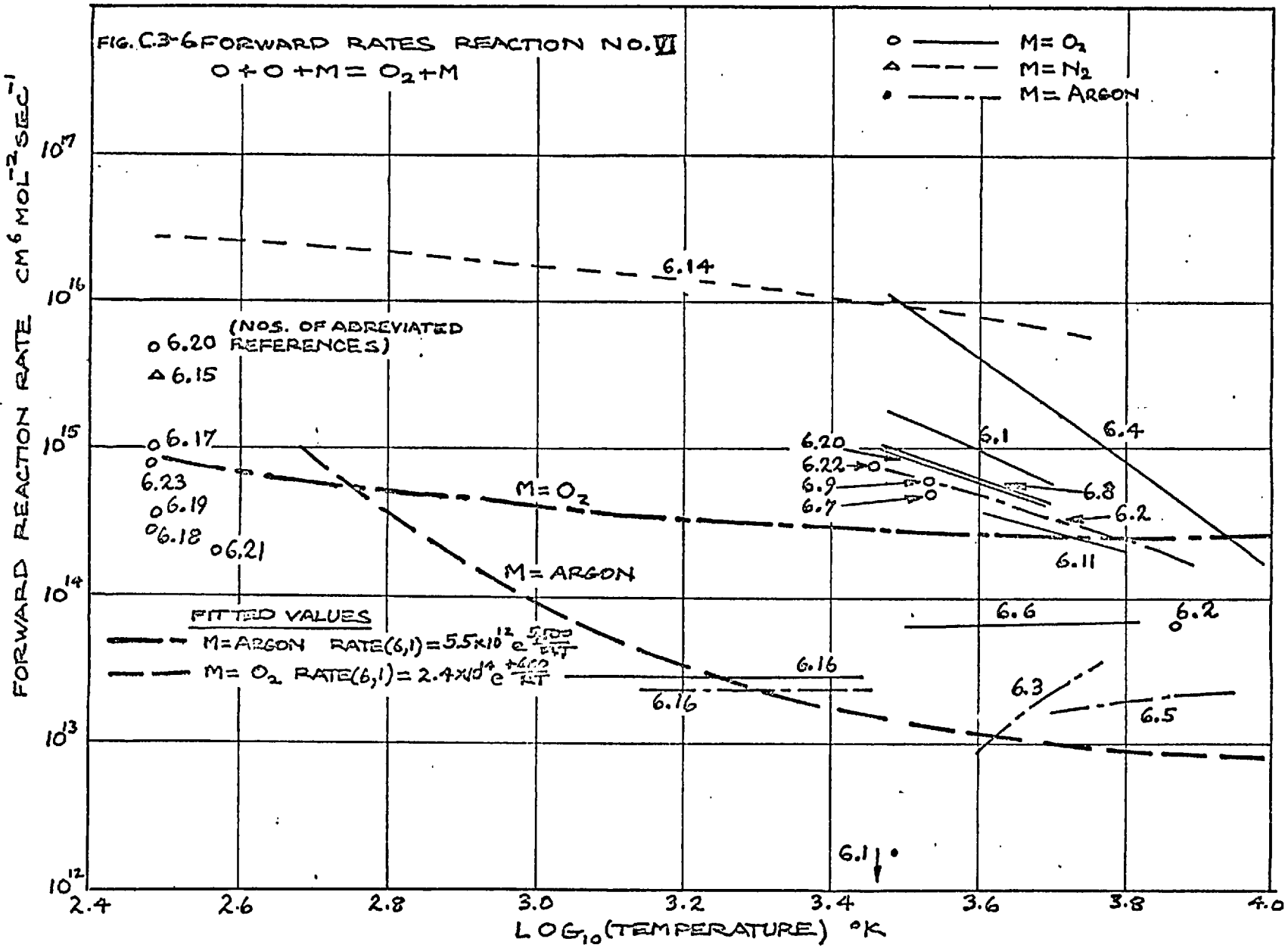
FIG. C.3-6 FORWARD RATES REACTION NO. VI
O + O + M = O2 + M
M = O2
M = N2
M = ARGON
(NOS. OF ABREVIATED REFERENCES)
6.20
6.15
6.17
6.23
6.19
6.18
6.21
6.14
6.1
6.4
6.22
6.9
6.7
6.8
6.2
6.11
M = O2
M = ARGON
FITTED VALUES
M = ARGON RATE(6,1) = 5.5x10^12 e^(-5000/RT)
M = O2 RATE(6,1) = 2.4x10^14 e^(+400/RT)
6.6
6.16
6.16
6.3
6.5
6.1
FORWARD REACTION RATE CM^6 MOL^-2 SEC^-1
LOG10 (TEMPERATURE) °K
10^17
10^16
10^15
10^14
10^13
10^12
2.4
2.6
2.8
3.0
3.2
3.4
3.6
3.8
4.0

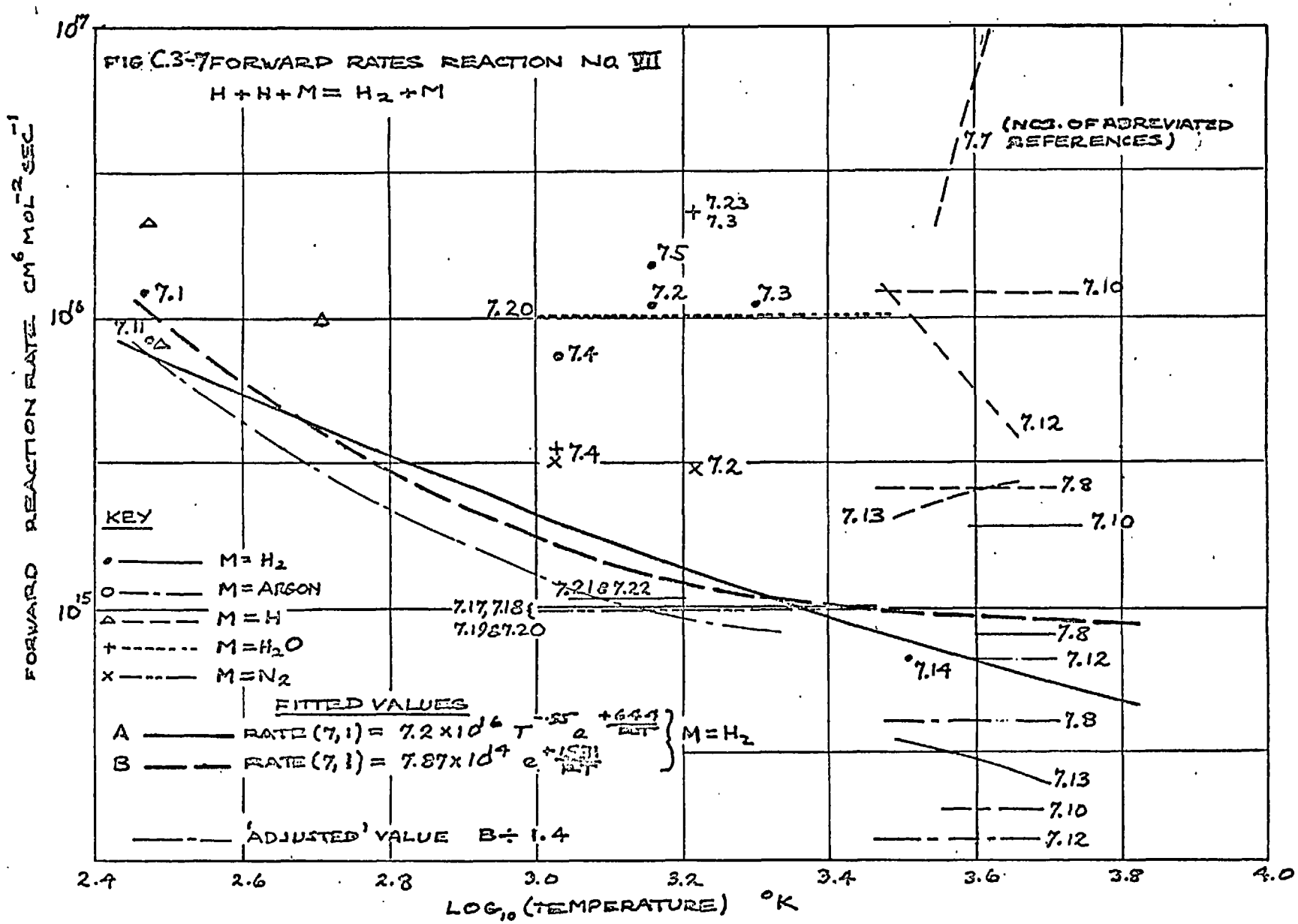
FIG C.3-7 FORWARD RATES REACTION NO VII
H + H + M = H2 + M
FORWARD REACTION RATE CM6 MOL-2 SEC-1
LOG10 (TEMPERATURE) °K
(NOS. OF ABREVIATED REFERENCES)
7.1
7.2
7.3
7.4
7.5
7.10
7.11
7.12
7.13
7.14
7.17, 7.18
7.19 & 7.20
7.21 & 7.22
7.23
KEY
M = H2
M = ARGON
M = H
M = H2O
M = N2
FITTED VALUES
A RATE (7,1) = 7.2 x 10-6 T-.55 e +644/RT
B RATE (7,1) = 7.87 x 10-4 e +1510/RT
M = H2
'ADJUSTED' VALUE B ÷ 1.4

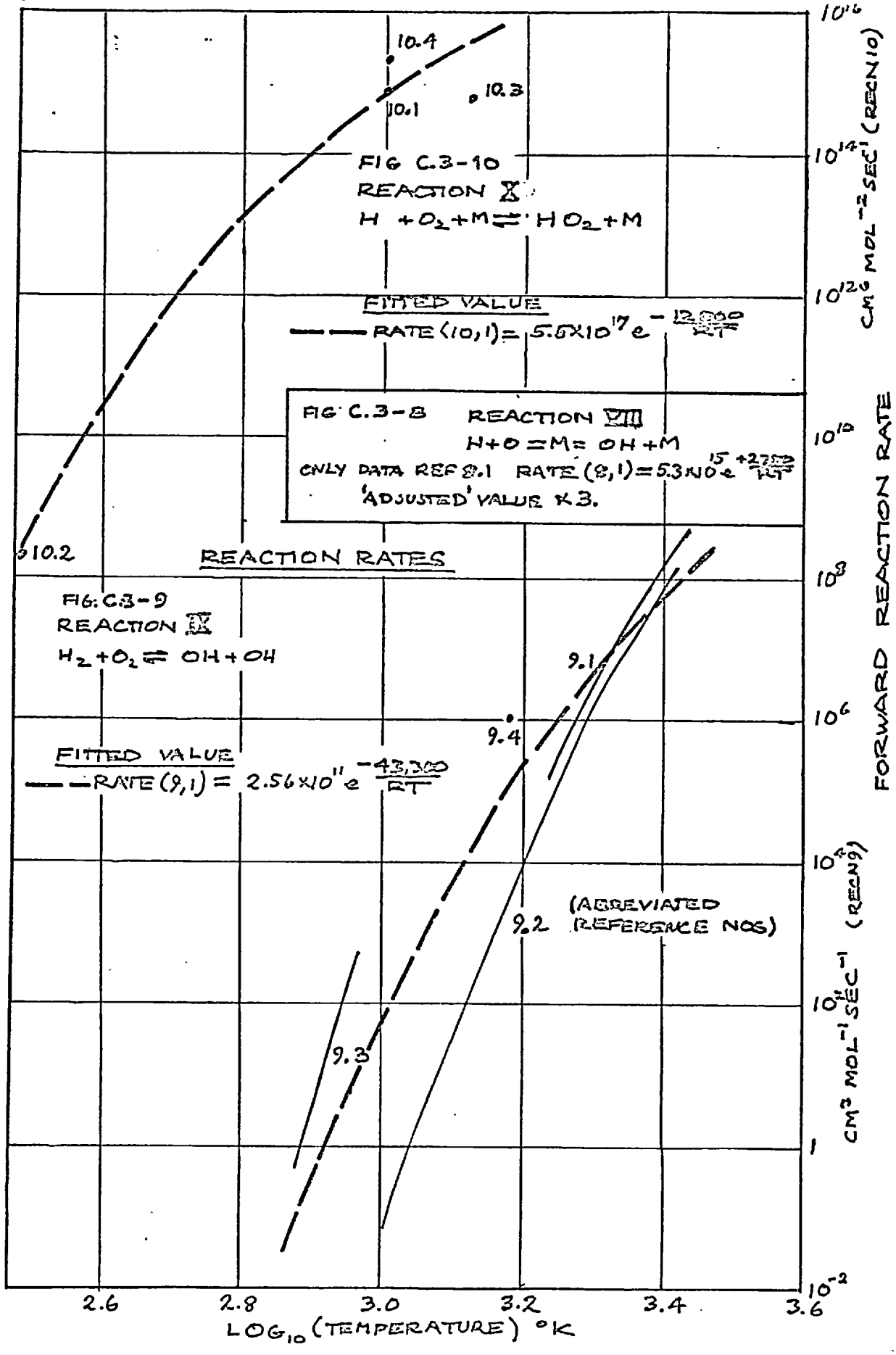
REACTION RATES
FIG C.3-10
REACTION X
H + O2 + M ⇌ HO2 + M
FITTED VALUE
RATE (10,1) = 5.6X10^17 e^-12,000/RT
FIG C.3-8 REACTION VIII
H+O=M=OH+M
ONLY DATA REF 8.1 RATE (8,1) = 5.3X10^15 e^+2750/RT
'ADJUSTED' VALUE X3.
FIG C.3-9
REACTION IX
H2 + O2 ⇌ OH + OH
FITTED VALUE
RATE (9,1) = 2.56X10^11 e^-43,500/RT
10.4
10.3
10.1
10.2
9.1
9.4
9.2
9.3
(ABBREVIATED REFERENCE NOS)
FORWARD REACTION RATE
CM^6 MOL^-2 SEC^-1 (REACN 10)
CM^3 MOL^-1 SEC^-1 (REACN 9)
10^16
10^14
10^12
10^10
10^8
10^6
10^4
1
10^-2
2.6
2.8
3.0
3.2
3.4
3.6
LOG10 (TEMPERATURE) °K

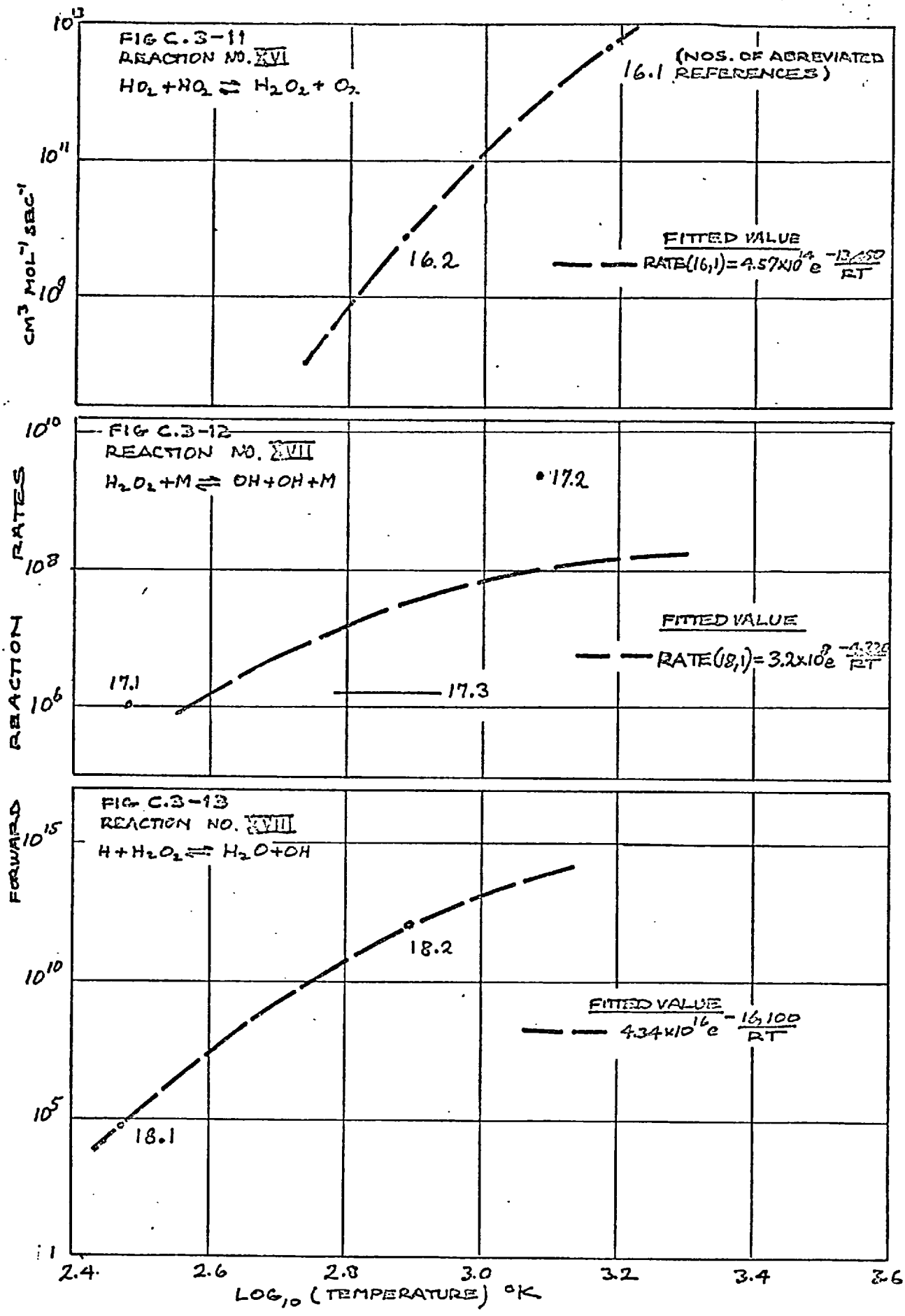
FIG C.3-11
REACTION NO. XVI
$HO_2 + NO_2 \rightleftharpoons H_2O_2 + O_2$
(NOS. OF ABREVIATED REFERENCES)
16.1
16.2
FITTED VALUE
RATE(16,1) = $4.57 \times 10^{14} e^{\frac{-13,450}{RT}}$
$CM^3\ MOL^{-1}\ SEC^{-1}$
10^{13}
10^{11}
10^{9}
FIG C.3-12
REACTION NO. XVII
$H_2O_2 + M \rightleftharpoons OH + OH + M$
17.2
17.1
17.3
FITTED VALUE
RATE(18,1) = $3.2 \times 10^{8} e^{\frac{-4,330}{RT}}$
REACTION RATES
10^{10}
10^{8}
10^{6}
FIG C.3-13
REACTION NO. XVIII
$H + H_2O_2 \rightleftharpoons H_2O + OH$
18.2
18.1
FITTED VALUE
$4.34 \times 10^{16} e^{\frac{-16,100}{RT}}$
FORWARD
10^{15}
10^{10}
10^{5}
1
2.4
2.6
2.8
3.0
3.2
3.4
3.6
LOG_{10} (TEMPERATURE) °K

The abbreviated references of the sources of the data

1.1 AVRAMENKO & LORENZO, Zhur. Fiz. Khim. 24, 207, 1950.

1.2 FENIMORE & JONES, J. Phys. Chem. 62, 693, 1958.

1.3 FENIMORE & JONES, J. Phys. Chem. 65, 993, 1961.

14. KAUFMAN & DEL GRECO, 9th Symposium on Combustion.

1.5 KONDRAT'EV, Chemical Kinetics of Gas Reactions 265, 1964.

1.6 DUFF, J. Chem. Phys, 29, 230, 1958.

1.7 SCHOTT & KINSEY, J. Chem. Phys. 29, 1177, 1958.

1.8 SEMENOV, Chem. Kinetics and Chain Reactions 1935.

1.9 WESTERNBERG, Chem. Digest, Oct. 1966, 6, NO.1.

2.1 SEMENOV, Acta. Physiochem, 1942, 20, 290.

2.2 BALDWIN, Trans. Faraday Soc. 1956, 52, 1344.

2.3 BALDWIN & CROWE, Trans. Faraday Soc. 1962, 58, 1768.

2.4 NALBANDYAN, KARMILWA & SEMENOV, Zhur. Fiz. Chem. 1958, 52, 1193.

2.5 FENIMORE & JONES, J. Phys. Chem. 1959, 63, 1154.

2.6 SCHOTT & KINSEY, J. Phys. Chem. 1958, 29, 1177.

2.7 KAUFMAN & DEL GRECO, 9th Symposium on Combustion.

2.8 VOEVODSKY & KONDRATIEV, Progress in Reaction Kinetics, Pergamon Press, 1961.

2.9 WAGNER et al. Z. Electrochem, 64, 501, 1960 and 65, 403, 1961.

2.10 CLYNE & THRUSH, 9th Symposium on Combustion.

2.11 KONDRAT'EV, Chemical Kinetics in Gas Reactions, 253, 1962.

3.1 KAUFMAN, Proc. Roy. Soc. A247, 123, 1958.

3.2 AZATYAN, NEODODSKY & NALBANDYAN, Pokl. Akad. Nauk. SSSR, 132, 864, 1960.

3.3 CLYNE & THRUSH, Nature, 189, 135, 1961.

3.4 FENIMORE & JONES, J. Chem. Phys, 65, 993, 1961.

3.5 DUFF, J. Chem. Phys. 28, 1193, 1958.

3.6 SEMENOV, Chemical Kinetics and Chain Reactions, 1935.

3.7 SCHOTT & KINSEY, J. Chem. Phys, 29, 1177, 1958.

4.1 SUDGEN & BULEWICZ, Trans. Faraday Soc. 54, 1855, 1958.

4.2 McANDREW & WHEELER, Thornton Res. Centre Report, M/IRM/44.

5.1 SCHOTT & BIRD, J. Chem. Phys. 41, 9, 1964.

5.2 BULEWICZ & SUGDEN, Trans. Faraday Soc. 54, 1855, 1958.

5.3 McANDREW & WHEELER, J. Chem. Phys. 24, 1256, 1956.

5.4 BLACK & PORTER, Proc. Roy. Soc. A266, 185, 1962.

5.5 KASKAN, Combustion and Flame, 2, 229, 1958.

5.6 DUFF, J. Chem. Phys. 28, 1084, 1958.

6.1 BYRON, J. Chem. Phys. 30, 1380, 1959.

6.2 CAMAC & VAUGHAN, J. Chem. Phys. 34, 460, 1961.

6.3 ANDERSON, United Aircraft Res. Labs. Report R-1828-1, 1961.

6.4 SCHEXNAYDER & EVANS, NASA T.R. R-108, 1961.

6.5 RINK, J. Chem. Phys. 36, 572, 1962.

6.6 RINK, WRIGHT & DUFF, J. Chem. Phys. 34, 1942, 1961.

6.7 LOSEN, Dokl. Akad. Nauk. 120, 1291, 1958.

6.8 MATTHEWS, Physics Fluids, 2, 170, 1959.

6.9 KISTIAKOWSKY & CHESICK, J. Chem. Phys. 28, 956, 1958.

6.10 ATTALLAH, Air Force Cambridge Res. Lab. Report AD1262017.

6.11 DUFF, J. Chem. Phys. 28, 1193, 1958.

6.12 ECKERMAN, Catholic University PhD Thesis, 1958.

6.13 DUFF & DAVIDSON, J. Chem. Phys. 1018, 1959.

6.14 HEIMS, NACA, Tech. Note 4144.

6.15 MORGAN, ELIAS & SCHIFF, J. Chem. Phys. 33, 948.

7.1 ADMUR, Amer. Chem. Soc. 60, 2247, 1938.

7.2 KASKAN, Combustion and Flame, 2, 229, 1958.

7.3 BULEWICZ, JAMES & SUGDEN, A235, 89, 1956.

7.4 DIXON-LEWIS, SUTTON & WILLIAMS, Disc. Faraday Soc. 1962.

7.5 DUFF, J. Chem. Phys. 28, 1194, 1958.

7.6 STEINER, Trans. Faraday Soc. 31, 623, 1935.

7.7 WIDAWSKY et al. 9th Symposium on Combustion.

7.8 RINK, J. Chem. Phys. 36, 262, 1962.

7.9 SCHOTKY, See Thornton Res. Centre Report, M/IRM/44.

7.10 PATCH, J. Chem. Phys. 36, 1919, 1962.

7.11 WISE, Project Squid, semi-annual Report.

7.12 SUTTON, J. Chem. Phys. 36, 2923, 1962.

7.13 GARDENER & KISTIAKOWSKY, J. Chem. Phys. 35, 1765, 1961.

7.14 CHESICK & KISTIAKOWSKY, J. Chem. Phys. 28, 956, 1958.

7.15 SMALLWOOD, J. Amer. Chem. Soc. 56, 1542, 1934.

7.16 LEWIS & von ELBE, Combustion, Flames and Explosions, 1961.

7.17 BUNKER & DAVIDSON, J. Amer. Chem. Soc. 28, 1089, 1958.

7.18 KUSHIDA, Liquids in Rocket Propellants, 385, 1960.

7.19 SCHOTT, J. Chem. Phys. 32,710, 1960.

7.20 FOWLER, Proc. 196 Ht. Trans. & Fluid Mechs. Inst. 279.

7.21 LIBBY, PERGAMENT & BLOOM, Report 250, Gen. Applied Science Labs. Inc. 1961.

7.22 OLSON, Amer. Rocket Soc. Paper, 2266-61, 1961.

7.23 ZIMNAN, ARS Journal, 30, 233, 1960.

8.1 SPALDING, JENKINS & YUMLU, 11th Symposium on Combustion, 779, 1967.

9.1 DUFF, J. Chem. Phys. 28, 1193, 1958.

9.2 SCHOTT & KINSEY, J. Chem. Phys. 29, 1177, 1958.

9.3 SEMENOV, Chemical Kinetics and Chain Reactions, 1935.

9.4 SPALDING, JENKINS & YUMLU, 11th Symposium on Combustion, 779, 1967.

10.1 KONDRAT'EV, Chemical Kinetics of Gaseous Reactions, 612, 1964.

10.2 NORRIS, Private Communication. 1966.

10.3 YUMLU, Private Communication. 1967.

10.4 BROKAW, 10th Symposium on Combustion, 1965.

16.1 YUMLU, Private Communication, 1967.

16.2 AVRAMENKO & KOLESNIKOVA, Izvest. Akad. Nauk SSSR, Otdel Khim. Nauk, 1971, 1961.

16.3 NORRIS, Private Communication, 1966.

17.1 NORRIS, Private Communication, 1966.

17.2 YUMLU, Private Communication, 1967.

17.3 HOARE, PROTHEROE & WALSH, Trans. Faraday Soc. 55, 548, 1969.

18.1 NORRIS, Private Communication, 1966.

18.2 BASCOMBE, Aer. Res. Council, LS/17934, 1966.

APPENDIX D

DESCRIPTION OF THE COMPRESSION MACHINE

D.1 The Compression Machine

Many of the design features of the compression machine are novel. It is because the design covered new ground that many months of development were required to arrive at the final form of the apparatus described in this Appendix. We shall only briefly mention this development.

Fig D.1-1 shows a view of the layout of the apparatus. The instrumentation, control panel and the compression machine are depicted. We begin by describing the compression machine.

The cylinder. Fig D.1-2 shows a detail drawing of the compression machine. The compression cylinder, item (13), is at the bottom of the apparatus. The cylinder is surrounded by an oil-heating-jacket (12) and the cylinder head (11) is recessed to minimise the heat path from the oil jacket at the head face, thus maintaining uniform wall temperatures. The 'W' section head gasket is designed for long life as the cylinder head may have to be cleaned, to remove combustion deposits from the cylinder walls between compression tests.

The cylinder head. The cylinder has a diameter of 2 inches, sufficient to mount a pressure transducer and an additional device, such as a sparking plug, fuel injector or quartz window, in the cylinder head. At present the cylinder head has a central hole for mounting the pressure transducer only. To reduce risk of surface activity the head face has a P.T.F.E. film sprayed on it.

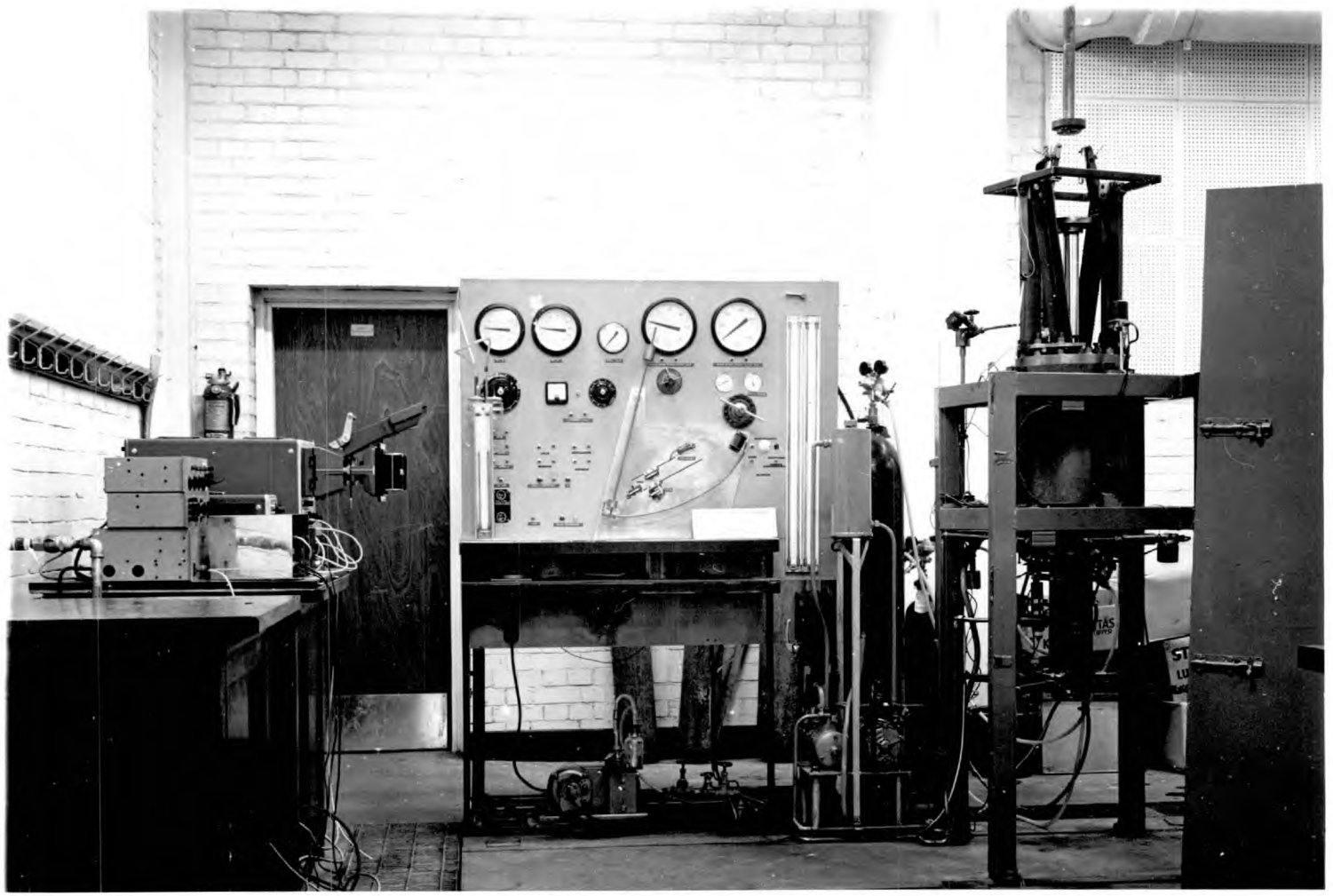

Fig D.1-1 The experimental apparatus, left to right: the recording equipment; the control panel; the compression machine.

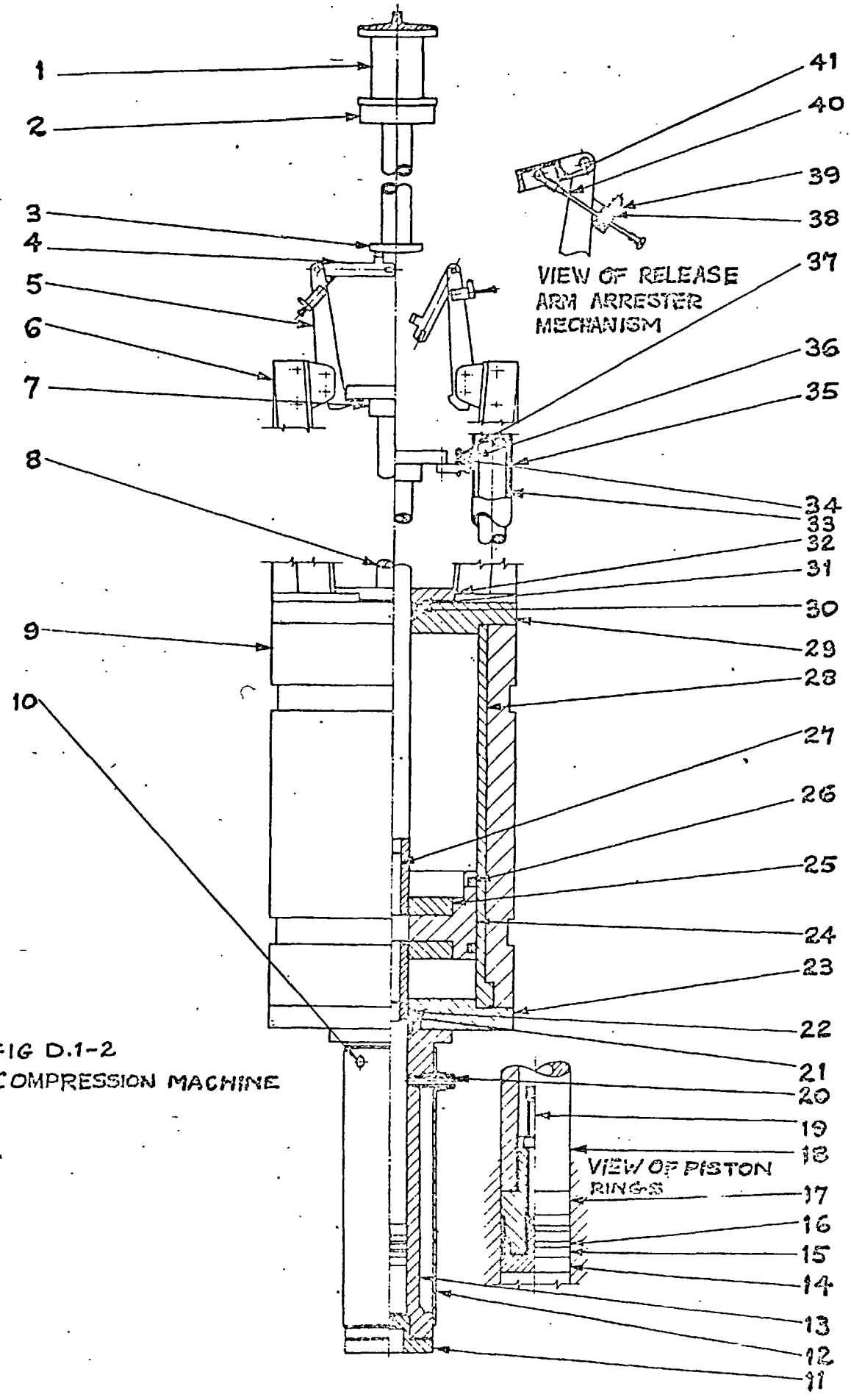

FIG D.1-2
THE COMPRESSION MACHINE

Key to Numbers appearing in Fig D.1-2

1 - Electromagnet
2 - a weight
3 - claw-release plunger
4 - release arm
5 - a claw
6 - release mechanism carrier
7 - retention pad
8 - upper shaft
9 - driving cylinder body
10 - exhaust ports
11 - cylinder head
12 - oil-jacket wall
13 - compression cylinder
14 - compression piston crown
15 - P.T.F.E. ring
16 - ring expander
17 - compression piston body
18 - lower shaft
19 - ring-expansion screw
20 - inlet port
21 - ring expander
22 - P.T.F.E. ring
23 - driving cylinder end-plate
24 - driving piston
25 - clamping plates
26 - two piece sealing ring
27 - piston boss
28 - liner
29 - driving cylinder end-plate
30 - ring expander
31 - P.T.F.E. ring
32 - ring loading plate
33 - wire-wound potentiometer
34 - follower loading screw
35 - potentiometer shield
36 - follower arm
37 - roller follower
38 - ball
39 - ball loading spring
40 - arresting shaft
41 - overshoot spring

The ports. At the end of the cylinder, remote from the head, 5 radial ports enter the cylinder. Four exhaust ports (10) lead through manually-operated ball-valves to atmosphere, so that the exhaust gases may be released, or contained, at the end of the first return stroke as desired. A single inlet port (20) contains three capillary tubes which end tangentially at the edge of the cylinder. Through these tubes gases may be independently introduced, so that there is no need for an external gas-mixing chamber and the associated explosion risks. The port itself is connected to a vacuum pump so that the cylinder may be evacuated prior to charging.

The length of the cylinder permits a maximum of 14 inches piston travel, so that a minimum surface area:volume ratio is attained at a compression ratio of 7:1.

The piston sealing system. Considerable attention has been given to devising a method of sealing the compression piston (17) in its cylinder. The most satisfactory systems previously used in the rapid-compression machines have required the use of lubricant [52.] or have given rise to small losses of charge [39.]. The present design uses three continuous P.T.F.E. rings (15) with floating, spacing ring-lands (16) between them.* The rings have tapered sections so that screwing the stainless-steel piston-crown (14) on to the body expands the rings radially, creating an excellent seal, (the combustion cylinder may be evacuated to less than 0.003 atmospheres and at 20 atmospheres the leakage rate is 0.3% per hour. Dynamic tests have shown charge loss per test to be less than 0.1% per shot). The piston crown is screwed on to the body by a cap

---

* To obviate the need to readjust ring tension with jacket temperature alterations, an additional ring and spacer have been added. The former is designed so that it expands to exactly compensate for the thermal expansion of the remaining rings.

screw (19) on the driving-piston side of the hollow lower shaft (18).

The driving system. The compression piston is rigidly coupled to the 10 inch diameter driving piston (24). Pneumatic control of the piston motion was chosen in preference to other methods employing impactive acceleration and arrestor springs [19., 20., 54.], where structural and instrumentational difficulties arise due to the vibration set up by the sudden acceleration of the piston. On the other side of the driving piston a similar shaft to that connecting the compression piston passes through the upper end-plate (29). Both shafts pass through P.T.F.E. tapered-ring glands. The diametral clearance of both shafts and pistons is .004 inches, calling for accurate concentricity and axial alignment of the components. The small clearance prevents extrusion of the plastic rings into the clearance spaces. Only the two-piece sealing rings (20) of the driving piston require lubrication.

D.2 Details of the Control Equipment

The external shaft of the piston assembly serves two purposes. Firstly, it carries the flange (7) with which the release mechanism engages, restraining the pistons against the driving-air charge. Secondly it carries the potentiometer follower (37) of the transducer which monitors the piston displacement.

The release mechanism consists of four hooked claws (5) which engage with hardened plates on the flange. Engagement is maintained by two abutting links (4) which form an unstable mechanism. Equilibrium of the linkage is disturbed by a plunger (3), itself actuated by a weight falling from an electromagnet down a guide shaft. A friction damper, seen in fig D.2-1 absorbs energy imparted to the

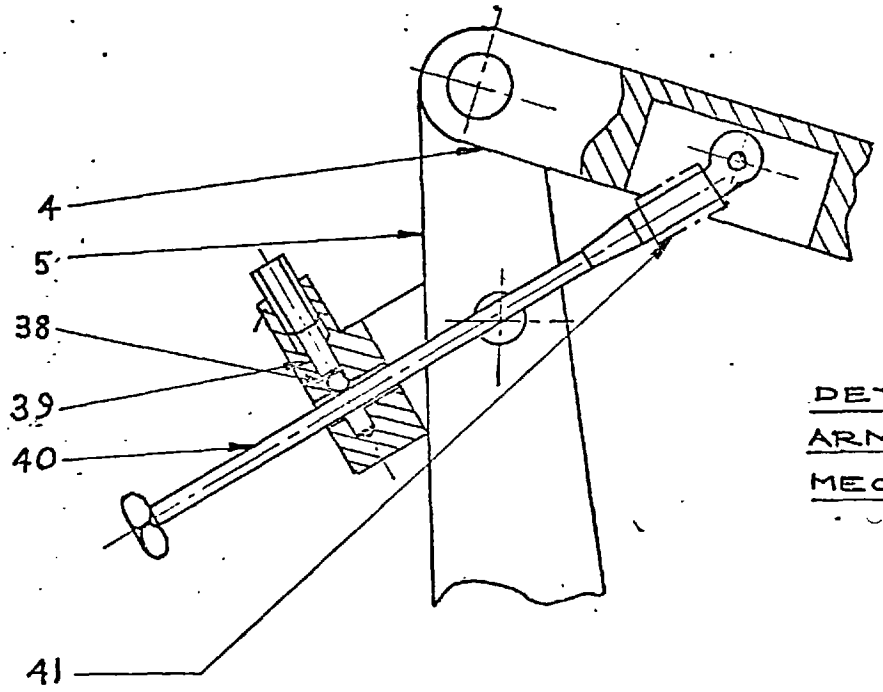

DETAIL OF RELEASE-ARM ARRESTER MECHANISM

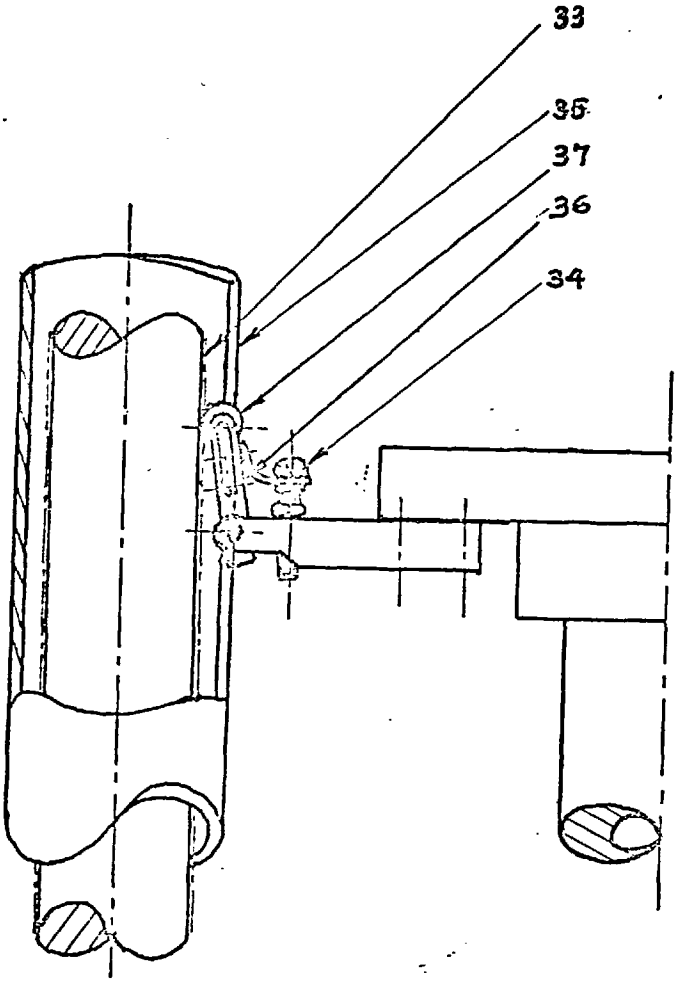

DETAIL OF POTENTIO-METER AND ROLLER FOLLOWER

FIGURE D.2-1

links on release of the pistons. The height of the release mechanism is adjustable so that the effective piston-stroke may be varied.

The potentiometer and its follower is shown in the lower half of fig D.2-1. The potentiometer consists of .004 inch diameter enamelled wire wound on to an insulating former on .005 inch pitch. To prevent the wire moving it is potted in epoxy-resin. One segment of the coil is bared of insulation to form a track for the follower. Several follower designs were tested before the final version was evolved. The need for development resulted from the tendency of the follower to bounce on its track at high piston speeds. The present roller follower (37) is maintained in contact with the track by a pivoting arm (36) and spring. The follower shaft runs in P.T.F.E. bearings and current path and lateral location of the shaft are maintained by leaf springs on each side of the arm.

Driving cylinder air control. Leakage of some driving air past the piston into the retarding chamber occurs, and it is necessary to supply 'make up' air via regulating valves to both chambers. Just before release of the piston the supplies are isolated by electro-pneumatic valves.

Event sequencing. The sequencing of the valves, the release of the weight from the electromagnet and the triggering of the oscilloscope are sequenced by a pendulum sweeping across a series of micro-switches. The pendulum has bobs both above and below its pivot point to give a period of approximately 4 s.

Other control equipment may be seen on fig 4.21-1, consisting of the automatic heating and regulating system of the oil circuit which is used to maintain the compression-cylinder jacket at a constant temperature within $\pm$ .25°C.

APPENDIX E

THE FLOW-VISUALISATION EXPERIMENT

E.1 The Object

The purpose of this investigation was to observe the flow patterns established in a piston-in-cylinder apparatus during the compression and expansion of non-reacting gases.

E.2 The Motivation

In the mathematical analysis of the reacting system (section 2.21) we assumed that the thermodynamic properties were uniform throughout the reactant gas. But in section 3.2 we supposed that the transport properties were spatially non-uniform because the gas-wall heat transfer could be correlated by an equation for forced convection. Nonetheless if we can establish that the fluid is well mixed, then the assumption about the thermodynamic properties will still be valid, despite the variability of the transport properties. If, however, we were, for example, to find that convection was confined to the fluid immediately in front of the piston, then we would have to conclude that the assumption was invalid. Hence the need to establish the nature of the fluid flow within the cylinder.

E.3 The Apparatus

As it was not possible to observe the fluid flow in the compression machine a transparent model was built. The model was designed so that model piston was driven by a pressure differential across it, and not by a separately-driven piston as in the compression

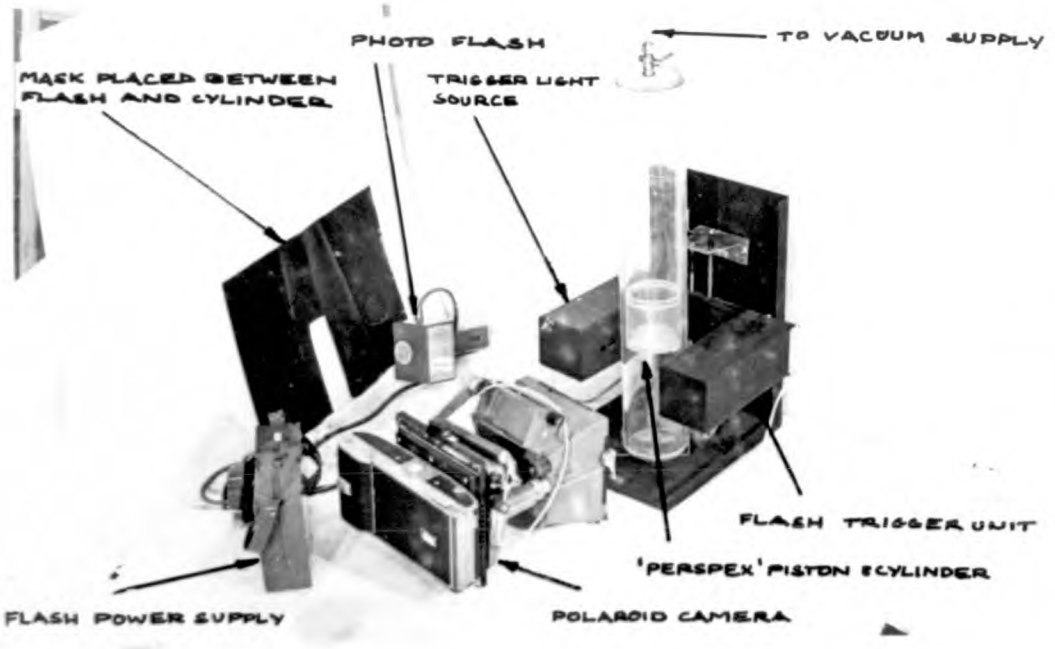

Fig E.3-1 Apparatus for the flow visualisation experiment

machine. The in-cylinder pressures in the model would be less than those in the machine and an analysis of dimensionless groups showed that to maintain similarity the length dimensions of the model should be 50% greater than those of the machine cylinder.

Fig E.3-1 shows a photograph of the model and its control equipment. The transparent 'perspex' cylinder, containing the piston, is supported between two arms of a cradle, whose height relative to the cylinder is adjustable. One arm contains a light source which shines across the cylinder on to a triggering unit in the other arm. A disc closes the lower end of the cylinder, while the upper end has a cylinder head lapped to it, so that the head may be slid quickly to one side forming, in effect, a quick-opening valve.

E.4 Test Procedure

The operational procedure is as follows: with the piston at its uppermost point of travel, the whole cylinder is evacuated to a predetermined pressure. The upper cylinder-head is slid aside, and the in-rush of atmospheric air drives the piston down the cylinder, compressing the air in front of it. As the piston travels down the cylinder it interrupts the light beam causing the triggering unit to actuate an electronic flash. The light beam from the flash is restricted by a narrow aperture to illuminate a diametral plane of the cylinder. Thus, a photograph of two-dimensional flow of particles suspended in the compressed gas may be taken by a Polaroid camera.

The piston speed is measured by raising the triggering unit and light source so that a photograph of the piston is obtained. Typically, the image of the piston is distorted by .3 in., which for the .001 ms duration of the flash corresponds to 25 ft s^{-1}.

If lycopodium powder and air are premixed prior to a shot, electrostatic precipitation of the powder on the cylinder walls obscures the photographic records. To avoid this, powder is suspended on a strip of paper gauze wedged across the mid-point of the cylinder in the plane of the light beam. The powder is then entrained by the flow past it during compression.

E.5 Results

The results of analysis of photographs taken at intervals from the beginning of compression through to expansion are shown in fig E.5-1a to E.5-1d. After the piston has travelled 30% of the way down the cylinder, (a) shows the turbulent front marking the limit of the particle penetration. Clearly, a velocity distribution has already developed. When the piston has travelled for 85% of the avail-

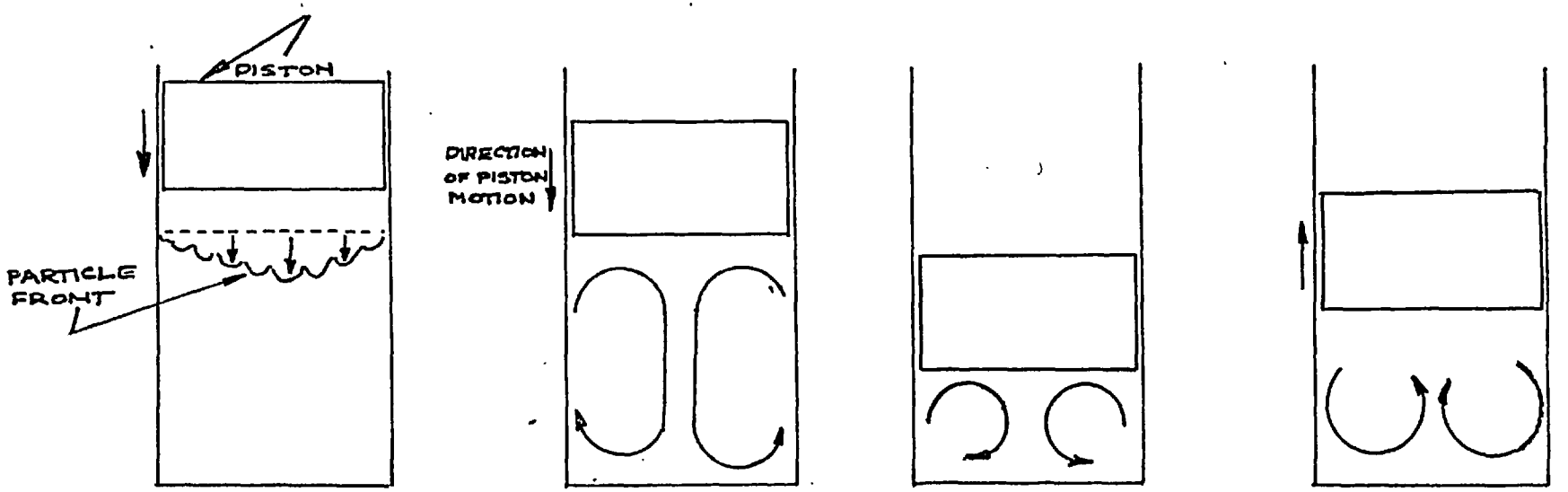

FIG E.5-1 Flow patterns observed during compression and expansion.

able stroke, a recirculation pattern is set up (b) which persists until the point of maximum compression. During expansion the direction of flow is reversed as in (d).

E.6 Conclusions

The tests demonstrated that, during compression, turbulent flow developed into a toroidal-vortex recirculation pattern.

A hypothesis for the development of the flow is as follows: The driving force behind the fluid motion is the variation in viscous shear-stress along any radius of the cylinder. The stresses are greatest close to the walls. Thus, as the piston moves down the cylinder, the gas in the central core of the cylinder moves in the direction of the piston motion more freely than that at the wall. The gas at the wall is removed by the piston and fed radially inwards across the piston face, creating the toroidal vortex observed in the experiments. When the piston moves away from the closed end, expanding the gas, the direction of the shear forces and vortex rotation is reversed.

It is this gas motion which leads to convective heat-transfer and enables us to correlate the gas-wall heat transfer by an equation for forced convection (equation 3.26-1).

It is concluded that the mixing established during recirculation is sufficient for us to assume that the thermodynamic properties are uniform throughout the fluid.

APPENDIX F

PREDICTION OF THE COMPRESSION-MACHINE PISTON-MOTION

F.1 The Task

The prediction of the compression-machine piston-motion, by way of mathematical analysis, would permit: i) the prediction of autoignition, using the method developed in Chapters 2 and 3, without recourse to experimental volume-time histories; ii) the selection, at the design stage, of control variables such that the finalised machine could produce density-time histories representative of reciprocating engines: that experienced by the end-gas in a gasoline engine; or that resulting from piston motion controlled by a crankshaft and connecting rod.

F.2 The Path

The derivation of the equation of motion from Newton's Second Law is straightforward. The equation has an exact integral which relates the piston velocity to its displacement, but to obtain displacement as a function of time numerical integration is required. A computer programme was written to obtain the arithmetic results.

F.3 The Predicted Piston-displacement

In calculating the piston displacement, a value of the frictional force F, between the pistons and their cylinders must be assumed.

Fig F.3-1 shows curves of observed and predicted compression ratios as a function of starting pressure in the retarding chamber p_{20}, for values of driving-chamber pressure p_{10}. The curves demon-

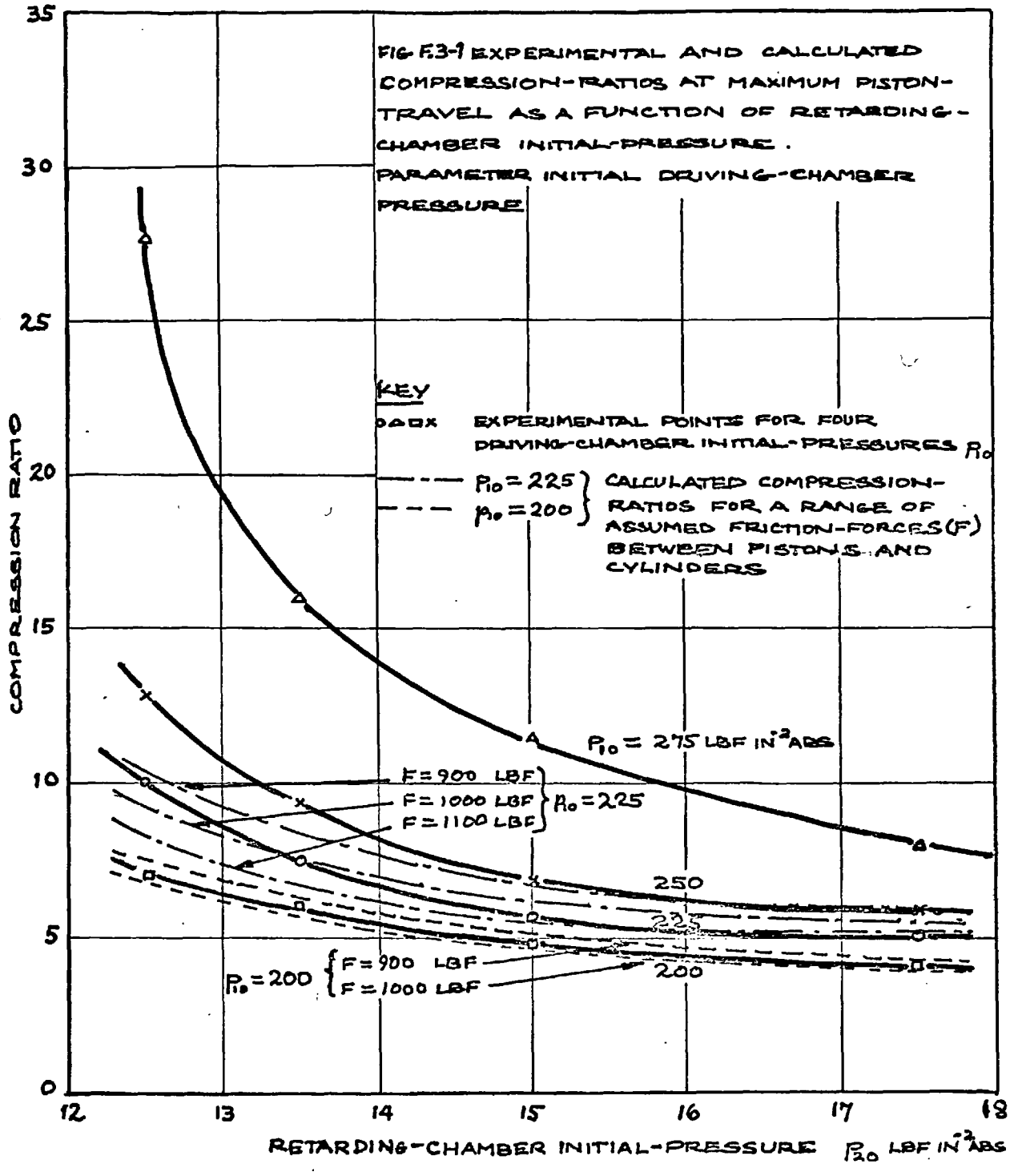
FIG F.3-1 EXPERIMENTAL AND CALCULATED COMPRESSION-RATIOS AT MAXIMUM PISTON-TRAVEL AS A FUNCTION OF RETARDING-CHAMBER INITIAL-PRESSURE.
PARAMETER INITIAL DRIVING-CHAMBER PRESSURE
KEY
EXPERIMENTAL POINTS FOR FOUR DRIVING-CHAMBER INITIAL-PRESSURES P_{10}
$P_{10}=225$
$P_{10}=200$
CALCULATED COMPRESSION-RATIOS FOR A RANGE OF ASSUMED FRICTION-FORCES (F) BETWEEN PISTONS AND CYLINDERS
$P_{10}=275$ LBF IN^{-2} ABS
F=900 LBF
F=1000 LBF
F=1100 LBF
$P_{10}=225$
250
225
200
$P_{10}=200$
F=900 LBF
F=1000 LBF
COMPRESSION RATIO
RETARDING-CHAMBER INITIAL-PRESSURE P_{20} LBF IN^{-2} ABS
0
5
10
15
20
25
30
35
12
13
14
15
16
17
18

strate that predicted and observed results agree for p_{10} = 200 lbf in^{-2}, and an assumed value of F = 950 lbf. At greater values of p_{10} agreement is not indicated.

It was concluded that F has no single value, but is a complex function of many parameters including the piston velocity, since the measured piston velocity was 300 lbf at slow speeds, much less than the apparent dynamic value. Because the friction function was uncertain, the decision was made to use experimental displacement-time records in the autoignition-prediction calculations.

F.4 The Predicted Range of Piston Motion

Experimental records of the pressure development in the end-gas of a gasoline engine* were used to calculate density-time histories. Spalding [50.] proposed a dimensionless relation between density ρ, and the rate of density change $\frac{d\rho}{dt}$, for comparing density-time histories in piston-engines. This relation is:

$$\frac{dt}{d\rho} \Big/ \left(\frac{dt}{d\rho}\right)_R = \left(\frac{\rho}{\rho_R}\right)^{\varepsilon} \qquad \text{F.4-1}$$

where R is a reference value at time t > 0.

The value of the index in the end-gas was found to be $\varepsilon \simeq -1.5$. The index, in the same engine, due to piston motion alone was $\varepsilon = -1.7$. This was the range of ε over which the machine should be able to operate.

Values of ε were calculated from the predicted piston-motion.+ The parameters which predominantly controlled ε were (see fig F.4-1)

---

* The results examined were those reported by Klat [32.] for a range of hydrocarbon fuels.

+ Although we showed in F.3 that with a constant friction-factor the prediction procedure was not accurate enough to apply to autoignition prediction, it is sufficiently precise for the derivation of approximate values of ε.

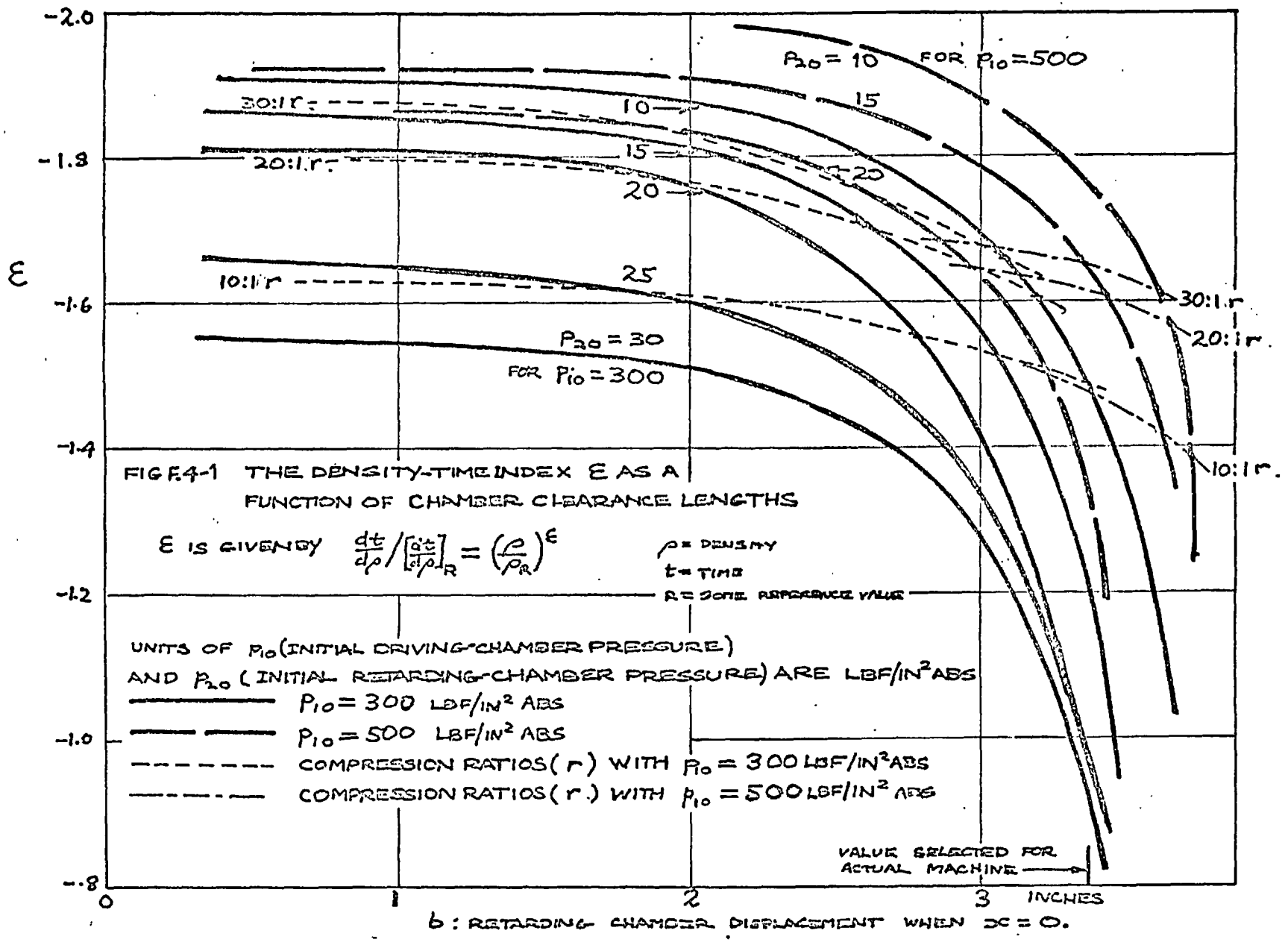

FIG F.4-1 THE DENSITY-TIME INDEX ε AS A FUNCTION OF CHAMBER CLEARANCE LENGTHS

ε IS GIVEN BY $\frac{dt}{d\rho} \Big/ \left[\frac{\partial t}{\partial \rho}\right]_R = \left(\frac{\rho}{\rho_R}\right)^{\epsilon}$

b : RETARDING CHAMBER DISPLACEMENT WHEN $x_c = 0$.

p_{10}, p_{20} and the geometrical parameter b (the driving-piston clearance in the retarding chamber at zero compression-piston displacement from the cylinder head). The value of b determines the length of the coupling shaft between the two pistons. It was apparent that the greatest range of ε was attained when b took values in the range 3.0 to 3.875 inches; with the larger value the driving chamber would have no starting volume.

A value of b = 3.375 inches was selected, giving a range of ε = -1.4 to -1.75, sufficient to include both engine end-gas and piston-motion density-time histories.